STRUCTURAL BASIS FOR THE ALLOSTERIC ACTIVATION OF *TRYPANOSOMA BRUCEI* S-ADENOSYLMETHIONINE DECARBOXYLASE BY A CATALYTICALLY DEAD HOMOLOG

APPROVED BY SUPERVISORY COMMITTEE

_____
Margaret A. Phillips, Ph.D.

_____
Kim Orth, Ph.D.

_____
Michael Roth, Ph.D.

_____
Jef De Brabander, Ph.D.

_____
Joseph Albanesi, Ph.D.

DEDICATION

To my parents, Carmen D. Aviles and Armando Velez, for their infinite love, support and encouragement in every step of the way. Thank you will never be enough!

STRUCTURAL BASIS FOR THE ALLOSTERIC ACTIVATION OF *TRYPANOSOMA BRUCEI S*-ADENOSYLMETHIONINE DECARBOXYLASE BY A CATALYTICALLY DEAD HOMOLOG

by

NAHIR AIMEE VELEZ

DISSERTATION

Presented to the Faculty of the Graduate School of Biomedical Sciences

The University of Texas Southwestern Medical Center at Dallas

In Partial Fulfillment of the Requirements

For the Degree of

DOCTOR OF PHILOSOPHY

The University of Texas Southwestern Medical Center at Dallas

Dallas, Texas

December, 2012

STRUCTURAL BASIS FOR THE ALLOSTERIC ACTIVATION OF TRYPANOSOMA BRUCEI S-ADENOSYLMETHIONINE DECARBOXYLASE BY A CATALYTICALLY DEAD HOMOLOG

NAHIR AIMEE VELEZ, Ph.D.

The University of Texas Southwestern Medical Center

Dallas, Texas 2012

MENTOR: MARGARET A. PHILLIPS, Ph.D.

Human African Trypanosomiasis (HAT) is caused by single-celled parasites, *Trypanosoma brucei*, which are transmitted to humans by infected tsetse flies. Trypanosomiasis has a profound impact on the health of a large number of people in sub-Saharan Africa and it is fatal when untreated. Unfortunately, current drug therapy is limited mostly because of toxic effects on the patients. The polyamine biosynthetic pathway is a validated target for the development of drugs. Enzymes involved in polyamine biosynthesis exhibit features that differ significantly between the parasites and the human host. Therefore, exploitation of such differences can lead to the design of new inhibitors that can selectively kill the parasites.

My work is focused on S-adenosylmethionine decarboxylase (AdoMetDC), which in the trypanosomatids is regulated by a unique mechanism, heterodimer formation with a catalytically dead homolog. This protein, designated prozyme, forms a high-affinity heterodimer with AdoMetDC and increases its activity by $>10^3$-fold. The heterodimer is confirmed to be the functional enzyme *in vivo*. Therefore, understanding the mechanisms that regulate *T. brucei* AdoMetDC activation by prozyme can provide essential information for more effective inhibitory strategies. The role of specific residues involved in the process was studied by deletion and site-directed mutagenesis. Results indicate that 12 key amino acids at the N-terminal portion of the enzyme, which are fully conserved in the trypanosomatids but absent from other eukaryotic homologs, play a crucial role since there is more than 50 percent less activation by prozyme when they are either removed or mutated to alanine. AdoMetDC L8 and L10 seem to be the strongest determinants for stimulation by prozyme in this region. Analytical ultracentrigugation analyses in the sedimentation velocity mode indicated that dimerization is not impaired when these essential residues are removed, since binding affinities between wildtype and mutant heterodimers remain similar (K_d= <0.5 and 1μM, respectively). Thus, these results imply that key residues in the area must be acting through an allosteric regulatory mechanism.

I have also characterized the activity of the *L. major* AdoMetDC/prozyme complex, the catalytic efficency from which increases by 170-fold upon binding of the homolog. Swapped complexes containing AdoMetDC and prozyme from different trypanosomatids (*T. brucei, T. cruzi* and *L.major*) are functional, supporting the idea that amino acid residues essential for the activation mechanism are conserved in all species.

TABLE OF CONTENTS

Chapter 2

Chapter 3

LIST OF FIGURES

LIST OF TABLES

LIST OF ABBREVIATIONS

AdoMet- S-Adenosylmethionine

AdoMetDC- S-Adenosylmethionine decarboxylase

AUC- analytical ultracentrifugation

BME- β-mercaptoethanol

BSO- buthionine sulfoximine.

CNS- central nervous system

CPM- counts per minute

dcAdoMet- decarboxylated S-Adenosylmethionine

DFMO- di-fluoromethylornithine

DMSO- dimethyl sulfoxide

DTT- dithiothreitol

E.coli- Escherichia coli

GS- glutathione synthetase

HAT- human African trypanosomiasis

HM-homodimer

HT- heterodimer

HTS- high-throughput screening

IPTG- isopropyl-beta-D-thiogalactopyranoside

Lm- Leishmania major

NECT- nifurtimox and eflornithine combination therapy

ODC- ornithine decarboxylase

PCR- polymerase chain reaction

PEP- phosphoenolpyruvate

PK- pharmacokinetics

PMSF- phenylmethylsulfonyl fluoride

SDS-PAGE- sodium dodecyl sulfate polyacrylamide gel electrophoresis

SpdSyn- spermidine synthetase

SUMO- small ubiquitin-like modifier

SV- sedimentation velocity

Tb- Trypanosoma brucei

Tc- Trypanposoma cruzi

TET- tetracycline

TEV- Tobacco Etch Virus

TR- trypanothione reductase

TS- trypanothione synthetase

ULP1- ubiquiting-like specific protease 1

VSG- variant surface glycoprotein

WHO- world health organization

WT- wild-type

γGCS- γ-glutamylcysteine synthetase

CHAPTER 1

INTRODUCTION

Human African Trypanosomiasis

Disease Aspects

Human African Trypanosomiasis (HAT), commonly known as sleeping sickness, is a fatal disease caused by subspecies of the protozoan pathogen *Trypanosoma brucei* and transmitted by the Tsetse fly insect vector [1-3]. It is most commonly found in the poorest regions of sub-Saharan Africa, covering about 37 countries. The world health organization estimated, in 1995, that 60 million people were at risk of getting infected [4, 5]. Approximately 300,000 new cases were identified each year but, unfortunately, only less than 30,000 were properly diagnosed and treated. Strong programs were developed to fight the outbreaks and more effectively assess diagnosis and treatments. Positive outcomes were obtained from these continuous efforts, since the number of cases reported in 2009 decreased below 10,000 (**Fig 1.1**). In recent years, these lower numbers have been maintained; with only 7139 cases reported in 2010 [4, 5]. Although this reduction was observed for the first time in 50 years, the disease still represents an extremely concerning health issue.

HAT occurs focally, in remote regions, and periodically reaches epidemic levels. The people that are most exposed to the disease are those living in rural areas. They commonly depend on agriculture, farming, fishing and hunting to survive and thus are more likely to have direct contact with the tsetse fly. Poverty in these affected populations and the fact that they have minimal access to proper health care are some of the reasons why surveillance is impaired. Therefore, if the cases cannot be properly monitored, diagnosis and treatments will be hampered as well.

There are three main *Trypanosoma brucei* sub-species, although only two of them are known to be human infective [1, 3]. *Trypanosoma brucei gambiense* is most commonly found in west and central Africa. It causes a chronic infection and represents more than 95% of the reported cases of sleeping sickness [5]. A person infected with *T.b.gambiense* could spend months or even years without showing any signs. The infection progresses slowly and quietly, and when the symptoms emerge the patient is already in an advanced point of the disease. Sleeping sickness is divided into two stages of infection: early and late. The parasites replicate extracellularly in the blood stream of the mammalian host during the early stage, which is characterized by high fever, itching, headaches, and joint pain. In the late stage, they cross the blood-brain barrier and invade the central nervous system, leading to severe neurological symptoms, including mental, sensory, and sleep anomalies, from which the disease takes its name. All of these symptoms can definitely progress to coma and death if not treated. *Trypanosoma brucei rhodesiense* is most commonly found in eastern and southern Africa. This form causes an acute infection and represents less than 5% of the reported cases [5]. In this case, the first signs of the disease are observed within a few months or weeks after infection, reaching the second stage very fast. *Trypanosoma brucei brucei* cannot infect humans, since it is susceptible to lysis by the apolipoprotein L1 circulating in the plasma of the mammalian host, as opposed to the other forms [6]. Although *T.b.gambiense* and *T.b.rhodesiense* are resistant to this trypanosome lytic factor, all three sub-species share many other important features and thus *T.b.brucei* is commonly used in laboratories as a model for human infections.

Another form of trypanosomiasis, known as Chagas disease, is common in Central and South America, and affects about 8-10 million people living in the endemic regions [7, 8]. It is caused by the protozoan *Trypanosoma cruzi* and, just like HAT, can be lethal if left untreated.

The disease is associated with failures in the nervous system, digestive system and the heart. Species and sub-species of the *Trypanosoma genus* can also infect wild and domestic animals. This increases the probability of transmission to humans, since they could act as a reservoir for the human pathogen parasites, *T.b. rhodesiense and T.b. gambiense.* In cattle, the disease is known as Nagana, which contributes to human protein malnutrition [5]. Animal trypanosomiasis also represents a potential threat for the economic development of the affected regions. Although protecting the animals from insect bites is difficult, continuous efforts focus on reducing or eliminating tsetse fly populations with traps and insecticides, among others.

Current Therapy

Trypanosma brucei undergoes extensive phenotypic (antigenic) variation of a protein known as variant surface glycoprotein (VSG), which surrounds the parasite cell creating a dense coat. This mechanism is utilized to avoid the host immune response and ensure pathogen survival [9, 10]. Obviously, the situation makes the development of a vaccine highly unlikely. Although HAT is always fatal if not treated, producing new HAT therapies is not a main priority for the pharmaceutical industry since the disease affects only the poorest nations. However, as one of the most neglected tropical diseases, African trypanosomiasis still gets the attention of an immense number of research institutions, control programs and international organizations that work hard on trying to fight this disease. The drugs that are available for treatment of HAT all present significant problems, particularly for the late stage disease, which go from toxicity and adverse reactions to extensive administration regimes [2, 11] (**Table 1.1**). Suramin and pentamidine are currently used for the treatment of the early stage, while only two drugs, melarsoprol and eflornithine, are available for the late stage disease. Melarsoprol is a highly toxic, arsenic-based compound that can be life-threatening by causing a fatal encephalopathy in

5-10% of the patients. Eflornithine, also called α-difluoromethylornithine (DFMO), is a suicide inhibitor of ornithine decarboxylase (ODC), which is required for the biosynthesis of polyamines. It is the most recently discovered drug for the treatment of HAT and the only one with a known mechanism of action. DFMO has low toxicity. However, it has to be administered in extremely high doses (400 mg/kg daily given as 6-hourly intravenous infusions for 14 days) because of the short half-life of the drug, which in turn is very expensive and not widely available on the market. This situation is not ideal for the affected people that commonly live in the poorest regions, who usually obtain the drug by donations from the manufacturers. In addition, while DFMO can cure infections of the West African sub-species *T. b. gambiense,* it is not considered effective against *T. b. rhodesiense,* the subspecies found in East Africa. Recently, nifurtimox, which is used for treating the Chagas disease, has been tested in combination with eflornitine yielding some encouraging results [12]. The dosage of the combination therapy, called NECT, decreased to 15mg/kg of oral nifurtimox for 10 days and 400mg/kg eflornithine in 12-hourly infusions for 7 days. However, despite this small accomplishment, the drug is still not efficient for treating *T. b. rhodesiense* infections. Thus, there is no available therapy for late stage disease that is effective against all forms of the disease, and which can be administered easily with acceptable toxicity profiles. This situation demonstrates the urge to develop new, safe and more effective drugs to fight this disease.

Polyamine Biosynthetic Pathway

Polyamines are essential organic cations found in all organisms and produced in the cells through highly regulated pathways [13]. In most eukaryotes, putrescine is synthesized from L-

ornithine and functions as the precursor for the formation of spermidine and spermine, with decarboxylated S-adenosylmethionine (AdoMet) working as the aminopropyl group donor (**Fig 1.2**). The enzymes catalyzing the rate-limiting steps in the mammalian biosynthetic pathway are ornithine decarboxylase (ODC) and S-adenosylmethionine decarboxylase (AdoMetDC), the levels from which are tightly controlled. Polyamines are ubiquitously expressed, present at high concentrations in the cells and usually associated with rapidly growing tissues. These important features were the key for researchers to start studying them more profoundly in order to better understand their biological roles. Apoptosis, cell cycle, cancer and embryonic development are some of the cellular processes in which they are involved [14, 15]. Important characteristics that make polyamines so versatile include their ability to bind RNA and DNA, influence DNA-protein interactions, bind ribosomes and stimulate protein biosynthesis [16]. As a result they are actively involved in both transcriptional and translational events. For example, hypusination (covalent modification) of the eukaryotic initiation factor 5A (eIF5A) is essential for its biological role in cell growth and survival [17, 18]. This important process is mediated by the polyamine spermidine, which is cleaved to produce the 4-aminobutyl moiety that will eventually lead to the formation of hypusine on eIF5A. Another important feature of polyamines is that they are known to modulate ion channels, which is a crucial mechanism for controlling membrane potential and cellular homeostasis [19].

Polyamine levels are known to directly influence cellular growth and transformation. Whenever these compounds are found in low quantities in the cell, growth arrest is observed. On the contrary, excess polyamines lead to cancer in mammalian cells, and as a consequence polyamine metabolism has been extensively studied as a potential drug target for infectious and proliferative diseases [20, 21]. Inhibitors of polyamine biosynthetic enzymes have been

developed and tested in cancer models [15, 22, 23]. In particular, eflornithine (DFMO), which irreversibly inactivates ODC, is the most widely studied example of a polyamine-metabolism inhibitor that suppresses cancer development in animal models and has been evaluated in clinical trials. As mentioned earlier, DFMO is currently used as a drug against African sleeping sickness, and it is the only fully validated, clinically proven target for the treatment of this disease. This finding demonstrates that the polyamine biosynthetic pathway is an essential tool from which potential new and more effective therapeutics against HAT can be obtained.

The polyamine metabolic pathway in the trypanosomatids *(Trypanosoma and Leishmania genera*) has several unique features that distinguish it from the mammalian host [24]. These species do not contain spermine, and spermidine is conjugated to two molecules of glutathione to form a novel cofactor, termed trypanothione (**Fig 1.2**). The main function of this cofactor is to help against oxidative stress and maintain a thiol redox balance in the parasites. Trypanothione reductase replaces the function of glutathione reductase, which in mammalian cells also controls oxidative stress by producing the reduced glutathione molecules that will scavenge reactive oxygen species [25]. In addition, the genomes of the trypanosomatids lack the catabolic enzymes, polyamine oxidase and spermidine/spermine N^1-acetyltransferase, required for converting the longer chain polyamines back to putrescine in mammalian cells [26]. This is an extremely important regulatory mechanism to ensure normal polyamine levels. Interestingly, trypanothione synthetase has been reported to contain both a synthetic domain for the formation of glutathionylspermidine (GSH-Spd) and trypanothione, and a catabolic amidase domain that hydrolyzes these compounds back to glutathione (GSH) and spermidine [27, 28]. An important difference in polyamine biosynthesis within the trypanosomatids relies on the fact that while *T. brucei* and *Leishmania spp* are able to synthesize putrescine, *T. cruzi* lacks ODC and instead

salvages both putrescine and cadaverine from the host cell [24]. This difference is very important, particularly for the development of new therapies against Chagas disease. Blocking polyamine uptake by the putrescine/cadaverine transporter or utilizing this transport mechanism to deliver cytotoxic compounds might be highly effective approaches against the parasites.

Several genetic and chemical studies in both *T. brucei* and *Leishmania spp* have demonstrated that the polyamine and trypanothione biosynthetic enzymes are essential for growth and survival of these parasites [29, 30]. *T. brucei* strains lacking both wild-type *ODC* alleles (*Δodc*-null mutants) require exogenous putrescine for proper proliferation [31, 32]. Trypanosomes deficient in ODC, injected into mice bloodstream, were unable to multiply and rapidly cleared from the blood. Additional studies on these cell lines established that ODC is the sole target of DFMO action in the parasite. *T. brucei* AdoMetDC knockdown also results in growth arrest, with cells dying by day 10 after induction, demonstrating the essentiality of this protein [33]. Similar results were obtain from irreversibly inhibiting AdoMetDC using 5_-*{*[(*Z*)-4- amino-2-butenyl]methylamino*}*-5_-deoxyadenosine (MDL73811), a structural analogue of decarboxylated AdoMet. While the ODC and AdoMetDC knockdowns are rescued by putrescine and spermidine, respectively, neither of these polyamines are found in significant quantities in the serum of the mammalian host. Thus, there is no possibility for the inhibition of these enzymes to be abolished *in vivo*. Furthermore, while *T. brucei* is capable of transporting both amines, it does so with very low efficiency particularly in the case of spermidine. Spermidine synthetase (SpdSyn) or the glutathione and trypanothione biosynthetic enzymes knockdown experiments yielded equal results in *T.brucei* [34-37]. In *Leishmania* knockout of ODC, AdoMetDC, SpdSyn or arginase lead to growth arrest of the promastigote stage, and both the

arginase and ODC knockout lines are significantly attenuated in animal models of the disease [38-41].

S-adenosyl Methionine Decarboxylase (AdoMetDC)

Structural Insights

Mechanistically, AdoMetDC uses a covalently-bound pyruvate group as a cofactor, which is involved in stabilizing the carbanion intermediate formed during the decarboxylation of AdoMet. This prosthetic moiety is generated after AdoMetDC undergoes an auto catalytic cleavage reaction, to generate the alpha (α) and beta (β) subunits of the active enzyme [42, 43]. Following this processing event, the pyruvoyl group is displayed at the N-terminus of the α-subunit. The crystal structure of human AdoMetDC has been determined and demonstrates that the enzyme is an $\alpha_2\beta_2$ homodimer, with the active sites sitting in a cleft between β-sheets away from the dimer interface [44, 45] (**Fig 1.3**). Catalytic residues include Cys82, His243, and Ser229 [46]. In addition, detailed structural studies show that the human enzyme binds ligands in a high energy *syn* conformation, which is stabilized by specific interactions involving residues Phe223, Phe7 and Glu67. Besides *Homo sapiens*, crystal structures have been obtained for *Solanum tuberosum*, *Thermotoga maritima*, and *Aquifex aeolicus*, but not for any of the trypanosomatid enzymes [46].

Putrescine Effect

The diamine putrescine is known to regulate the activity of AdoMetDC by influencing the rates of autoprocessing and decarboxylation [45]. Interestingly, this effect seems to be species specific. The autoprocessing reaction is stimulated by putrescine in humans particularly. However, decarboxylation of AdoMet is enhanced by this amine not only in humans, but also in *Trypanosoma brucei*, *Trypanosoma cruzi*, *Caenorhabditis elegans* and *Neurospora crassa*. The hAdoMetDC putrescine-binding site is formed by a group of acidic residues (Asp174, Glu178, and Glu256) and located 16-20Å away from the active site [45, 47] (**Fig 1.3**). But, although they are far from each other, a group of hydrophilic residues connect both sites through a series of electrostatic interactions, rearranging conformation and placing the key catalytic residues in the correct orientation. Studies have demonstrated that binding of putrescine to the wild type dimeric protein is cooperative [47]. The putrescine-binding is not present in the structure of the monomeric plant enzyme, which is fully active without putrescine [48], but it is partially conserved in the trypanosomatid enzymes. Interestingly, even after rate stimulation by this diamine, the recombinant trypanosomatid enzymes have significantly lower catalytic efficiency than the mammalian and plant homologs [45, 49].

AdoMetDC Inhibitors

The effectiveness of DFMO, which is an ODC suicide inhibitor, for treating sleeping sickness validates the polyamine biosynthetic pathway as target for the development of new anti-trypanosomal drugs. Basically, most of the enzymes involved in the biosynthesis have proven to be necessary for parasite growth [29, 30]. Several very promising *in vivo* trials were undertaken

demonstrating that AdoMetDC inhibitors can cure *T. brucei* infections in mice, including a synthetic adenosine analog that is a mechanism-based inhibitor of AdoMetDC (MDL 73811), and various aryl and heteroaryl bis-(guanylhydrazones), which are potent reversible inhibitors of the enzyme[50-52]. The basis for the selective toxicity of these compounds seems to be derived from extensive differences in the function and regulation of both AdoMetDC and polyamines in *T. brucei.* Some of the most crucial differences include the requirement for spermidine to synthesize trypanothione [24], the regulation of AdoMetDC synthetase, which may lead to hypermethylation of macromolecules in trypanosomes but not mammalian cells [51-54], and the presence of a novel AdoMet transporter in *T. brucei* that is absent in mammalian cells [55, 56]. These studies serve to chemically validate AdoMetDC as a target; however most of these compounds displayed significant pharmacokinetic (PK) and /or tissue (CNS) distribution issues, and could not proceed to further trials. Thus, there is a clear need to identify new classes of *T. brucei* specific AdoMetDC inhibitors before this enzyme can be exploited as a tool for chemotherapeutic intervention against sleeping sickness.

Novel Mechanism for Activation of Trypanosomatid AdoMetDCs

Polyamine levels are tightly controlled in eukaryotes for normal cellular function However, how these cations are modulated in trypanosome parasites was not well understood. Recently, our lab demonstrated that trypanosomatid AdoMetDCs are activated by a unique mechanism [57]. These species encode two types of AdoMetDC genes: an ortholog to the functional enzyme, AdoMetDC, and a paralog that we term prozyme, which is not present outside of the trypanosomatids. Prozyme shares only ~30% amino acid sequence identity with

the AdoMetDC from the same trypanosomatid species. It appears to have arisen by gene duplication of the ancestral enzyme after the divergence of the trypanosomatids from other eukaryotes. In addition, this homolog is neither processed to generate the pyruvute cofactor, nor does it display any activity on its own. However, it was demonstrated that prozyme forms a high affinity heterodimer with *T. brucei* AdoMetDC, and upon binding stimulates AdoMetDC activity by $>10^3$-fold, when compared to the homodimeric enzyme [57] (**Fig 1.4**). Analysis in *T. brucei* blood form extracts demonstrated that the AdoMetDC/prozyme heterodimer is the functional enzyme in the parasite. Further experiments provided the first evidence that prozyme is a key component for the regulation of polyamine biosynthesis in *T. brucei*, as inhibition or knockdown of AdoMetDC leads to a up to 20-fold induction of prozyme protein levels [33] (**Fig 1.5**). Putrescine does not seem to have a strong effect on the activity of the *T. brucei* heterodimer, as opposed to the human enzyme [57]. However, this polyamine is absolutely necessary for the *T. cruzi* heterodimer to reach full activation [58].

Research Goals

The structural basis for the activation of trypanosomatid AdoMetDC by prozyme remains an open question, since no crystallographic information is available to this date. Understanding the mechanisms that regulate this process could represent an important advance in the task of identifying potent inhibitors of this enzyme and the development of new anti-trypanosomal drugs. Therefore, the goal of this research project was to elucidate specific amino acid residues or regions in *T.brucei* AdoMetDC essential for proper activation by prozyme, and to study how these are related in other trypanosomatid species.

Chapter 2 describes in detail the different approaches taken for optimizing *T.brucei* AdoMetDC protein expression in *E.coli*, as well as the purification procedure. In chapter 3, we employ several biochemical techniques, including site-directed mutagenesis, enzyme kinetics and sedimentation velocity, to evaluate the role that the N-terminal portion of AdoMetDC and specific amino acids may have in the activation by prozyme. Chapter 4 focuses on the characterization of the *Leishmania major* AdoMetDC/prozyme complex and evaluates the functionality of cross-species heterodimers. And, finally, chapter 5 discusses the relevance of all findings and takes on perspectives and future directions.

Figure 1.1. Human African trypanosomiasis (HAT): evolution of reported cases from 1998 to 2009 (Taken from [4])

Graph presents the number of cases per year for both forms of the disease, caused by either *T. brucei rhodesiense* (red) or *T. brucei gambiense* (blue). [4]

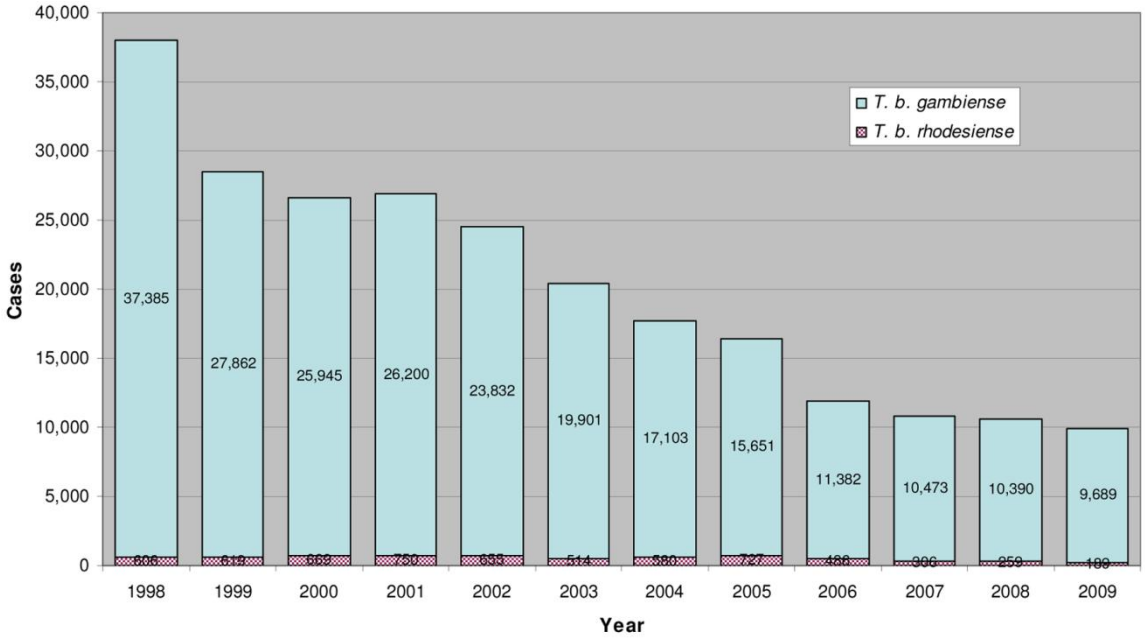
40,000
35,000
30,000
25,000
20,000
15,000
10,000
5,000
0
Cases
T. b. gambiense
T. b. rhodesiense
37,385
27,862
25,945
26,200
23,832
19,901
17,103
15,651
11,382
10,473
10,390
9,689
1998
1999
2000
2001
2002
2003
2004
2005
2006
2007
2008
2009
Year

Table 1.1. Current drugs available for the treatment of HAT (Adapted from [3])

	Stage	Route of application	Dosing	Main adverse drug reactions
Trypanosoma brucei gambiense				
Pentamidine	First	Intramuscular	4mg/kg at 24h intervals for 7 days	Hypoglycemia, injection site pain, diarrhea, nausea, vomiting
Eflornithine	Second	Intravenous	400mg/kg at 6h intervals for 14 days	Diarrhea, nausea, vomiting, convulsions, anemia, leucopenia, and thrombocytopenia
Melarsoprol	Second	Intravenous	2.2mg/kg at 24h intervals for 10 days	Encephalopathic syndromes, skin reactions, peripheral motoric or sensorial neuropathies, thrombophlebitis
NECT combination therapy	Second	Intravenous and oral	Eflornithine: 400mg/kg at 12h intervals for 7 days Nifurtimox: 15mg/kg at 8h intervals for 10 days	Diarrhea, nausea, vomiting, anorexia, tremors
Trypanosoma brucei rhodesiense				
Suramin	First	Intravenous	Test dose of 4-5mg/kg at day 1, then 5 injections of 20mg/kg every 7 days	Hypersensitivity reactions, albuminuria, cylinduria, haematuria, peripheral neuropathy
Melarsoprol	Second	Intravenous	Three series of 3.6, 3.6, 3.6mg/kg, spaced by intervals of 7 days	Encephalopathic syndromes, skin reactions, peripheral motoric or sensorial neuropathies, thrombophlebitis

Figure 1.2. Polyamine biosynthetic pathway in *Trypanosoma brucei*

Enzymes involved are labeled in purple, and the respective inhibitors are depicted by the red arrows. ODC, ornithine decarboxylase; AdoMetDC, S-adenosylmethionine decarboxylase; SpdSyn, spermidine synthetase; γGCS, γ-glutamylcysteine synthetase; GS, glutathione synthetase; TS, trypanothione synthetase; TR, trypanothione reductase; DFMO, difluoromethyl-ornithine; BSO, buthionine sulfoximine.

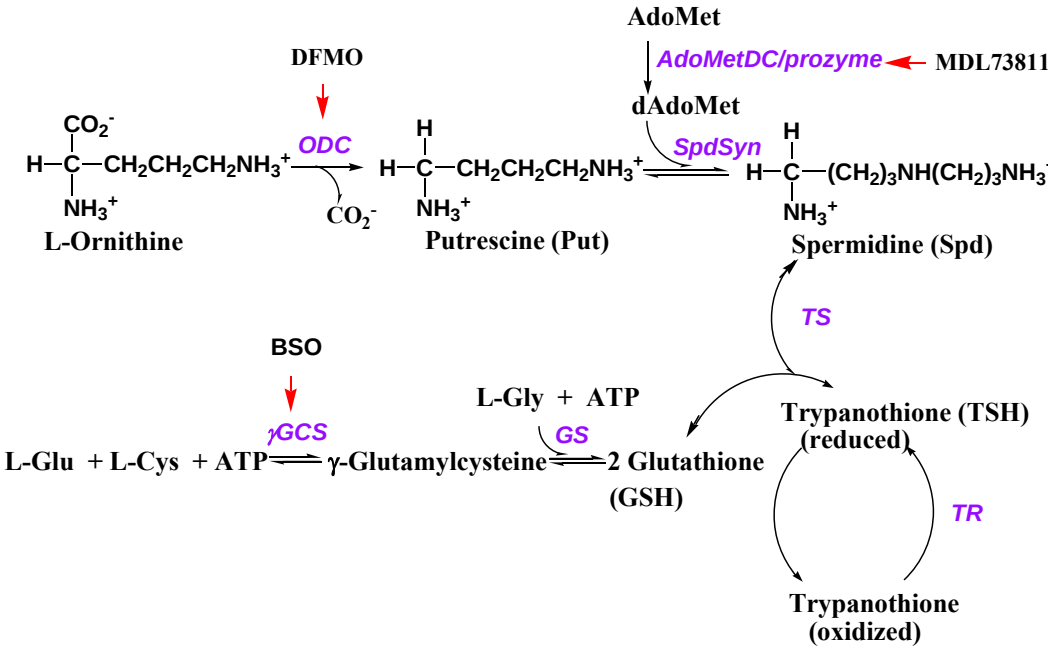
AdoMet
DFMO
AdoMetDC/prozyme
MDL73811
dAdoMet
ODC
SpdSyn
L-Ornithine
Putrescine (Put)
Spermidine (Spd)
TS
BSO
L-Gly + ATP
γGCS
GS
L-Glu + L-Cys + ATP
γ-Glutamylcysteine
2 Glutathione (GSH)
Trypanothione (TSH) (reduced)
TR
Trypanothione (oxidized)

Figure 1.3. Dimeric structure of the processed human AdoMetDC enzyme (Taken from [46])

Image is viewed down the two-fold axis. The α-chains from each monomer are colored red and blue, while the β-chain chains are presented in yellow and gray. Putrescine and the MeAdoMet substrate are shown in ball and stick. Protein data bank access code: 1I7B [46]

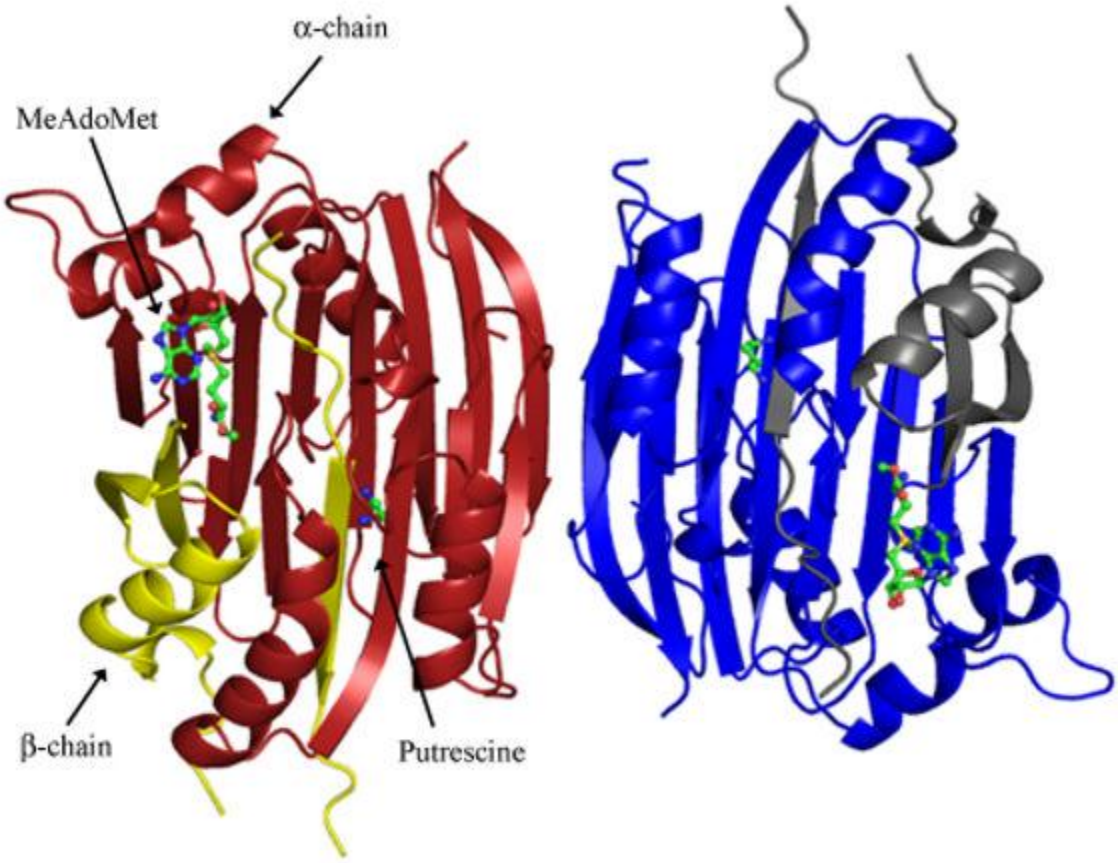
α-chain
MeAdoMet
β-chain
Putrescine

Figure 1.4. Steady-state kinetic analysis of *T.brucei* AdoMetDC alone and in complex with the catalytically dead homolog, prozyme (Taken from [57])

(A) Specific activity of homodimeric AdoMetDC as a function of substrate concentration (0-160μM) in the presence and absence of 5mM putrescine. Concentration of enzyme used was 2μM. (B) Specific activity of AdoMetDC/prozyme co-purified complex as a function of substrate concentration (0-1mM) in the presence and absence of 5mM putrescine. Concentration of enzyme used was 50-100nM. [57]

A.

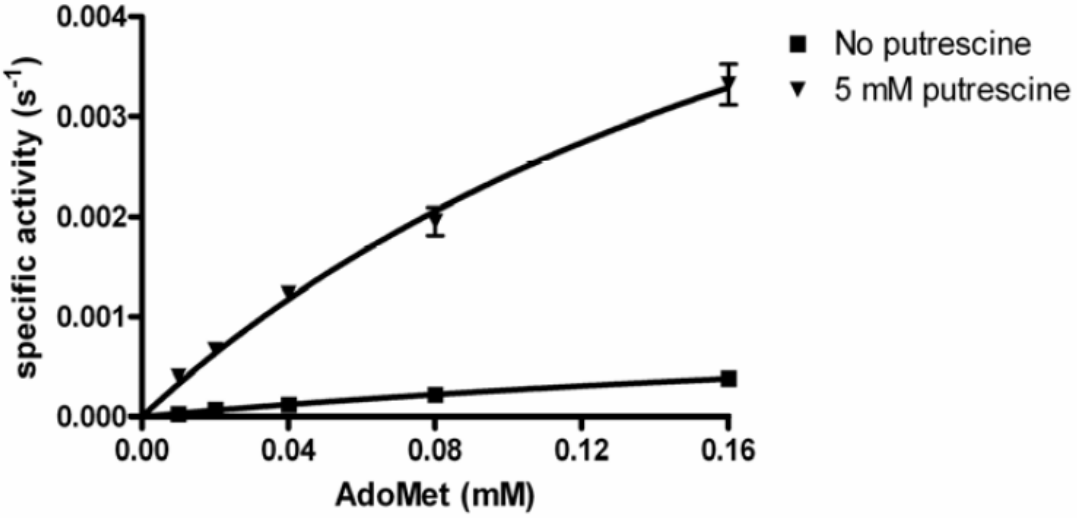
0.004
0.003
0.002
0.001
0.000
specific activity (s-1)
0.00
0.04
0.08
0.12
0.16
AdoMet (mM)
No putrescine
5 mM putrescine

B.

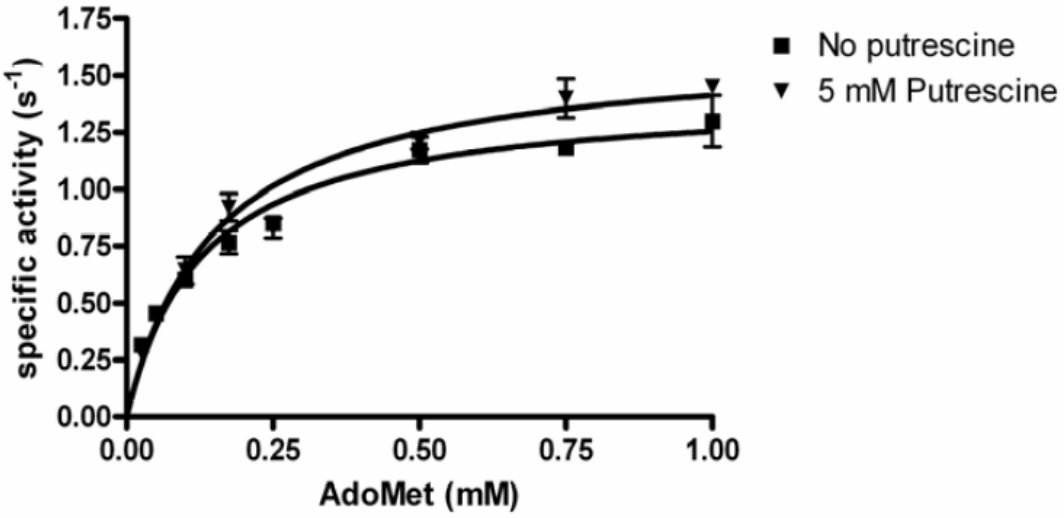
1.75
1.50
1.25
1.00
0.75
0.50
0.25
0.00
specific activity (s-1)
0.00
0.25
0.50
0.75
1.00
AdoMet (mM)
No putrescine
5 mM Putrescine

Figure 1.5. AdoMetDC RNAi knockdown in blood form trypanosome parasites (Taken from [33])

(A) Log cell number as a function of days in culture. Purple triangles: uninduced control cells (AdoMetDC RNAi line without Tet); orange circles: induced cells (AdoMetDC RNAi line plus 1 mg/ml Tet); green squares: induced cells plus spermidine (AdoMet RNAi line plus 1 mg/ml Tet and 0.1 mM Spd). (B) Western blot analysis of polyamine/trypanothione biosynthetic enzymes after AdoMetDC RNAi knockdown induction with Tet. Experiment was performed in the absence (left) and presence (right) of spermidine (0.1 mM). Total protein amount was 20 µg. The control lane (day 0) on the right panel was cultured in the presence of spermidine for six days prior to the addition of Tet. Prozyme is denoted by (*). [33]

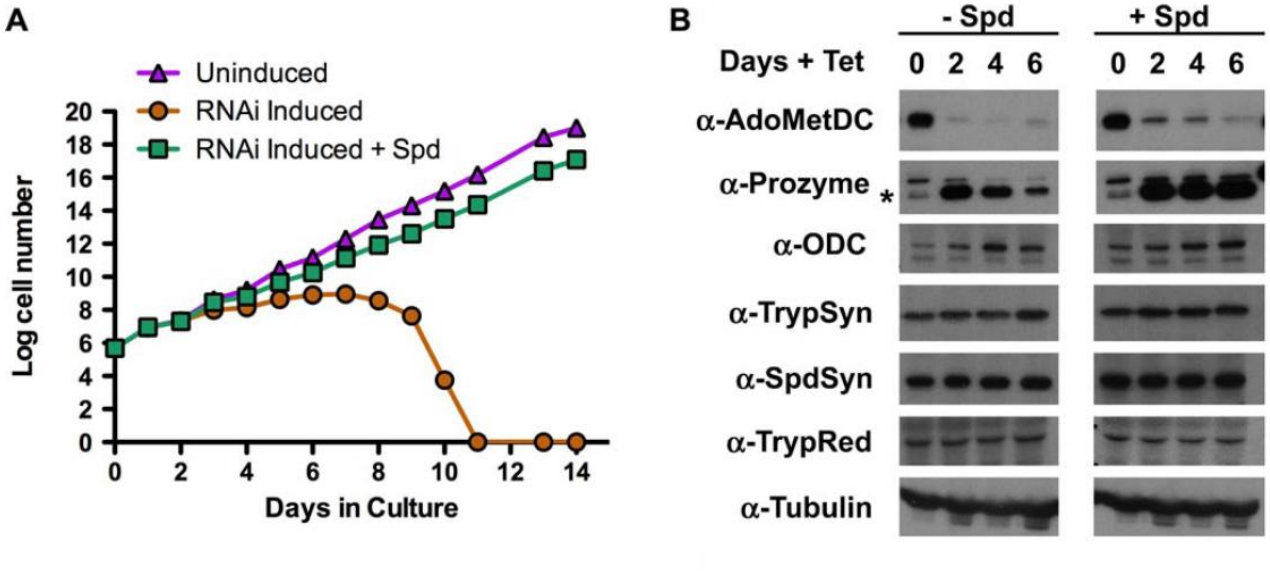
A
Uninduced
RNAi Induced
RNAi Induced + Spd
Log cell number
Days in Culture
B
- Spd
+ Spd
Days + Tet
0 2 4 6
0 2 4 6
α-AdoMetDC
α-Prozyme *
α-ODC
α-TrypSyn
α-SpdSyn
α-TrypRed
α-Tubulin

CHAPTER 2

T.BRUCEI ADOMETDC PROTEIN EXPRESSION AND PURIFICATION

Introduction

Biological systems are formed by a complex network of functional and physical interactions, the core of which is represented by proteins, lipids, nucleic acids and other essential molecules. To understand how these networks work, in order to find solutions to any life-threatening issues, usually involves careful investigation and characterization of a particular protein activity. Thus, they have to first be isolated from a specific resource. There is a large number of cell-based expression systems currently used by researchers for the production of proteins. These include bacteria [59], yeast [60], baculovirus/insect [61] and eukaryotic [62] systems. They all have unique features and advantages that would make them more suitable for a particular experimental approach. However, the Gram-negative bacterium *Echerichia coli* remains one of the most widely used mature and cost-effective model organisms. Many details are known about the biology of *E. coli*, including careful characterization of its genetics, which makes its use in a variety of biotechnology applications more suitable [59, 63]. Some other important characteristics this organism possesses are the ability to grow very fast, and to reach high density levels on inexpensive substrates. In addition, a large number of well-characterized expression vectors and mutant host strains are available. Obviously, there is no guarantee that a recombinant gene product will always accumulate in *E.* coli at high levels in a full-length and biologically active form, since potential issues can occur along the way. For example, there is a tendency for overexpressed proteins to accumulate in bacteria in an insoluble form (inclusion bodies), which results in a denatured and inactive product. Some meticulous procedures must be followed in order to avoid this problem, and although there are other disadvantages inherent to this organism as a model system, a considerable amount of effort is always been directed towards improving its performance and versatility.

Recombinant AdoMetDCs from several species have been successfully expressed in *E. coli* for a variety of investigative purposes [57, 64, 65]. Initially, my project was focused on the advance of *T. brucei* AdoMetDC as a target for the treatment of Human African Trypanosomiasis (HAT), through the identification of novel and more potent inhibitors that can block this essential enzyme in the parasites. High-throughput screening (HTS) of a small molecule compound library was the method of choice to achieve this goal, since it provides one of the most robust ways to identify active compounds that can modulate a particular target. In order to utilize this strategy, an enzyme assay that would be amenable for high-throughput robotic techniques was needed. To this end, the standard spectrophotometric ODC activity assay [66] commonly used in the lab had to be adapted for AdoMetDC. In this method, the decarboxylase activity is measured by coupling the production of 1 mol of CO_2 to the oxidation of 1 mol of NADH, which is monitored at 340 nm. The coupling enzymes and substrates are commercially available as a CO_2 detection kit (Infinity). This kit is meant for the detection of CO_2 in clinical samples, but it was adapted for the measurement of enzymatic decarboxylation. In order for the assay to be functional, the rate of NADH oxidation must depend on the concentration of AdoMetDC added to the assay. While the standard kit components worked well for the assay of ODC, they did not produce a functional AdoMetDC assay. It was found, however, that addition of extra phosphoenolpyruvate (PEP) to the system allowed for proper assaying of AdoMetDC, as it was illustrated by the proportional relationship between the rate of NADH oxidation and the AdoMetDC concentration (**Fig. 2.1**). Using this assay, steady-state kinetic parameters were obtained, which resembled those previously calculated using the standard $^{14}CO_2$-trapping method.

Pilot experiments to fully adapt the assay to the robots and the 384-well plate format were performed at the St. Jude children's research hospital screening facility, for the identification of inhibitors against the AdoMetDC/prozyme heterodimer. Subsequently, a pre-screen on a subset of the library (~ 6,000 compounds) was conducted to determine the hit frequency. Statistical analysis of the data revealed a Z factor of 0.3, which is considered not ideal but workable (**Fig 2.2**). A Z factor between 0.5 and 1.0 corresponds to a highly significant and functional assay. However, several issues were encountered as the screen was performed. These include: extremely high substrate concentration needed in order to get a decent signal (5mM), limited amounts of enzyme available, and temperature variations (screen performed at room temperature, as opposed to 37°C). Thus, some optimization was needed before we can utilize this method to conduct the full scale HTS, which required large amounts of protein. Unfortunately, AdoMetDC's expression in *E.coli* was extremely low and, after a couple purification steps, only about 2-4mgs of pure/active protein were recovered from 6L of culture.

In this chapter, specific information will be discussed regarding the approaches followed in order to obtain good *T. brucei* AdoMetDC expression levels in *E. coli*. However, in order to do this, we must first understand a bit more about this enzyme. AdoMetDC depends on a covalently bound pyruvoyl cofactor for the decarboxylation of AdoMet. It is expressed as an inactive proenzyme, which eventually undergoes an autocatalytic cleavage reaction to generate the active enzyme. This leads to the formation of two chains (α and β), with the pyruvate group formed at the N-terminus of the alpha chain. Human AdoMetDC is a homodimer ($\alpha_2\beta_2$) and putrescine, an essential polyamine, is required for both the processing reaction of this enzyme and the decarboxylation of AdoMet. Recently, our lab demonstrated that the trypanosomatid AdoMetDC is regulated by a unique mechanism, heterodimer formation with a catalytically dead

AdoMetDC homolog. This protein, designated prozyme, forms a high-affinity complex with AdoMetDC and increases its activity by $>10^3$-fold. Further, it was confirmed that the heterodimer is the functional enzyme *in vivo*.

We will discuss the general protocol for expression and purification of *T. brucei* AdoMetDC, followed by the strategies used in attempt to improve expression in *E. coli*. These include: temperature variations, putrescine addition to the media, several *E. coli* strains tested, codon optimization, tag removal, and the use of different expression vectors. Our findings show that fusion of AdoMetDC to a His_6-SUMO protein allows for the production of high levels of soluble material.

Experimental Procedures

T. brucei AdoMetDC and Prozyme Constructs

The initial pET15b-AdoMetDC expression construct used was provided by Erin Willert [57], which generated an N-terminal His_6 fusion. The codon optimized AdoMetDC gene (AdoMetDC-G), from GenScript, was provided as pUC57-AdoMetDC plasmid DNA. AdoMetDC-G was amplified by PCR from this plasmid, using specific primers, and ligated into the pET28a (Novagen, San Diego, CA), pET28b (Novagen, San Diego, CA) and pE-SUMO (LifeSensors, Malvern, PA) vectors. Primer sequences and respective restriction sites are presented on **Table 2.1**. The main difference between the pET28a and pET28b expression vectors, besides the frame shift, is that the second one was engineered, by Xiaoyi Deng, to

contain a TEV protease cleavage site to remove the N-terminal His_6 tag generated after protein expression. The pE-SUMO vector generates an N-terminal His_6 –SUMO fusion protein.

AdoMetDC Expression and Purification (General Protocol)

E.coli BL21/DE3 cells were transformed with the construct of interest and grown in LB broth (usually 6L for AdoMetDC) at 37°C until OD_{600} reached between 0.6 - 0.8. Protein expression was induced by the addition of 0.2mM IPTG and cells grown overnight at 20°C. Subsequently, cells were harvested by centrifugation and resuspended in 90mL of lysis buffer (50mM Hepes, 100mM NaCl, 10mM Imidazole, 5mM β-mercaptoethanol). Protease inhibitors were added directly to the resuspension (Cocktail 1 (1:1000)- 1mg/mL Leupeptin, 2mg/mL Antipain and 10mg/mL Benzamidine; Cocktail 2 (1:1000)- 1mg/mL Pepstain, 1mg/mL Chymostatin; and 0.2M Phenylmethyl-sylfonyl fluoride (PMSF) in a 1:500 ratio) (Sigma, St.Louis, MO). Bacterial cells were lysed using an EmulsiFlex-C5 homogenizer (3 passages at 15,000- psi), followed by centrifugation (Beckman Ti-45 rotor) at 15,000rpm for 30min. The soluble fraction was then subjected to Ni^{2+} -agarose (Qiagen, Valencia, CA) column chromatography, as previously described [57, 66]. Purification details include: Column- HiTrap Chelating HP 5/5; Buffer A- 50mM Hepes pH 8, 100mM NaCl, 1mM β-mercaptoethanol, 10mM Imidazole; Buffer B- 50mM Hepes pH 8, 100mM NaCl, 1mM β-mercaptoethanol, 800mM Imidazole; Flow-rate- 2mL/min, Wash- 15 to 20 column volume (CV) at 4 % Buffer B (~40mM Imidazole); Elution- 10 CV at 4-40 % Buffer B (40-325mM Imidazole) linear gradient. Subsequently, a 16% SDS-PAGE analysis was performed and the protein containing fractions were pooled together, concentrated and diluted back in buffer A, to remove excess imidazole.

Extinction coefficient for the enzyme (AdoMetDC: 65.3 $mM^{-1}cm^{-1}$, determined by ExPASy Prot Param) was used to obtain protein concentration after measuring absorbance at 280nm. These calculations were performed by using the Beer's law equation, $A=\varepsilon lc$; where A is absorbance, ε is extinction coefficient, l is the path lengh and c is concentration.

If purity was less than 90% after the first affinity purification step, then anion-exchange chromatography was performed to provide additional purification, as previously described [57, 66]. In this case, purification details include: Column- Mono Q 5/50 GL; Buffer A- 50mM Tris pH 8, 50mM NaCl, 1mM DTT; Buffer B- 50mM Tris pH 8, 1000mM NaCl, 1mM DTT; concentrated sample (<1 mL) is diluted to 10 mL with Buffer A and cleared through a 22 nm filter before injecting in the instrument; Flow-rate- 1ml/min; Elution- 0-20% Buffer B (50-200mM NaCl) linear gradient. Just like after the first purification step, a 16% SDS-PAGE analysis was performed and the protein containing fractions are pooled together, concentrated and stored at -80 °C.

TEV Protease Expression, Gluthatione Beads Conjugation and Cleavage Reaction

Proteins generated from the pET28b-AdoMetDC construct had a TEV protease cleavage site engineered, allowing the N-terminal His_6 fusion tag to be removed after purification. Richard Baxter kindly provided us the pGEX-4T-1-TEV construct (generates a GST tag), which was fully sequenced and transformed into *E.coli* BL21cells. Expression of the GST-TEV fusion protein was performed in 1L culture of LB and incubated at 37°C until an OD_{600} between 0.4-0.6. Induction was performed by adding IPTG to a final concentration of 200µM. Cells were harvested (4 hours later) by centrifugation, resuspended in lysis buffer (50mM Hepes, 100mM

NaCl, 10mM Imidazole, 5mM Bme, 1mL/20g cells protease inhibitors cocktail) and lysed using the cell disruptor (EmulsiFlex-C5 homogenizer; 3 passages at 15,000- psi). High speed centrigugation (15,000 rpm) for 30 min followed and both supernatant and pellet fractions were evaluated through 16%SDS-PAGE analysis.

Gluthatione-agarose gel- Lyophilized powder was swelled in water at 200ml/g for 1 hour at 4°C. Then, beads were washed thoroughly with 10 volumes of water. Supernatant (containing the expressed TEV protease) was incubated with the beads for 1 hour at room temperature. Conjugated beads were washed three times with Arnie buffer (1M Hepes, 5M NaCl, 1M DTT, 0.5M EDTA, 10% Triton-X and protease inhibitors). Then, beads were resuspended in 50% glycerol/50% lysis buffer, aliquoted (1mL), freezed in liquid N_2 and stored at -80°C. 2mgs of protein were incubated (gentle agitation) with 20µL of GST-TEV beads for 16 and 24 hours at room temperature. Then, samples were centrifuged for 10 minutes at 4°C to remove beads. Ni^{2+} purification was performed again, following the protocol presented above, and flow-through, wash and elution fractions were collected and evaluated through 16% SDS-PAGE analysis.

ULP-1 Protease Expression, Purification and Cleavage Reaction

Proteins generated from the pESUMO-AdoMetDC construct contained an N-terminal His_6-SUMO tag, which could also be easily removed. The SUMO protease 1, known as ULP1, recognizes the tertiary structure of SUMO in the fusion protein and cleaves with high specificity. The pET15b-ULP1 plasmid was provided by Kim Orth. The protocol followed to express this N-terminal His-tagged protease was the same one used for obtaining GST-TEV, explained above. In this particular case, overnight IPTG induction was performed at 30°C. Lysis buffer contained

50 mM Tris-HCl (pH=7.5), 350 mM NaCl, 1 mM BME, 10 mM imidazole, 0.2% IGEPAL and 20% glycerol. Ni^{2+} -affinity purification Buffer A contained 50 mM Tris-HCl (pH=7.5), 350 mM NaCl, 1mM BME, 10 mM imidazole and 20% glycerol, while Buffer B had the same components, with the exception of imidazole at 800mM concentration. Purified His_6-SUMO AdoMetDC was incubated with approximately 300 µg of ULP1 for every 20-35mgs of protein, during 2 hours at 4°C with gentle agitation. After this cleavage reaction, a second Ni^{2+} -agarose purification step was performed in which the now tagless-enzyme was collected in the flow-through fractions. Successful cleavage was evaluated through 16% SDS-PAGE analysis.

Western Blot

Several small (25mL) AdoMetDC cultures were set up to test different conditions for protein expression optimization. About 5mL from these bacterial cultures were harvested at 4,000 rpm for 20 minutes. Media was then removed and the pellet was resuspended in 500µL of SoluLyse reagent (Genlantis, Inc), followed by shaking at room temperature for 10 minutes. The soluble and insoluble fractions were separated by centrifugation at 14,000 rpm for 5 minutes. Supernatant was collected and total protein concentration was measured using the Bradford assay [67]. Pellet was resuspended in 1mL of SoluLyse reagent and total protein concentration was measured similarly. From these lysates, 40µg of total protein per lane were separated by 16% SDS/PAGE and transferred to a PVDF membrane (Hybond-P; Amersham). In occasions, 10ng of pure recombinant *T. brucei* AdoMetDC per lane were also added as a control. Membranes were blocked with 5% non-fat dry milk in Tris-buffered saline (TBS: 20 mM Tris-HCl, 137 mM

NaCl, pH 7.6), overnight at 4ºC with gentle agitation. Then, blots were incubated with rabbit polyclonal antibody to *T. brucei* AdoMetDC at 1:2,500 for 1 hour at room temperature with gentle agitation. After three washes with TBS-T (0.1% Tween-20 added), blots were incubated with Horseradish peroxidase-linked donkey anti-rabbit (Amersham Biosciences) at 1:10,000 for 1 hour at room temperature. Blots were washed again with TBS-T and the antigen was visualized by using the ECL Western Blotting Analysis system (Amersham).

Results

Approaches to Enhance AdoMetDC Expression in *E. coli*

Temperature Variations

As mentioned earlier, one of the most important pitfalls of using *E. coli* is the fact that it could sometimes be challenging to obtain soluble, folded and active recombinant protein, since the whole bacterial expression occurs really fast. Usually, lowering the expression temperatures improves solubility because the process slows down, leading to reduced rates of transcription, translation, and cell division, while also leading to reduced protein aggregation [68, 69]. Initial western blots on several AdoMetDC cultures showed that, although protein was been recovered in the soluble fraction, much of it was found in the pellet (**Fig 2.3**). Thus, we started by evaluating a wide range of expression temperatures and lengthening time of induction in order to overcome this. Conditions included: 37º C for 2-4 hrs, 30º C for 4-6 hrs, 20º C for 16 hrs (O/N)

and 16º C for 18 hrs (O/N). Unfortunately, none of these seem to have a strong effect on protein yield and solubility (**Table 2.2**).

E. coli Cell Lines

Two different cell lines were also used in an attempt to enhance AdoMetDC's expression and alleviate solubility issues. Some eukaryotic proteins contain codons that are rarely used in *E. coli.* The Rosetta strain allows for broader translation by supplying tRNAs for seven different rare codons, thus resulting in higher probabilities for better protein expression [69]. On the other hand, Arctic Express competent cells have been engineered for improved protein processing at very low temperatures [70]. As thoroughly known, some chaperones are essential to help macromolecular structures fold or prevent them from aggregating. *Oleispira antarctica* Cpn10 and Cpn60 chaperonins are cold-adapted and provide high protein refolding activities at temperatures of 4–12°C. The Artic Express cells co-express these chaperonins, which have 74% and 54% amino acid identity with the *E. coli* GroEL and GroES chaperonins, respectively. It has been demonstrated that, when expressed in Artic cells, these chaperonins help improve protein processing at lower temperatures, which can potentially lead to a more active and soluble recombinant protein [70]. However, AdoMetDC protein yields obtained after using each of these strains were not significantly enhanced (**Table 2.2**).

Putrescine Addition to the Media

Putrescine is known to stimulate both the auto-processing reaction and the catalytic activity of human AdoMetDC [45]. The impact of this polyamine on the *T. brucei* enzyme

varies, since it influences the activity of the homodimeric AdoMetDC, but not the AdoMetDC/prozyme complex [57]. Species differences are however observed even within the trypanosomatids as the *T. cruzi* heterodimer is stimulated 5-fold by the addition of putrescine, but there is no effect on processing [57, 58]. Initial western blot analyses revealed, in addition to some minor solubility issues, that significant amounts of enzyme were still un-processed (inactive proenzyme) and found in both pellet and supernatant fractions (**Fig 2.3**). Svensson, et al. showed that addition of putrescine to the growth medium appeared to stimulate the conversion of AdoMetDC proenzyme into its subunits, indicating a physiological role for this polyamine in the regulation of mammalian AdoMetDC expression [71]. Since, the putrescine binding site is not very well conserved between eukaryotic AdoMetDCs and because there is so much variability on the effect that it can exert over different enzymes, we decided to add this polyamine to the growth medium as well, and evaluate the effect on solubility and processing of *T. brucei* AdoMetDC. There was a possibility that the presence of this polyamine could lead us to obtain better yields of more soluble and fully active enzyme. However, that was not the case. When putrescine was added to the expression medium the amount of un-processed enzyme did not seem to change much, and in fact, more AdoMetDC was observed in the insoluble fraction. (**Fig 2.3**).

Codon Optimization for Expression in E. coli

Codon optimization is one of the most recent and widely used techniques for improving protein translation efficiency and expression in a particular system. Each organism has a specific codon usage frequency. For example, plants generally prefer G and C rich codons [72], while a

huge variability is found in mammals [73]. On the other hand, correlation and regression analyses by Gutierrez, et al. showed that increasing expression levels in some *E. coli* genes are accompanied by higher frequencies of base G at first, base A at second and base C at third codon positions [74]. The nucleotide sequences used less in a particular organism are denoted as "rare codons", and usually correlate with reduced intracellular levels of aminoacyl-tRNAs [69]. If no tRNA is available, the synthesis process will potentially fail or slow down, yielding very low levels of protein. Earlier we mentioned that Rosetta cells were used to try to improve AdoMetDC's expression because they are supplemented with tRNAs for seven different rare codons in *E. coli*. Thus, we tried to approach the same problem with a newer technology that might result more effective. The *T. brucei* AdoMetDC nucleotide sequence was submitted to GenScript for optimization and synthesis. Basically, codons in the trypanosomatid gene that could be considered "rare" for the *E. coli* host were replaced with higher frequency ones, without changing the actual amino acid composition. Gene synthesis has the added benefit that most gene optimization algorithms optimize not only rare codons, but also mRNA secondary structure, which has also been shown to affect translation efficiency [69, 75]. The newly optimized AdoMetDC gene was subcloned into the pET28a expression vector and transformed into *E. coli* BL21 cells. Results from western blots show some improvement in protein expression levels when comparing wild-type versus optimized sequences (**Fig 2.4**). Unfortunately, whenever the large scale expression/purification was performed only 6mgs of protein were collected after Ni^{2+} -agarose column chromatography. However, we continued using this optimized gene for further experiments.

Expression Vectors and tTag Removal

Expression vectors must contain important signals for directing the transcription and translation of a target gene [69]. These include promoters, regulatory sequences, transcriptional terminators, origins of replication, and a translation initiation sequence, among others. In addition, they have an antibiotic-resistance gene, which works as a selectable marker that helps in the identification of host cells that successfully had the foreign DNA internalized. Fusion tags are another very essential feature that *E. coli* expression vectors possess. These are sequences transcribed in-frame with the construct of interest and, after the translation process, they result in short peptides fused either at the C- or N-terminal of the target protein [76]. Fusion tags are added to the protein for purification, detection or localization purposes. However, some of them are also known to improve expression and solubility.

The initial construct we used to produce AdoMetDC was provided by Erin Willert, and contained the gene subcloned into the pET15b expression vector through the NdeI and BamH1 restriction sites. This generated an N-terminal His_6-tag fusion protein. However, when we started working with the optimized AdoMetDC sequence from GenScript (AdoMetDC-G), which showed a mild improvement in expression, the gene was first subcloned into the pET28a vector, which we had available at that time. This expression vector not only carries an N-terminal His_6-tag /thrombin/T7-tag configuration, but also has the ability to generate a C-terminal His_6-tag sequence. In this case, we decided to generate the tag at the N-terminus as well, since it seemed to work fine before. The location of the fusion tag is very important because it can have strong effects on protein solubility and expression, although the His_6-tag is not really known for it [69, 76]. In fact, because this tag is so small (<1kD), researchers frequently use it in conjunction

with solubility-enhancing fusion tags, in order to dually improve solubility and obtain a pure protein. However, a very important caveat of fusing tags to recombinant proteins is that they can potentially interfere with activity. In addition, since our studies were going to be focused on the N-terminal region of AdoMetDC, where the His_6-tag was located, we thought it was crucial to remove the tag after purification and evaluate catalytic efficiency *in vitro*. To do this, AdoMetDC-G had to first be subcloned into the pET28b vector, which was engineered by Xiaoyi Deng in our lab to contain a TEV-protease cleavage site. This cysteine protease, found in the Tobacco Etch Virus (TEV), recognizes the Glu-Asn-Leu-Tyr-Phe-Gln-(Gly/Ser) (ENLYFQ(G/S)) sequence and cleaves with high specificity between the Gln and Gly/Ser residues [77]. Its most common use is to remove affinity tags from recombinant proteins after purification. The His_6-tag at the N-terminus of AdoMetDC did not seem to influence activity, since catalytic efficiency (k_{cat}/K_m) numbers obtained after tag removal were similar to those previously determined [57].

As stated before, the main reasons for cloning AdoMetDC into the pET15b, pET28a and pET28b vectors were not really to improve expression levels and/or solubility. Thus, thinking about alternative possibilities to enhance these features we discovered the SUMOpro gene fusion technology (LifeSensor, Inc.). SUMO stands for small ubiquitin-like modifier, which when covalently attached (SUMOylation) to proteins in cells can regulate various processes such as nuclear-cytoplasmic transport, apoptosis, protein activation and stability, stress response and cell cycle progression [69, 76, 78-81]. In eukaryotic systems, SUMOylation is a common modification and the protein is conserved from yeast to humans. It has been demonstrated that yeast SUMO (Smt3), whenever fused with a protein of interest, can greatly enhance expression and promote solubility, which might be explained by the detergent-like effect it exerts on less

soluble proteins [78-81]. Cloning into the pESUMO vector generates an N-terminal His_6-SUMO tag that facilitates purification. Importantly, ULP1 (SUMO Protease 1) is a very efficient protease that recognizes the tertiary structure of the SUMO moiety, instead of a short linear sequence, and cleaves immediately after the C-terminal residue of the SUMO, generating a partner protein with a native N-terminus and no extra residues. Cloning AdoMetDC-G into the pESUMO expression vector produced excellent results. From 6L of culture, which would normally generate about 5-9mgs of protein after the first purification step, we were able to recover about 30mgs. After subsequent ULP1 cleavage reaction and second Ni^{2+} -agarose purification step, AdoMetDC yield was about 12-15mgs of 80-85% pure and active protein. **Table 2.2** summarizes AdoMetDC protein yields obtained from the different approaches taken.

Conclusion

Generation of large quantities of recombinant protein is often required for a variety of investigative purposes. This brings great attention to both the practical and theoretical aspects of protein expression/purification, and the difficulties researchers encounter during the whole process. Common issues that relate to low levels of soluble and biologically active material involve the host system, expression vector and/or growth conditions. Sometimes careful troubleshooting is necessary when attempting to express a particular protein and the use of small-scale cultures is advantageous for determining the right conditions that can be translated into a large-scale system. Here, we presented detailed information on the strategies followed, using this small-scale approach, to optimize *T. brucei* AdoMetDC protein expression in *E. coli*. Extensive

time and effort were devoted to generate this optimal protocol, since huge amounts of active recombinant protein were needed to perform a high-throughput screening (HTS) of a small molecule compound library, in order to identify potent inhibitors of the parasite enzyme. The main goal is to advance AdoMetDC as a target for the treatment of Human African trypanosomiasis (HAT), which is endemic in some regions of Sub-Saharan Africa and represents a potential public health and economic burden.

Our results demonstrate that AdoMetDC can be expressed at high levels in a BL21 (DE3) bacterial system, only when fused to a SUMO protein at the N-terminus, which resulted in about six times (12-15 mgs) more purified material than what was initially obtained (2-4 mgs). Neither induction temperature and time variations, nor codon optimization and the addition of known stimulators to the medium were able to increase protein yield. Fusion tag technologies have become one of the most advantageous and practical methods for the production of recombinant proteins over the past few decades. Not only has the use of SUMO as fusion partner been demonstrated to increase protein solubility and prevent proteolytic degradation, but the SUMO system also allows for the efficient removal of the tag, leaving the recombinant protein of interest with its native N-terminus [78-81]. This is accomplished by the availability of naturally occurring SUMO proteases, like ULP 1, which specifically recognizes both the C-terminal sequence and tertiary structure of SUMO. Removing expression tags is very important because they can obstruct structure and function of the target protein. In fact, whenever a specific protein is to be used for therapeutic purposes, it is requisite that the final product contains only the native amino acid sequence.

In summary, the optimal AdoMetDC protocol includes cloning the gene into an expression vector that generates a solubility-enhancing fusion tag (His_6-SUMO), using *E. coli* as

a bacterial system, inducing protein expression overnight at 20ºC, cleaving the fusion tag with a highly specific protease, and utilizing an effective affinity purification method to obtain clean material. This procedure works equally effective whenever we want to generate the heterodimeric *T. brucei* AdoMetDC/prozyme enzyme. In that particular case, while AdoMetDC is still His_6-SUMO tagged, prozyme will be either tagless or Flag-tagged (for western blot purposes). Usually, 4L of AdoMetDC and 2L of prozyme (which expresses in great quantities) cultures are generated. Lysates are then mixed and co-purified as described in the experimental procedures section.

While time-consuming, generating high yields of soluble and active AdoMetDC was essential to successfully carry out the initial part of the HTS project. The discovery of prozyme and its ability to stimulate AdoMetDC activity upon binding is a key finding that will aid in the identification of potent inhibitors of this enzyme and, thus, in the generation of lead compounds that can exploit this target. Blocking the complex formation or stabilizing the inactive conformation might be crucial ways for inhibition. Oleg Volkov in our laboratory took over this project and is now working in collaboration with Genzyme to use a new technology, called RapidFire (Biocius Lifesciences, Inc.), which enables label-free screening of many targets using mass spectrometry. One of the most important benefits of this technique is that decreases considerably the time required for HTS assay development and compounds identification, and the data is obtained in a format easy to interpret and analyze.

The availability of new commercial tools for successful recombinant protein expression, combined with advanced protein purification techniques, has made protein production a less painful task to achieve. Importantly, these tools facilitate scientific research focused on the study

of thousands of novel proteins, from a large variety of organisms, which could represent potential targets for therapeutic drug discovery.

Figure 2.1. Development of a spectrophotometric assay for the *T.brucei* AdoMetDC/prozyme heterodimer

AdoMetDC/prozyme complex (0.3 – 2.4 μM) was mixed with Infinity^{TM} CO_2 detection reagent, 2 mM S-adenosylmethionine and 2.4 mM PEP. Reaction rates were monitored at 340 nm for 10 min.

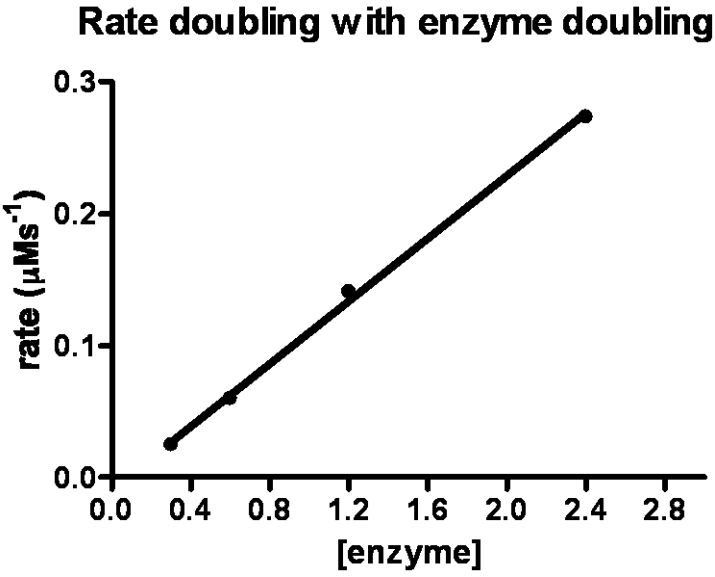
Rate doubling with enzyme doubling
rate (μMs-1)
0.3
0.2
0.1
0.0
0.0 0.4 0.8 1.2 1.6 2.0 2.4 2.8
[enzyme]

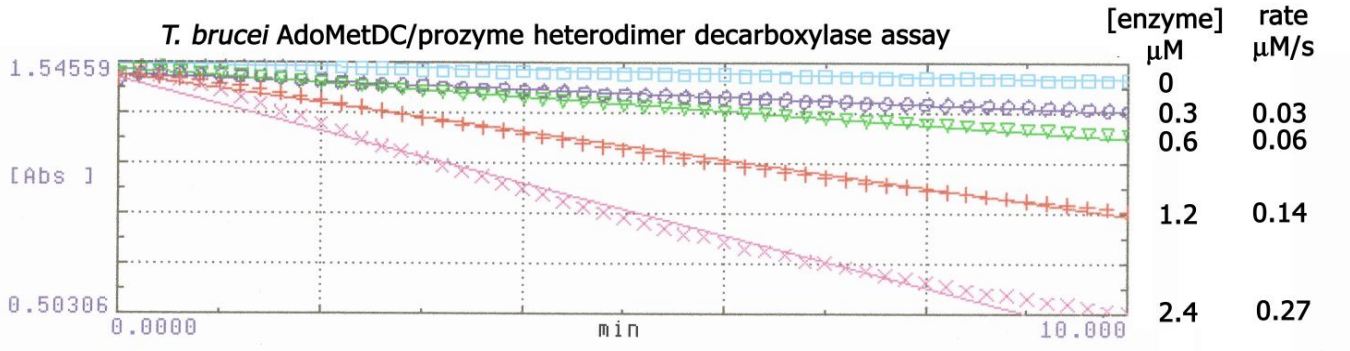
T. brucei AdoMetDC/prozyme heterodimer decarboxylase assay
[enzyme] μM
rate μM/s
1.54559
[Abs]
0.50306
0.0000
min
10.000
0
0.3 0.03
0.6 0.06
1.2 0.14
2.4 0.27

Figure 2.2. Scatterplot of activity values for *T. brucei* AdoMetDC/prozyme pre-screen

Percent inhibition is presented for each compound tested. Sample wells contained enzyme (0.6μM), AdoMet (5 mM), 60 % CO_2 detection reagent, 2.4mM PEP and 3- 10μM compound. DMSO and no enzyme were used as negative and positive controls, respectively. Green: positive control, red: negative control, black: inactive compounds, blue: active compounds, orange: 95th activity quantile, purple: 99th activity quantile.

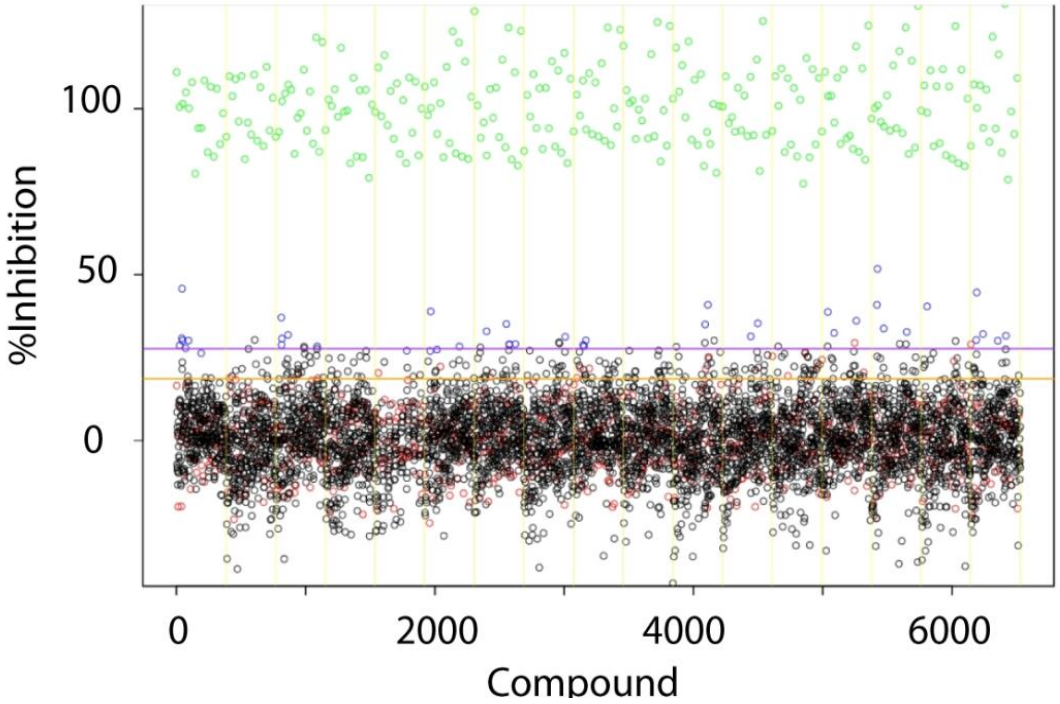
%Inhibition
100
50
0
0
2000
4000
6000
Compound

Table 2.1. Primer sequences and restriction sites

Construct (Optimized Gene)	Restriction Site	Primer Sequence
pET28a-AdoMetDC	BamH1(F), XhoI(R)	Forward (5’ to 3’): GAAAAAGGATCCATGAGCAGCTGCAAAGAT Reverse (5’to 3’): CTTTTTCTCGAGTTATTCTTTCGCGCCGCTCGC
pET28b-AdoMetDC	BamH1(F), XhoI(R)	Forward (5’ to 3’): GAAAAAGGATCCGATGAGCAGCTGCAAAGAT Reverse (5’to 3’): CTTTTTCTCGAGTTATTCTTTCGCGCCGCTCGC
pESUMO-AdoMetDC	Bsa1(F), XbaI(R)	Forward (5’ to 3’): GAAGGTCTCGAGGTATGAGCAGCTGCAAAGAT Reverse (5’to 3’): CTTTCTAGATTATTCTTTCGCGCCGCTCGC

Fig 2.3. Western blot analysis of *T.brucei* AdoMetDC in presence and absence of putrescine

40 µg of total protein isolated from *E. coli* cells were loaded per lane. Blots were probed with α-*T.brucei* AdoMetDC antibody. Un-processed AdoMetDC corresponds to the ~42kDa band, α-AdoMetDC to the ~32kDa band, and β-AdoMetDC to the ~10kDa band. The band observed around 22kDa is non-specific binding of the antibody. Lanes 1 and 2 represent supernatant (S) and pellet (P) fractions, respectively, when putrescine was added to the media. Lanes 3 and 4 represent supernatant and pellet fractions, respectively, with no putrescine added.

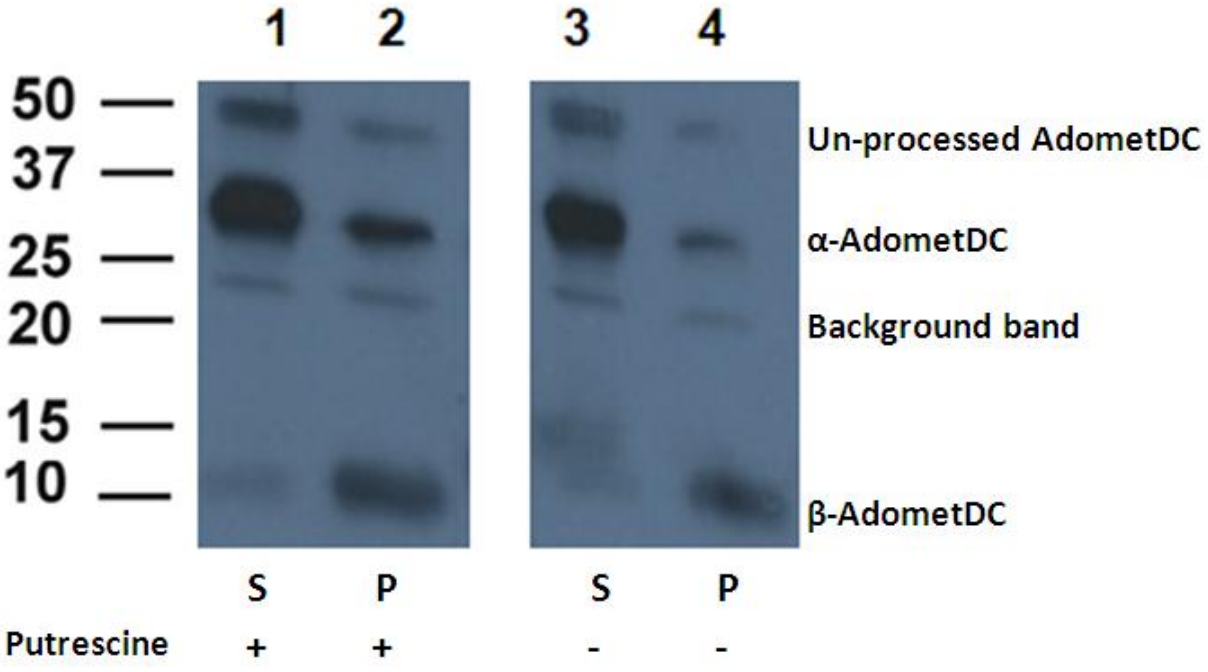
1
2
3
4
50
37
25
20
15
10
Un-processed AdometDC
α-AdometDC
Background band
β-AdometDC
S
P
S
P
Putrescine
+
+
-
-

Table 2.2. Summary of approaches taken to improve *T. brucei* AdometDC expression in *E. coli* and protein yields obtained

Strategy	Protein Yield (mgs)
Initial expression conditions	5-9
20, 30 and 37°C expression temperatures	5-9
Artic cells expression	6
Rosetta cells expression	5
Putrescine addition to expression medium	5
Codon optimization of AdoMetDC sequence	6
Cloning into the pET28a expression vector	7
Cloning into the pET28b expression vector	7
Cloning into the pESUMO expression vector	30

Note: Protein yields presented here were obtained from 6L of culture, after the after first Ni^{2+} -agarose column.

Fig 2.4. Western blot analysis *T.brucei* AdoMetDC protein levels obtained from wild-type versus optimized gene sequences

40 µg of total protein isolated from *E. coli* cells were loaded per lane. Blots were probed with α-*T.brucei* AdoMetDC antibody. Un-processed AdoMetDC corresponds to the ~42kDa band and α-AdoMetDC to the ~32kDa band. The β-AdoMetDC portion could not be detected because the SDS-PAGE gel ran for too long, while the band observed around 22kDa is non-specific binding of the antibody. Lane 1 represents protein obtained from the wild-type (WT) AdoMetDC sequence, while lane 2 is the optimized version synthesized by GenScript.

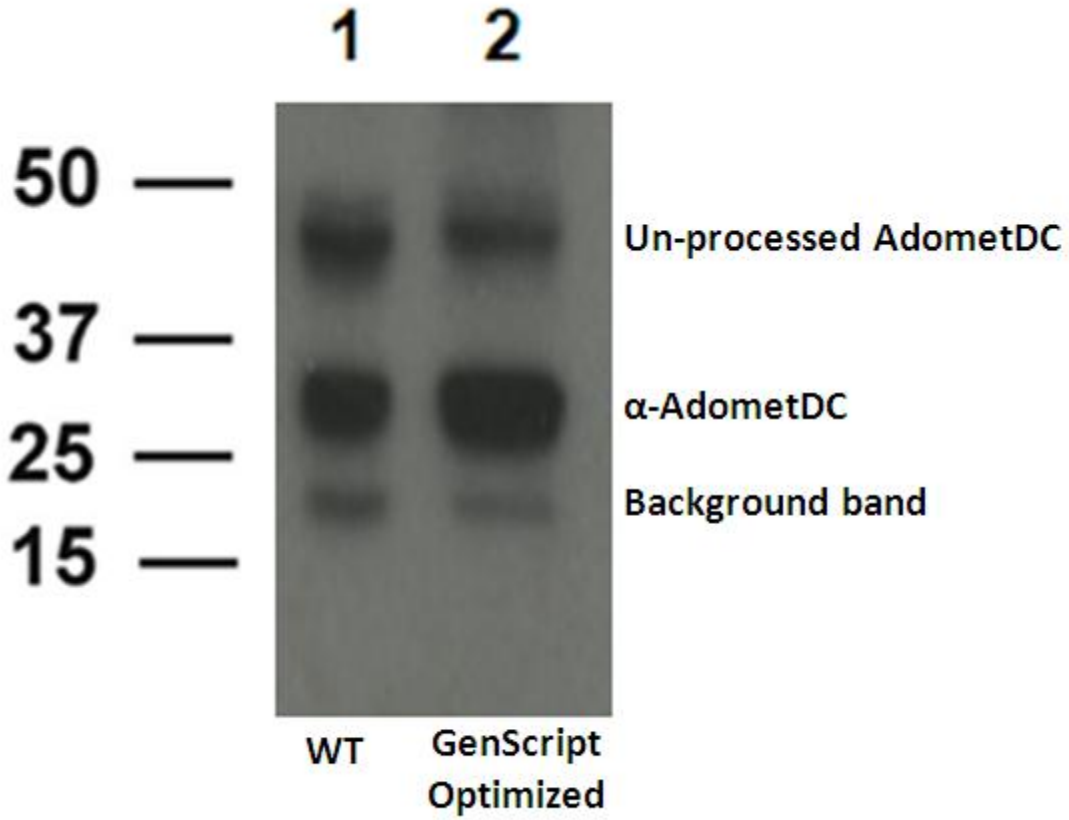
1
2
50
37
25
15
Un-processed AdometDC
α-AdometDC
Background band
WT
GenScript
Optimized

CHAPTER 3

STRUCTURAL BASIS FOR THE ALLOSTERIC ACTIVATION *TRYPANOSOMA BRUCEI* ADOMETDC BY PROZYME

Introduction

Human African trypanosomiasis (HAT), also known as sleeping sickness, is a vector-borne parasitic disease caused by the protozoan pathogen *Trypanosoma brucei* [1, 3]. The WHO estimates that 10 – 30 thousand people in Sub-Saharan Africa are infected yearly, with up to 50 million Africans at risk [5]. In the early stages of the disease the parasite replicates in the blood stream leading to fevers and flu like symptoms, however eventually the parasite crosses the blood brain barrier and the late stage of the disease is characterized by neurological symptoms, including disruption of the sleep cycle leading to eventual coma and death. HAT is 100% fatal if untreated yet current therapy is limited by toxicity and difficult dosing regimens, particularly for late stage disease [2, 11]. Furthermore there is no single drug that is effective against both stages or both sub-species of the disease. Current recommendations are that late stage *T.b. gambiense* (accounting for 95% of the cases) be treated with a combination of nifurtimox and eflornithine (NECT) therapy. Eflornithine, also known as α-difluoromethylornithine (DFMO) is a suicide inhibitor of ornithine decarboxylase, implicating polyamine biosynthesis as a key target for HAT therapy. Polyamines are small organic cations that are required for cell growth and play important roles in a number of other cellular processes such as replication, transcription and translation [13, 16, 82]. In trypanosomes the polyamine pathway has several unique features that differ significantly from the human host, and which contribute to selective toxicity of inhibitors that target the pathway [14, 20, 25, 83]. These include differences in protein turnover rates, the finding that a key polyamine spermidine is conjugated with glutathione to form a novel molecule termed trypanothione, which is key to redox chemistry in the parasite, and novel mechanisms of regulation of pathway enzymes. Genetic and chemical studies have demonstrated that the

polyamine and trypanothione biosynthetic enzymes are essential for *T. brucei* growth and survival [29, 30, 34-36]. Of these, in addition to ODC, S-adenosylmethionine decarboxylase (AdoMetDC) and trypanothione synthetase (TS) have been shown to be druggable targets in the parasite by the discovery of enzyme inhibitors that show good anti-trypanosomal activity [20, 31, 32, 84, 85].

AdoMetDC catalyses the decarboxylation of S-adenosylmethionine (AdoMet) to produce the amino propyl group that will be used for the synthesis of the polyamine spermidine from putrescine. Several inhibitors have been developed against this enzyme, some of which are able to cure *T. brucei*-infected mice suggesting that AdoMetDC is a promising target for the development of new antitrypanosomal agents [50, 86]. Unfortunately most of these compounds displayed significant pharmacokinetic (PK) and /or tissue (CNS) distribution issues, and could not proceed to further trials [86]. Thus the discovery of new classes of AdoMetDC inhibitors will be needed before this target can be exploited. Mechanistically, AdoMetDC uses a covalently-bound pyruvate group as a cofactor during the decarboxylation of AdoMet. The pyruvate is generated by an auto processing reaction, which also leads to cleavage of the peptide bond into the α and β chains [42, 46]. The crystal structure of human AdoMetDC has been determined and shows that the enzyme is an $\alpha_2\beta_2$ homodimer, with the active sites sitting in a cleft between β-sheets away from the dimer interface [44, 45]. Putrescine stimulates both the processing and decarboxylation reactions [44, 46]. Currently, no structure is available for any of the trypanosomatid enzymes.

Polyamine levels are tightly controlled throughout the cell cycle in eukaryotes cells, but the regulatory mechanisms established in mammalian and yeast cells are not found in *T. brucei* [87, 88]. Instead, our lab demonstrated that the trypanosomatid AdoMetDC is allosterically

activated by heterodimer formation with a catalytically dead homolog, designated prozyme, which is present only in the trypanosomatid species [57]. Prozyme is neither processed to generate the pyruvute cofactor, nor does it display any activity on its own. However, upon binding, prozyme stimulates AdoMetDC activity by $>10^3$-fold. Putrescine, which stimulates the activity of human AdoMetDC, does not affect the activity of the *T. brucei* heterodimer [44], though it is required for the *T. cruzi* heterodimer to reach full activation [58]. In *T. brucei,* prozyme expression levels appear to be translationally regulated in response to inhibition or knockdown of AdoMetDC, suggesting that the parasite controls polyamine synthesis at least in part through this mechanism [33].

The structural basis for the activation of trypanosomatid AdoMetDC by prozyme remains an open question. To gain insight into this query, herein we evaluate the role of specific amino acid residues involved in the activation of AdoMetDC by prozyme through deletion and site-directed mutagenesis. Results indicate that the unique trypanosomatid N-terminal 16-amino acid peptide of AdoMetDC is important for this process. We found that deletion of these residues led to a loss in the ability of prozyme to activate the enzyme. Subsequent site-directed mutagenesis identified two leucine residues (8 and 10) in *T. brucei* AdoMetDC that are key for prozyme activation. Interestingly, when putrescine is present the effect of these two point mutants on activity is diminished. Sedimentation velocity experiments demonstrate that the mutant enzyme, lacking the peptide, forms a weaker heterodimer than wild-type, but enzyme activity analysis suggests that the weakened dimer is not the cause of the reduced catalytic activity, suggesting that these residues are involved in a conformational change that is essential for activation. The 16 amino acid unique N-terminus is partially conserved in prozyme, but deletion of these residues in prozyme does not significantly affect the activation process. Our findings provide the

first insight into the structural basis and mechanisms that control AdoMetDC activation by prozyme, demonstrating the importance of a unique N-terminal peptide in the process.

Experimental Procedures

Multiple Sequence Alignment

AdoMetDC and prozyme sequences were obtained from the Pubmed (*Homo sapiens* gi:178518, *Solanum tuberosum* gi:416883) and GeneDB (Tb927.6.4460, Tc00.1047053504257.30, LmjF30.3110, Tb927.6.4470, Tc00.1047053509167.110, LmjF30.3120) databases, and converted into a FASTA format. Alignment was performed using the ClustalW2 program (http://www.ebi.ac.uk/Tools/msa/clustalw2/).

Construction of Wild-type and Mutant E. coli Expression Constructs

T. brucei AdoMetDC was amplified by PCR from the pET15b-AdoMetDC plasmid DNA, provided by Erin Willert [57], and cloned into the pE-SUMO (LifeSensors, Malvern, PA) vector. This newly generated construct was then used as a template to produce the Δ16 AdoMetDC mutant, using complimentary primer pairs encoding the sequence alteration. Point mutants were created using a Quick-Change Site-directed Mutagenesis Kit (Stratagene, CA, USA). *T. brucei* prozyme was also previously cloned into the pT7-Flag1 (Sigma, St.Louis, MO) vector [33, 57]. The truncated version of prozyme was produced by amplifying the gene from the

pT7-Flag1-prozyme plasmid and cloning it into the pET28b vector, which was engineered to generate a tag less protein. Cloning primers are provided in **Table 3.1**. *E. coli* TOP10 competent cells were transformed with each plasmid, and mutations were confirmed by DNA sequencing.

AdoMetDC/prozyme Expression and Purification

E.coli BL21/DE3 cells were transformed with the construct of interest and grown at 37°C until OD_{600} reached between 0.6 - 0.8. Protein expression was induced by the addition of 0.2mM IPTG and cells were grown overnight at 20°C. Cells were harvested by centrifugation and resuspended in lysis buffer (50mM Hepes, 100mM NaCl, 10mM imidazole, 5mM β-mercaptoethanol). Protease inhibitors were added directly to the cell lysate (Cocktail 1 (1:1000)-1mg/mL Leupeptin, 2mg/mL Antipain and 10mg/mL Benzamidine; Cocktail 2 (1:1000)-1mg/mL Pepstain, 1mg/mL Chymostatin; and 0.2M Phenylmethyl-sylfonyl fluoride (PMSF) in a 1:500 ratio) (Sigma, St.Louis, MO). Bacterial cells were lysed using an EmulsiFlex-C5 homogenizer, followed by centrifugation (Beckman Ti-45 rotor) at 15,000rpm for 30min. The soluble fraction was subjected to Ni^{2+} -agarose (Qiagen, Valencia, CA) column chromatography (Buffer A: 50mM Hepes pH 8, 100mM NaCl, 1mM β-mercaptoethanol, 10mM imidazole; Buffer B: 50mM Hepes pH 8, 100mM NaCl, 1mM β-mercaptoethanol, 800mM imidazole), as previously described [57, 66]. The heterodimeric enzymes were obtained by mixing the separate lysates and co-purifying the His_6-SUMO-tagged AdoMetDC with the Flag-tagged prozyme. The protein containing fractions were pooled together, concentrated and diluted back in buffer A, to remove excess imidazole. The protein sample was then incubated with ULP1, also known as SUMO protease 1, which recognizes the tertiary structure of SUMO in the fusion protein and

cleaves with high specificity. This resulted in the removal of the His_6-SUMO tag generating AdoMetDC such that no tag region remained. AdoMetDC (wild-type or mutant) sample was incubated with approximately 300 µg of ULP1 for every 20-35mgs of protein for 2 h at 4°C with gentle agitation. After cleavage, a second Ni^{2+} -agarose purification step was performed in which the now tagless-enzyme was collected in the flow-through fractions. Anion-exchange chromatography was subsequently performed, as previously described [57, 66], only for WT homodimer/heterodimer, Δ16 homodimer/heterodimer and the AdoMetDC LSL-AAA heterodimer, all of which underwent careful binding analyses and had to be > 90% pure. Remaining mutants were sufficiently clean after the second Ni^{2+} -agarose purification step. Extinction coefficients (**Table 3.1**) for the wild-type and mutant enzymes were obtained through the ExPASy- ProtParam program (http://web.expasy.org/protparam/), and used to quantify protein by measuring absorbance at 280nm. These calculations were performed using the Beer's law equation ($A=\varepsilon lc$, where A is absorbance, ε is extinction coefficient, l is the path lengh and c is concentration).

Expression and Purification of ULP-1

The pET15b-ULP1 plasmid was provided by Kim Orth. Expression of this N-terminal His-tagged protease was performed as above with the following modifications. IPTG induction was performed at 30°C overnight and lysis buffer contained 50 mM Tris-HCl (pH=7.5), 350 mM NaCl, 1 mM BME, 10 mM imidazole, 0.2% IGEPAL and 20% glycerol. Ni^{2+} -affinity purification Buffer A contained 50 mM Tris-HCl (pH=7.5), 350 mM NaCl, 1mM BME, 10 mM

imidazole and 20% glycerol, while Buffer B had the same components, with the exception of imidazole at 800mM concentration.

Steady-state Kinetic Analysis

The enzymatic activity of AdoMetDC was assessed using a $^{14}CO_2$-based method [89]. A constant amount of AdoMetDC (1-3 µM homodimers; 0.1 and 1-6 µM for wild-type and mutant heterodimers, respectively) was titrated into reactions containing 25µM $^{14}CO_2$-AdoMet (American Radiolabeled Chemicals), a range of unlabeled AdoMet concentrations (25-1475 µM, Affymetrix), 100mM Hepes pH 8, 50mM NaCl, 1mM DTT and 5mM putrescine (analyses were also performed in the absence of putrescine). Test tubes were capped and placed in a water bath at 37ºC. The CO_2 liberated from the substrate would get trapped on a filter paper soaked in 80 µL of saturated $Ba(OH)_2$. After 5 min, reactions were quenched using 6M HCl. The filter paper was then transferred to a scintillation vial containing 5mL of CytoScint. Samples were placed on the scintillation counter, and the counts per minute (cpm) obtained were converted into velocity (s^{-1}) values using the specific activity of the substrate. Data was fitted to the Michaelis-Menten equation to determine the steady-state kinetic parameters (k_{cat}, K_m) using Prism (GraphPad, San Diego, CA). Enzyme doubling experiments were performed similarly. In that particular case a range of enzyme concentrations were tested at a fixed concentration of substrate (250µM total AdoMet).

Sedimentation Velocity

All analytical ultracentrifugation (AUC) experiments were performed in a Beckman-Coulter (Indianapolis, IN) Optima XL-I ultracentrifuge. The Beckman An50Ti rotor was used, and all studies were carried out at 20° C and 50,000 rpm. The samples of co-purified wild-type or mutant AdoMetDC/prozyme were diluted to their final concentrations in AUC buffer (50 mM HEPES pH 8, 50 mM NaCl, 1 mM β-mercaptoethanol) and incubated overnight at 4° C before being loaded into dual-sectored, charcoal-filled Epon centerpieces that had been sandwiched between sapphire windows in a centerpiece housing. The assembled housings were placed in the rotor, and the rotor was placed in the centrifuge and allowed to incubate at the experimental temperature for approximately 2.5 hr. before the centrifugation commenced. Radially dependent concentration profiles were acquired at approximately 10 min. time intervals using the absorption optics tuned to 280 nm.

All data were analyzed using either SEDFIT or SEDPHAT (www.analyticalultracentrifugation.com). In all cases, $c(s)$ distributions were used to fit the data [90, 91]. Regularization levels of 0.68 were used. In the case of the Δ16 mutant, these distributions exhibited strong concentration dependence. Thus, these data were fitted to solutions of the Lamm equation with explicit consideration of the thermodynamics and kinetics of the AdoMetDC/prozyme interaction [92, 93]. For wild-type AdoMetDC mixture, a fixed fraction (23%) of the AdoMetDC did not participate in the heterodimeric AdoMetDC complex, regardless of the concentration of the complex. From this observation, it was inferred that this fraction of one of the proteins (AdoMetDC) was incompetent to form the complex. Going forward, we assumed that this incompetent fraction was identical and constant in all wild-type

and mutant AdoMetDC expressions. In order to carry out the analysis of the association of Δ16 and the prozyme, six sedimentation experiments were analyzed globally in SEDPHAT, with several other assumptions and constraints: 1) Monomeric AdoMetDC and monomeric prozyme behaved identically hydrodynamically, 2) The sedimentation coefficient of the complex was the same as that of the wild-type complex, 3) The material that sediments with an $s_{20,w}$-value of 4.9 S is all heterodimeric, with no homodimers of either protein present, 4) no hyper- or hypochromicity accompanied the interaction, 5) all proteins and the complex have the same partial-specific volume (0.73 cm^3/g), 6) an observed 7-S species did not participate in the interaction and could be treated as "non-participating", and 7) the molar ratio of AdoMetDC and prozyme was constant (a consequence of the preparation procedure). The error interval for the association constant was calculated using the projection method [94] with the F-statistic described by Johnson [95]. All AUC-derived figures were made using GUSSI (biophysics.swmed.edu/MBR/software.html). The same software was used to convert $c(s)$ distributions to standard conditions. SEDNTERP [96] was used to calculate buffer viscosity, buffer density, and protein partial-specific volumes.

Tertiary Structure Prediction

The *T. brucei* AdoMetDC sequence (Tb927.6.4460) was submitted to the automated homology modeling program ESyPred3D Web Server 1.0 (http://www.fundp.ac.be/sciences/biologie/urbm/bioinfo/esypred/) for tertiary structure prediction. The human AdoMetDC (PDB code 1I7B [44, 46]) information was used as a model,

and both 3-D structures were visualized and superimposed using the graphics program PyMOL [97].

Results

Sequences Analysis of Eukaryotic AdoMetDCs

In order to elucidate the structural requirements for AdoMetDC activation by prozyme in the absence of a crystal structure for any of the parasitic enzymes we performed a sequence alignment of representative AdoMetDCs to determine if any sequence signatures that were unique to the trypanosomatid enzymes were present (**Fig 3.1**). This analysis indicates that the N-terminal region contains a unique 16-20 amino acid peptide, present in the trypanosmatids (*T. brucei, T. cruzi and Leishmania major*) AdoMetDCs, but absent from other eukaryotic homologs (e.g. human and plant; **Fig 3.1**). In this region, 12 specific amino acids are particularly conserved between the parasitic enzymes. Interestingly, although prozyme contains this stretch of residues as well, the degree of conservation with the respective AdoMetDC or prozyme from different species is less. The human enzyme is fully active as a homodimer and does not contain this peptide. Thus this conserved N-terminal extension is only present in the AdoMetDCs that are activated by prozyme, suggesting that it might play a role in the activation of the trypanosomatid enzymes.

Unique N-terminus of T. brucei AdoMetDC is Essential for Activation by Prozyme

A mutant version of *T. brucei* AdoMetDC was constructed lacking the N-terminal 16 amino acids to determine if this region was required for activation. Both homodimeric (Δ16AdoMetDC) and heterodimeric (Δ16AdoMetDC/prozyme) enzymes were expressed and purified from *E. coli*. Like wild-type AdoMetDC, Δ16AdoMetDC undergoes a self-processing reaction to generate the active enzyme consisting of two chains, α (32kDa) and β (8 kDa) (data not shown). In addition, Δ16AdoMetDC like the wild-type enzyme, forms a stable complex with prozyme that co-purified over Ni^{2+}-agarose and ion exchange chromatography. In the absence of putrescine, the Δ16AdoMetDC homodimer has a k_{cat}/K_m of 16 $M^{-1}s^{-1}$, which is similar to that of the wild-type homodimer (**Table 3.2 and Fig 3.2**). However, prozyme is unable to activate the mutant enzyme, which displays a catalytic activity for the Δ16AdoMetDC/prozyme heterodimer that is 100-fold lower than the wild-type heterodimer (**Fig 3.2**). This strong decrease in catalytic efficiency is the consequence of an effect on both substrate binding (K_m) and catalysis rate (k_{cat}) (**Table 3.2**). Putrescine stimulates the activity of the wild-type AdoMetDC homodimer and has no effect on the heterodimer. The activity of the truncated dimeric enzymes (Δ16AdoMetDC and Δ16AdoMetDC/prozyme), was not significantly affected by the addition of putrescine.

Identification of Residues within the N-terminal Peptide that are Essential for Prozyme Activation

To identify specific residues within the N-terminal peptide that were involved in activation by prozyme ala-scanning mutagenesis was performed. The key residues were initially narrowed down by construction of four mutants each containing three consecutive amino acids

substituted with alanine. Similar to the Δ16 homodimer and heterodimer, these mutants were all capable of self-processing and the complexes held together through all purification steps. Results indicate that AdoMetDC L8A/S9A/L10A has the strongest effect (**Table 3.2 and Fig 3.2**). The catalytic efficiency of this triple mutant heterodimer is 250-fold lower than wild-type and, interestingly, 3-fold lower than the Δ16 heterodimer. AdoMetDC M11A/M13A also showed reduced enzyme activity, but only in the absence of putrescine, which whenever added to the reactions increases catalysis efficiency to within 20-fold of wild-type heterodimer levels.

To further study AdoMetDC L8A/S9A/L10A, individual point mutations were constructed for each of these residues (**Fig 3.2**). S9 was not essential since no significant changes were observed. On the contrary, whenever L8 is replaced by Ala, the enzyme behaves similarly to the truncated Δ16AdoMetDC, but only in the absence of putrescine. L10 has a mild effect on activity, and it was putrescine dependent as well.

Analysis of Dimer Formation by Sedimentation Velocity

While all of mutant enzymes could be copurified as heterodimers, in order to assess the relative strengths of the associations between the prozyme and various AdoMetDC constructs, we worked in collaboration with Chad Brautigam to perform AUC experiments in the sedimentation velocity (SV) mode (**Fig 3.3**). The wild-type heterodimer binding affinity (K_D) was compared to those mutations that led to the largest decrease in activity. The AdoMetDC/prozyme complexes were purified as described in the experimental procedures section and diluted to three different concentrations. These samples were subjected to SV. If the dissociation constant for the heterodimers was near the concentrations used, a concentration-

dependence for the observed sedimentation coefficients or for the populations of the resolved species should be present [98, 99].

For the wild-type protein, $c(s)$ distributions, which relate the signal populations of sedimenting species directly to the SV data, revealed two well-resolved peaks (**Fig 3.3A**). One peak occurred at an $s_{20,w}$-value of 3.3 S, and the other at 4.8 S; these values were not dependent on the concentration of the complex. Further, the relative signal populations of the two species do not change significantly over the concentration range studied. From these data, from the manner of the complex was purified, and from the fact that an SDS-PAGE analysis (**Fig 3.3D**) demonstrate that AdoMetDC/prozyme preparations contain equal concentrations of the two proteins, we concluded that the 3.3-S material was equimolar mixture of free AdoMetDC and free prozyme. That is, at least one of the proteins must be incompetent to bind the other (see below). We also inferred that the 4.8-S species was the complex between AdoMetDC and the prozyme. The estimated molar masses associated with the two species (40 kg/mol and 70 kg/mol) buttress this conclusion. Also, we conclude from the lack of relative population variation that the dissociation constant of the wild-type complex must be well below the lowest complex concentration studied, 0.3 μM. This result conforms to our earlier report using sedimentation equilibrium analysis that found the dissociation constant for the two proteins to be below 0.5 μM [57].

As mentioned above, we surmise that the 3.3-S peak represents a mixture of both free species. For our observations to be consistent with this supposition, AdoMetDC, prozyme, or both must have become incompetent for binding during the steps subsequent to the affinity purification. Because it seems unlikely that both proteins would simultaneously suffer this defect, we speculated that only AdoMetDC became incompetent, causing the dissociation of the

incompetent fraction of AdoMetDC and the prozyme. The cause of this phenomenon is unknown. Also, the hypothesis that the 3.3-S peak contains both proteins requires that they are hydrodynamically indistinguishable from one another; this requirement is compatible with our observations with the Δ16 AdoMetDC, described in detail below.

The same lack of concentration trend is observed in the L8A/S9A/L10A mutant of AdoMetDC (**Fig 3.3B**). Indeed, this AdoMetDC variant exhibited a very similar level of incompetent material (21%). Two conclusions may be drawn from these data. First, the LSL mutations did not significantly increase the dissociation constant of AdoMetDC and prozyme, providing a clear indication that the reduced activity of this mutant does not result from loss of dimerization. Second, the amount of incompetent AdoMetDC does not strongly vary from preparation to preparation.

The Δ16 mutant of AdoMetDC is clearly different from the wild-type protein and the L8A/S9A/L10A mutant. The size distributions obtained from the Δ16/prozyme mixture displays robust concentration dependence in the SV studies (**Fig 3.3C**). Specifically, when going from low to high concentrations, the signal population (the areas of the peaks in **Fig 3.3C**) of the 3.3-S species decreases, while that of the 4.8-S species increases, consistent with mass action law. This observation and our experiences with the wild-type AdoMetDC allowed us to construct a constrained Δ16 + prozyme ↔ Δ16:prozyme interaction model and use it to fit the SV data using the Lamm equation with explicitly considered thermodynamics and kinetics (see Experimental Procedures section for the assumptions and constraints built into the model). Given the assumptions and constraints, we found that the dissociation constant was 1.0 [0.9-1.4] μM (the numbers in brackets indicate the 68.3% error interval). The quality of the fits to the data was judged to be high based on the low overall root-mean-square of the differences between the data

and the fits (0.0065 AU) and the non-systematic nature of the residuals. Our ability to resolve the complex from the uncomplexed material in the *c*(*s*) distributions indicates a slow off rate for the interaction.

In summary, SV results reveal values of <0.3, 1 and <0.7μM for wild-type, Δ16 and L8A/S9A/L10A AdoMetDC heterodimers, respectively. Thus, while wild-type and the triple mutant heterodimers bind very tightly, there is a decrease in affinity in the Δ16 heterodimer. This implies that truncation at the N-terminus weakens the dimer interface, but that it does not block dimer formation.

To further confirm that poor dimer formation did not contribute to the lack of activation of the Δ16 heterodimer, an enzyme concentration titration was performed (**Fig 3.4**). The concentration of Δ16 AdoMetDC heterodimer was varied from 1 – 16 μM and the activity determined. Results demonstrate that as the concentration of Δ16 AdoMetDC/prozyme was doubled, the enzyme velocity also doubled and there was no indication of a greater than proportional increase in rate as would be expected if monomers were contributing to the lowered rate of the reaction (**Fig 3.4A**). Thus, truncation at the N-terminus weakens the dimer interface, based on the sedimentation velocity results, but the dimer is fully formed under the conditions of the enzyme assay.

N-terminus Region of T. brucei Prozyme is not Important to Activate AdoMetDC

Since *T. brucei* prozyme also contains residues at the N-terminus with similarity, though not full conservation, to the trypanosomatid AdoMetDC N-terminal signature, we evaluted the effects of trunctation of the prozyme N-terminus (first 25 residues) as well. Results demonstrate

that when wild-type AdoMetDC is co-purified with Δprozyme, a catalytically efficient enzyme is still obtained (**Table 3.2 and Fig 3.5**). On the contrary, Δprozyme was not able to stimulate Δ16 AdoMetDC activity, demonstrating once again the essentiality of this region for AdoMetDC proper catalysis.

Discussion

The polyamine metabolic pathway in the trypanosomatids has several important characteristics that differ from the mammalian host, making it a suitable target for the development of drugs. Enzymes involved in the production of polyamines are constantly under study and it was recently shown that in *T. brucei* parasites, AdoMetDC activity is stimulated by $>10^3$-fold upon heterodimer formation with an inactive homolog, called prozyme. This homolog proved to play an essential part in regulating polyamine levels and metabolism, together with AdoMetDC and ODC as key control points. The studies described herein demonstrate that the *T. brucei* AdoMetDC N-terminus is necessary for proper activation by prozyme and might be involved in any associated conformational changes. In particular, residues L8 and L10 seem to be playing a crucial role during catalysis.

There are a large number of examples in nature that link N-terminal protein extensions and domains to function, interactions, structural organization, regulatory roles, and localization, among others. Conversion of trypsinogen into its active form, trypsin, is achieved after hydrolysis of the $Lys_{(6)}$-$Ile_{(7)}$ bond by enterokinase, which results in the release of an N-terminal peptide known to be essential for the recognition and further activation of the enzyme [100-102]. The whole process becomes autocatalytic, since trypsin can subsequently activate more

trypsinogen by cleaving off these residues as well [103]. In protozoan parasites, specifically, N-terminal regions in some proteins are known to be required for gene silencing, telomeric localization, association of argonaute proteins (AGOs) with polyribosomes, fibril formation and structure stabilization [104-111]. The prozyme discovery provided the first parasite-specific mechanism to control polyamine homeostasis in trypanosomes. Depletion of either AdoMetDC or prozyme resulted in a reduction of spermidine and trypanothione levels, and eventually in parasite death, demonstrating that prozyme activation of AdoMetDC is essential [33]. In mammalian cells, ornithine decarboxylase levels are regulated by a protein inhibitor, termed antizyme, which blocks enzyme activity and accelerates degradation. This control mechanism is very similar to what happens to AdoMetDC upon binding to prozyme, with the main difference that prozyme is stimulatory instead of inhibitory. Interestingly, the N-terminus of antizyme, although not required for the interaction with ODC, must be present to induce degradation by the proteosome [112]. Just the covalent link of the N-terminus portion of antizyme to ODC is sufficient to direct protein destruction. This provides another example of the importance of these unique N-terminal regions, and raises the possibility for the AdoMetDC N-terminus to be equally important and necessary for parasite growth and survival.

The genomes of the trypanosomatids (*T. brucei, T. cruzi* and *L. donovani*) all contain the sequence for both a functional AdoMetDC and a catalytically dead prozyme. *T. cruzi* is the causative agent of Chagas disease, commonly found in South America, with over 13 million people infected. Similar to HAT, there is an urgent need for the development of new and more effective therapies. The *T.cruzi* AdoMetDC/prozyme heterodimer has been characterized, and the catalytically dead homolog is also able to stimulate AdoMetDC activity by 110-fold, when compared to homodimeric enzyme [58]. Sequence alignment demonstrated the presence of the

highly conserved stretch of residues at the N-terminus of all trypanosomatid enzymes (Fig 1). Thus, it remains to be determined if the requirement of this region, together with prozyme, is a common mechanism to control AdoMetDC activity in these species.

The N-terminus of *T. brucei* AdoMetDC could be playing a role in the activation by prozyme either by influencing dimer formation or through an allosteric regulatory mechanism. Our results are consistent with the second possibility, since sedimentation velocity experiments on the Δ16 heterodimer demonstrated that truncation in the region weakens the dimer interface, but does not disrupt binding. Importantly, the AdoMetDC L8A/S9A/L10A mutant forms a dimer with prozyme that is as strong as wild-type, but displays impaired activity. Thus, suggesting that these mutated residues, in particular L8 and L10, might be influencing catalysis through an allosteric mechanism. Structural knowledge about AdoMetDC relies on the human homodimeric enzyme, which is activated by putrescine and does not have an N-terminal extension. Homology modeling of *T. brucei* AdoMetDC, which shares a 58% sequence identity with human AdoMetDC, predicted a tertiary structure where the N-terminal region of the enzyme is exposed to the water (**Fig 3.6A**). Thus, our data could be supporting a model in which binding of prozyme results in a conformational change that rearranges the N-terminus closer to the active site residues, allowing key interactions to take place in order to enhance catalysis (**Fig 3.6B**).

The structural basis for the requirement of putrescine to pronouncedly activate the *T.brucei* AdoMetDC M11A/M13A, L8A and L10A mutant heterodimers is unclear, since no X-ray structure is currently available for the wild-type parasitic enzyme. In the human enzyme, the putrescine binding-site is composed of acidic residues (D174, E178, E256) distant from the active site, and closer to the dimer interface. Structural studies demonstrate that putrescine influences the orientation of essential catalytic residues through a hydrogen-bonding network,

mediated by K80, H243, E11 and S229 [47]. However, although D174 and E256, in addition to some of the residues involved in connecting the putrescine-binding pocket to the active site, are conserved between the trypanosomatid and human enzymes, they do not seem to play the same roles. Clyne et al. showed that, just like for the human enzyme, D174 is essential for putrescine to bind *T. cruzi* AdoMetDC and stimulate its activity, while the remaining amino acids known to be important had no effect [113]. It is possible that the M11, M13, L8 and L10 residues at the N-terminus of *T. brucei* AdoMetDC are involved in essential hydrophobic interactions during the decarboxylation process, which when mutated to alanine are compensated by the methylene groups in putrescine.

Novel AdoMetDC inhibitors that can potentially lead to the treatment of HAT are urgently needed. The finding that AdoMetDC is regulated by a catalytically dead homolog is an important accomplishment, and provides an alternative for more efficient enzyme inhibition. Compounds targeted to disrupt the AdoMetDC-prozyme complex interface could be a successful approach. Current inhibitors developed for the homodimeric enzyme might also be more potent against the heterodimer. In fact, MDL 73811, an irreversible inhibitor *of* AdoMetDC, has shown efficacy in *T.brucei* animal models and is also highly active against the *T. brucei* AdoMetDC heterodimer (k_{inact}/K_iapp = 1.5 μM^{-1} min^{-1}) [86]. Although several pharmacokinetic issues have slowed down the development of MDL73811 as a drug, hu*g*e efforts are currently ongoing to modify the compound structure in order to increase potency. One of the analogs synthesized (Genz-644131) was shown to be highly active against *T .b. rhodesiense in vitro*. Importantly, enzyme kinetic studies demonstrated that Genz-644131 is approximately 5-fold more potent than MDL 73811 against the *T. b. brucei* AdoMetDC-prozyme complex [86]. Discovering that AdoMetDC's N-terminus is essential for activation by prozyme provides yet another crucial

approach for inhibition. Small molecules could be designed to target this region and block interaction with key residues during catalysis. In addition, allosteric activation suggests a conformational change that allows seeking for inhibitors that lock the protein in the inactive conformation. Gleevec, a drug used for the treatment of certain cancers including chronic myelogenous leukemia (CML) is an inhibitor of the constitutively active Bcr-Abl tyrosine kinase [114, 115]. Its mechanism of action represents a good example of a ligand exploiting the inactive conformation of a protein kinase. Basically, the compound molecule sits between the two lobes of the inactive structure, spanning the width of the protein and forming several key interactions [114, 115]. Another crucial example for this type of mechanism is the development of bi-aryl urea inhibitors of P38 MAP kinase [116]. More detailed structural information on the *T. brucei* AdometDC/prozyme heterodimeric enzyme is needed before these ideas can be exploited.

Table 3.1. Primer sequences and extinction coefficients

Construct	Restriction Site	Primer Sequence	Protein Extintion Coeficients ($mM^{-1}cm^{-1}$)
pESUMO-AdoMetDC	Bsa1(F), XbaI(R)	Forward (5' to 3'): GAAGGTCTCGAGGTATGAGCAGCTGCAAAGAT Reverse (5'to 3'): CTTTCTAGATTATTCTTTCGCGCCGCTCGC	65.3
pESUMO-Δ16AdoMetDC	Bsa1(F)	Forward (5' to 3'): GAAGGTCTCGAGGTATTGCGCGTTTTGATCCG	59.8
pESUMO-AdoMetDC(KDS-AAA)	n/a	Forward (5' to 3'): GAGCAGCTGCGCAGCTGCCCTGAGCCTGATG Reverse (5'to 3'): CATCAGGCTCAGGGCAGCTGCGCAGCTGCTC	65.3
pESUMO-AdoMetDC(LSL-AAA)	n/a	Forward (5' to 3'): GCAAAGATAGCGCGGCCGCGATGGCGATGTGG Reverse (5'to 3'): CCACATCGCCATCGCGGCCGCGCTATCTTTGC	65.3
pESUMO-AdoMetDC(MAM-AAA)	n/a	Forward (5' to 3'): GCCTGAGCCTGGCGGCGGCGTGGGGCAGCATTG Reverse (5'to 3'): CAATGCTGCCCCACGCCGCCGCCAGGCTCAGGC	65.3
pESUMO-AdoMetDC(WGS-AAA)	n/a	Forward (5' to 3'): GATGGCGATGGCGGCCGCCATTGCGCGTTTTG Reverse (5'to 3'): CAAAACGCGCAATGGCGGCCGCCATCGCCATC	65.3
pESUMO-AdoMetDC(L8A)	n/a	Forward (5' to 3'): GCAAAGATAGCGCGAGCCTGATGGC Reverse (5'to 3'): GCCATCAGGCTCGCGCTATCTTTGC	65.3
pESUMO-AdoMetDC(S9A)	n/a	Forward (5' to 3'): GATAGCCTGGCCCTGATGGCG Reverse (5'to 3'): CGCCATCAGGGCCAGGCTATC	65.3
pESUMO-AdoMetDC(L10A)	n/a	Forward (5' to 3'): GATAGCCTGAGCGCGATGGCGATGTGG Reverse (5'to 3'): CCACATCGCCATCGCGCTCAGGCTATC	65.3
pET28a-Prozyme (no tag)	NcoI (F), XhoI (R)	Forward (5' to 3'): GAAAAACCATGGGGATGTCGGTCACGCGGATTAAC Reverse (5'to 3'): CTTTTTCTCGAGTCAGGCACTGCGTGCGTATGTGGC	35.9
pET28a-Δprozyme (no tag)	NcoI (F)	Forward (5' to 3'): GAAAAACCATGGGGTGCACCCAATCTAAAACCTCC	30.4

Note: Extinction coefficients for the complexes were obtained by adding the coefficients of the individual proteins.

Figure 3.1. N-terminus sequence alignment of eukaryotic AdoMetDCs with prozyme

Highlighted in turquoise are some residues essential for activity. Highlighted in yellow is the conserved 12 amino acid peptide found only in the trypanosomatid AdoMetDCs. *T. br= Trypanosoma brucei*, *T. cr= Trypanosoma cruzi*, *L. ma= Leishmania major*, pr= prozyme

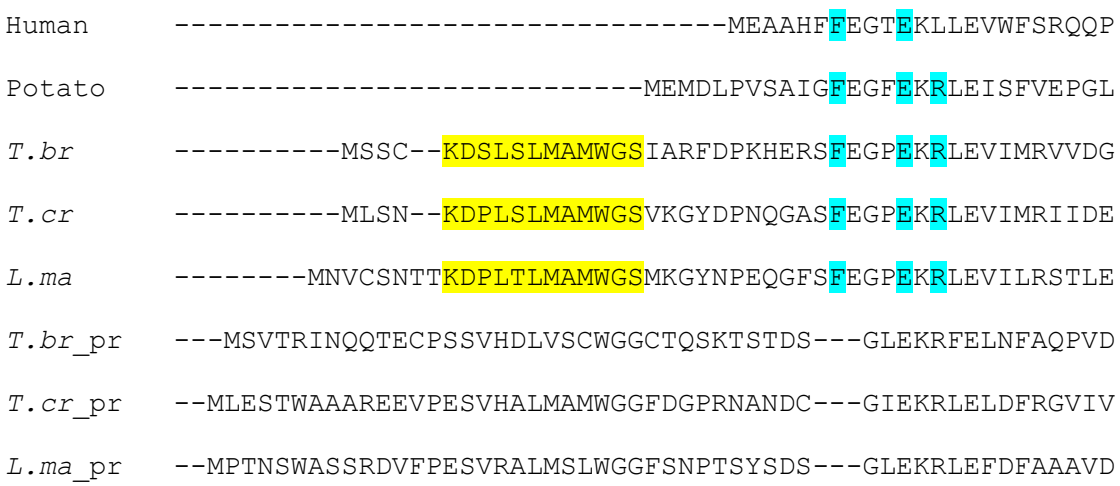
Human ----------MEAAHFFEGTEKLLEVWFSRQQP
Potato ----------MEMDLPVSAIGFEGFEKRLEISFVEPGL
T.br ----------MSSC--KDSLSLMAMWGSIARFDPKHERSFEGPEKRLEVIMRVVDG
T.cr ----------MLSN--KDPLSLMAMWGSVKGYDPNQGASFEGPEKRLEVIMRIIDE
L.ma --------MNVCSNTTKDPLTLMAMWGSMKGYNPEQGFSFEGPEKRLEVILRSTLE
T.br_pr ---MSVTRINQQTECPSSVHDLVSCWGGCTQSKTSTDS---GLEKRFELNFAQPVD
T.cr_pr --MLESTWAAAREEVPESVHALMAMWGGFDGPRNANDC---GIEKRLELDFRGVIV
L.ma_pr --MPTNSWASSRDVFPESVRALMSLWGGFSNPTSYSDS---GLEKRLEFDFAAAVD

Figure 3.2. Catalytic efficiency of wild-type and several mutant *T. brucei* AdoMetDCs

Bar graphs represent k_{cat}/K_m ($M^{-1}s^{-1}$) values for the *T.brucei* enzymes in the presence (purple) and absence (blue) of 5mM putrescine. Inset represents the N-terminal region and highlighted in yellow are the conserved trypanosomatid residues. HM=Homodimer and HT=heterodimer

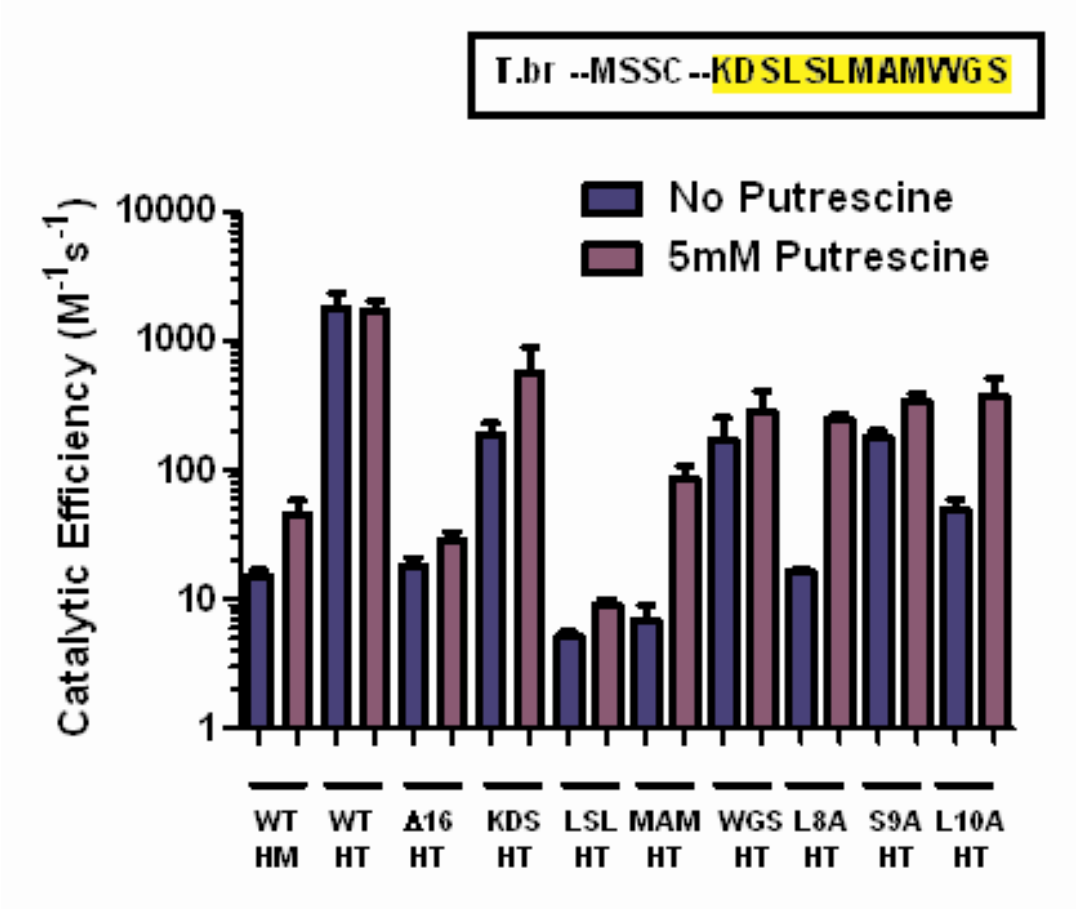
T.br --MSSC--KDSLSLMAMVVGS
No Putrescine
5mM Putrescine
Catalytic Efficiency ($M^{-1}s^{-1}$)
10000
1000
100
10
1
WT HM
WT HT
Δ16 HT
KDS HT
LSL HT
MAM HT
WGS HT
L8A HT
S9A HT
L10A HT

Figure 3.3. Sedimentation velocity analysis of wild-type, Δ16 and the L8A/S9A/L10A AdoMetDC/prozyme heterodimers

(A) Size distributions for the wild-type AdoMetDC/prozyme heterodimer. The distributions have been normalized by the total signal present between 2 S and 7 S in the respective distributions. Slowly sedimenting material of < 1 S (probably resulting from a buffer mismatch) has been excluded from the plot. The concentrations of the complex used were 0.3 μM (*red*), 1.7 μM (*black*), and 3.8 μM (*blue*). (B) Size distributions of the L8A/S9A/L10A AdoMetDC/prozyme heterodimer. The distributions have been normalized by the total amount of signal present. The concentrations of the complex used were 0.7 μM (*red*), 2.2 μM (*black*), and 3.7 μM (*blue*). (C) Size distributions of the Δ16 AdoMetDC/prozyme heterodimer. The distributions were normalized by the total amount of signal present between 2 S and 6 S. Slowly sedimenting material of < 1 S has been excluded. The concentrations of the (potential) complex used were 0.7 μM (*red*), 1.9 μM (*black*), and 3.3 μM (*blue*). (D) SDS-PAGE evaluation of the AdoMetDC heterodimeric samples used in the SV analysis. Bands were quantified using ImageJ (http://rsbweb.nih.gov/ij/). Relative AdoMetDC to prozyme ratios were obtained for the wild-type (WT, lane 1), Δ16 (lane 2) and L8A/S9A/L10A (lane 3) co-purified complexes. Calculated values were 0.89, 0.96 and 0.89, respectively, indicating equal concentrations of the two proteins for each sample. α-AdoMetDC (32kDa), β-AdoMetDC (8-10kDa) and prozyme (37kDa).

A.

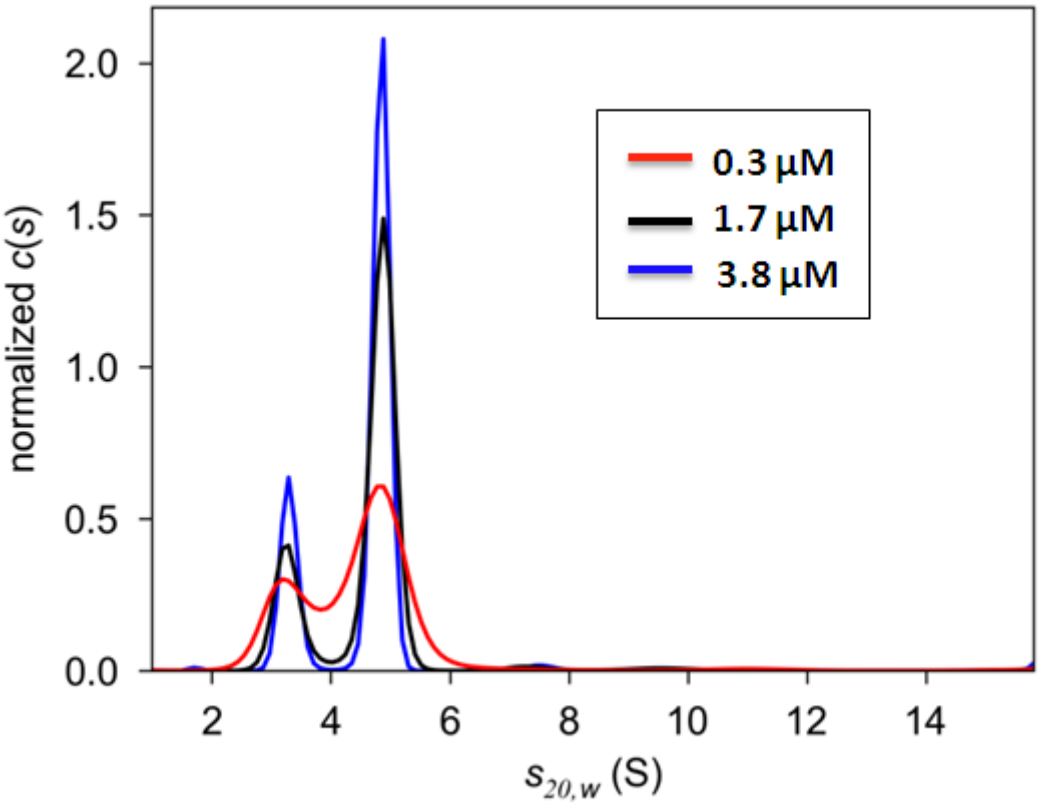

B.

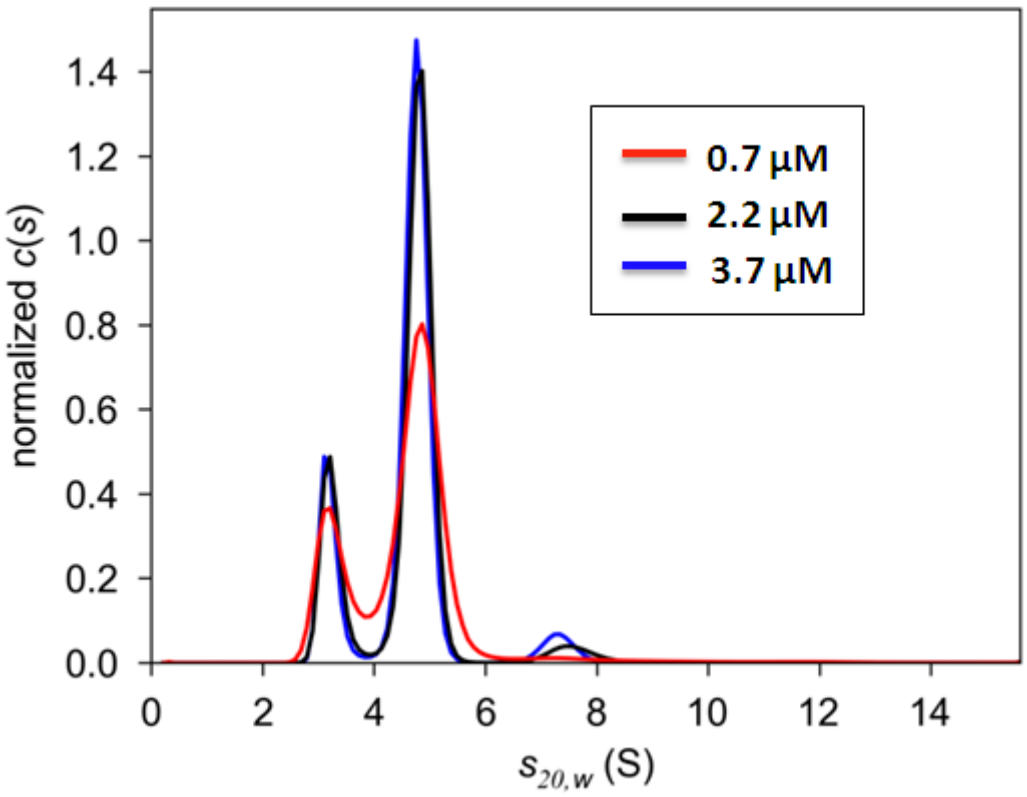
normalized c(s)
1.4
1.2
1.0
0.8
0.6
0.4
0.2
0.0
0
2
4
6
8
10
12
14
$s_{20,w}$ (S)
0.7 µM
2.2 µM
3.7 µM

C.

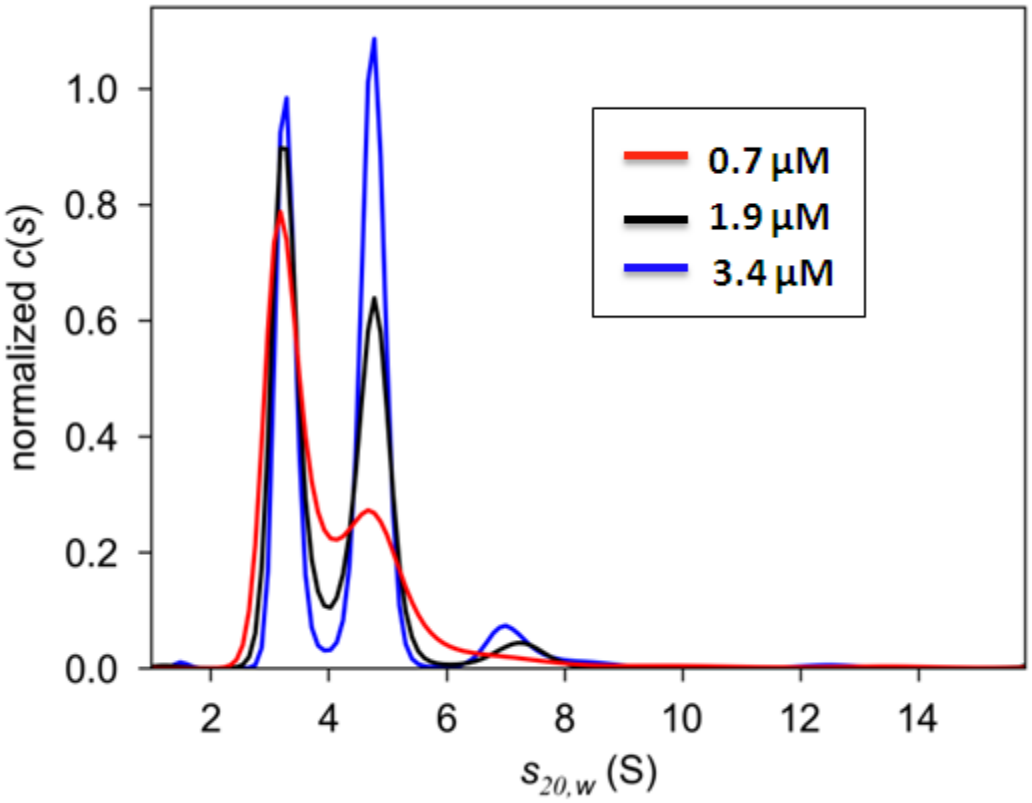
normalized c(s)
1.0
0.8
0.6
0.4
0.2
0.0
2
4
6
8
10
12
14
$s_{20,w}$ (S)
0.7 µM
1.9 µM
3.4 µM

D.

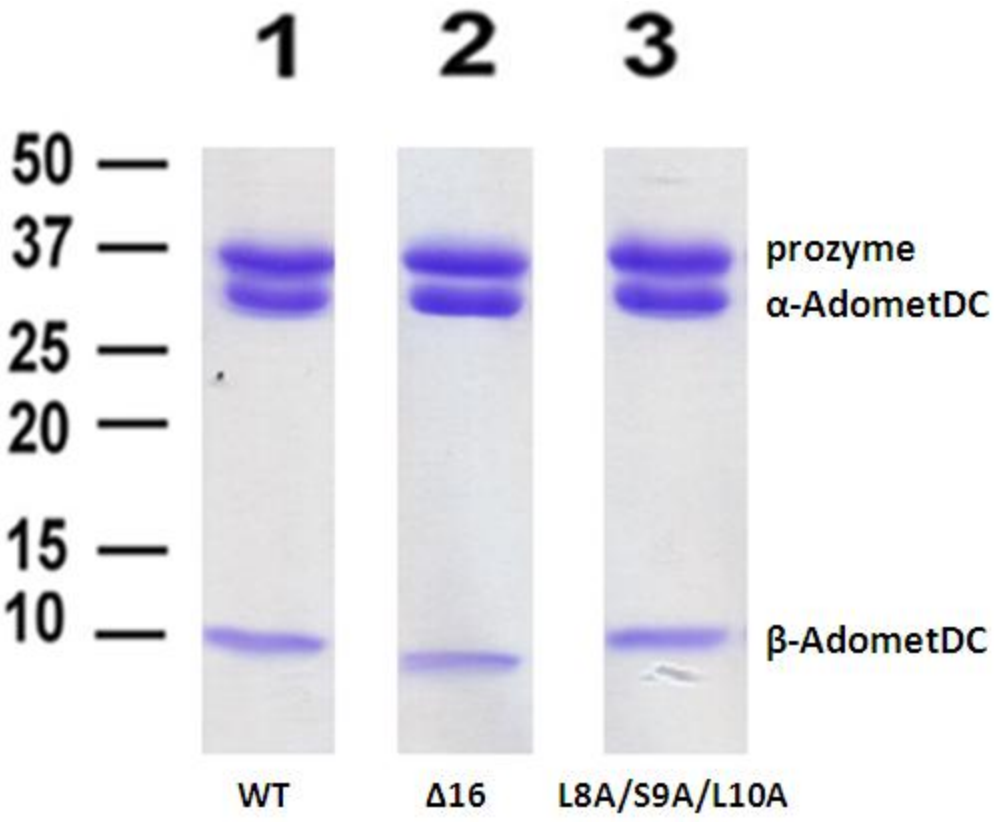
1
2
3
50
37
25
20
15
10
prozyme
α-AdometDC
β-AdometDC
WT
Δ16
L8A/S9A/L10A

Figure 3.4. Test for dimerization impairment of mutant *T. brucei* AdoMetDC/prozyme heterodimers.

Graph represents the μmoles per minute obtained as a function of enzyme concentration for the (A) Δ16 and (B) L8A/S9A/L10A AdoMetDC/prozyme heterodimers.

A.

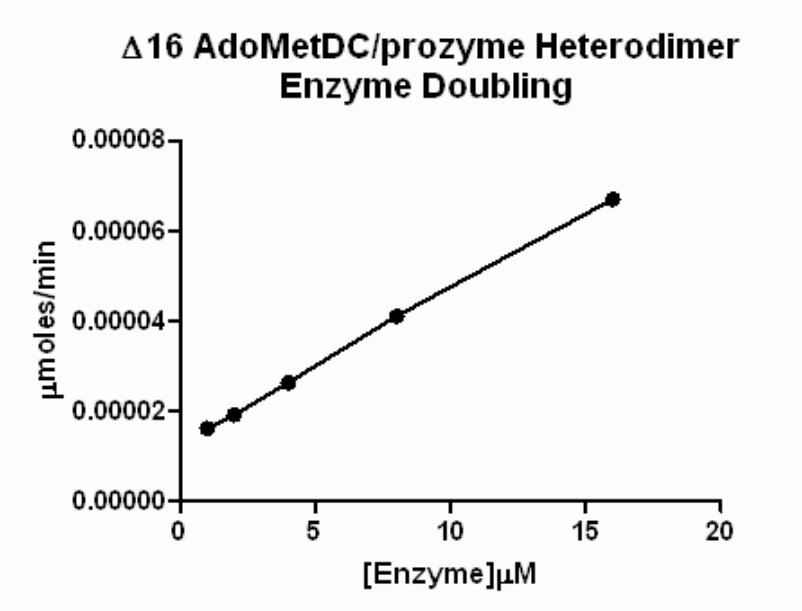
Δ16 AdoMetDC/prozyme Heterodimer
Enzyme Doubling
µmoles/min
0.00008
0.00006
0.00004
0.00002
0.00000
0
5
10
15
20
[Enzyme]µM

B.

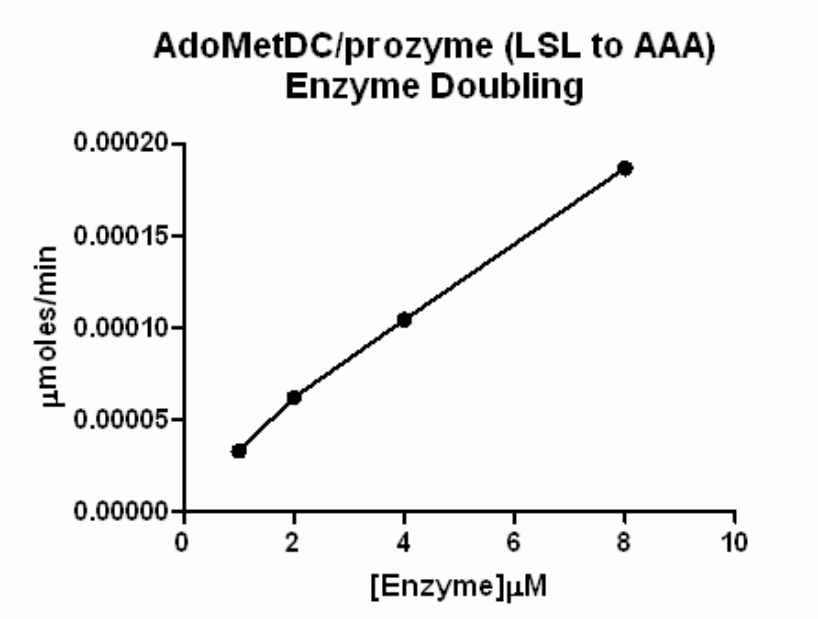
AdoMetDC/prozyme (LSL to AAA)
Enzyme Doubling
µmoles/min
0.00020
0.00015
0.00010
0.00005
0.00000
0
2
4
6
8
10
[Enzyme]µM

Figure 3.5. Catalytic efficiency of different *T. brucei* AdoMetDCs co-purified with either wild-type or Δprozyme

Bar graphs represent k_{cat}/K_m ($M^{-1}s^{-1}$) values for the *T.brucei* enzymes in the presence (purple) and absence (blue) of 5mM putrescine. WT=wild-type, Ado= AdoMetDC, proz= prozyme and HT=heterodimer.

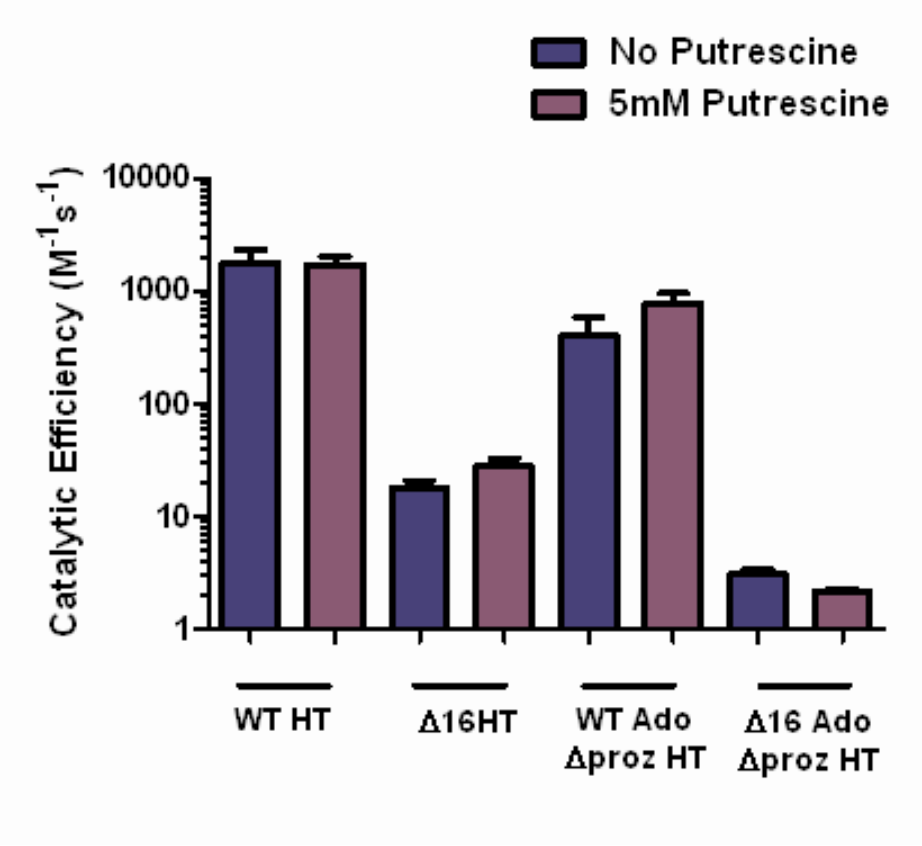
No Putrescine
5mM Putrescine
Catalytic Efficiency ($M^{-1}s^{-1}$)
10000
1000
100
10
1
WT HT
Δ16HT
WT Ado Δproz HT
Δ16 Ado Δproz HT

Figure 3.6. Tertiary structure analysis

(A, left) Human AdoMetDC monomeric structure. In light blue is the α-subunit, and in dark blue the β-subunit. Highlighted in red are essential active site residues. (A, right) Superimposed monomeric structures of human and *T. brucei* (obtained from homology modeling) AdoMetDC. The trypanosomatid protein is represented in magenta and the N-terminal region is highlighted in green. (B) Hypothetical model for *T. brucei* AdoMetDC activation.

A.

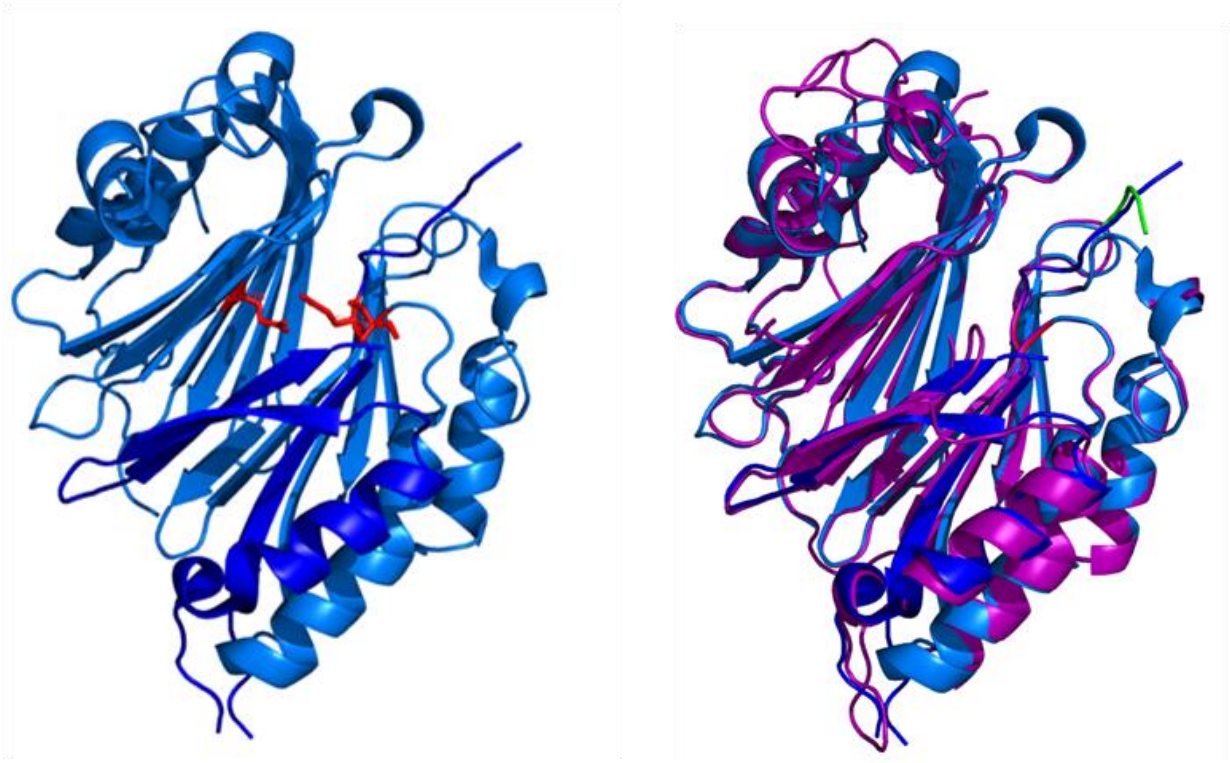

B.

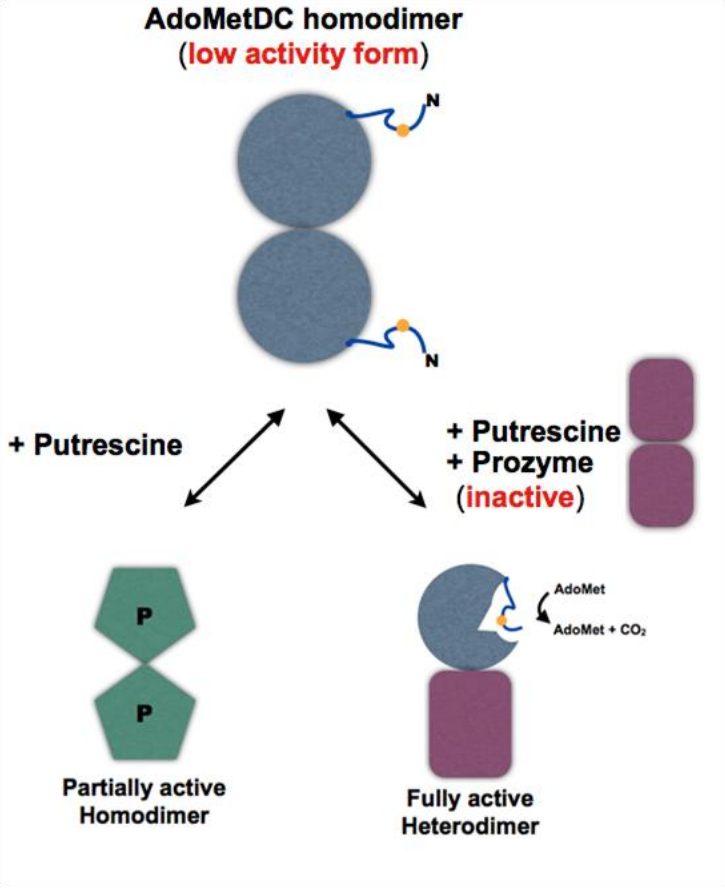
AdoMetDC homodimer
(low activity form)
N
N
+ Putrescine
+ Putrescine
+ Prozyme
(inactive)
P
P
Partially active
Homodimer
AdoMet
AdoMet + CO2
Fully active
Heterodimer

Table 3.2. Steady-state kinetic analysis of wild-type and several mutant *T. brucei* AdoMetDC enzymes.

	5 mM Putrescine			No Putrescine		
Enzyme	k_{cat} (s^{-1})	K_m(mM)	k_{cat}/K_m($M^{-1}s^{-1}$)	k_{cat} (s^{-1})	K_m(mM)	k_{cat}/K_m($M^{-1}s^{-1}$)
WT AdoMetDC homodimer	0.0065±0.0004	0.14±0.04	46±12	0.0058±0.0003	0.40±0.06	15±2
WT AdoMetDC/prozyme	0.21±0.01	0.13±0.02	(1.7±0.3)x 10^3	0.25±0.02	0.14±0.02	(1.8±0.5)x 10^3
Δ16 AdoMetDC homodimer	>0.03	>2	*16±3	>0.032	>2	*16±11
Δ16 AdoMetDC/prozyme	0.017±0.001	0.60±0.1	28±5	0.014±0.001	0.80±0.1	18±3
AdoMetDC(KDS-AAA)/prozyme	0.33±0.07	0.60±0.3	(5.7±0.3)x 10^2	0.071±0.005	0.37±0.07	(1.9±0.4)x 10^2
AdoMetDC(LSL-AAA)/prozyme	0.011±0.001	1.2±0.2	9.0±1.0	>0.01	>2	*5.1±0.5
AdoMetDC(MAM-AAA)/prozyme	0.026±0.002	0.31±0.08	85±22	>0.01	>2	*4.8±0.1
AdoMetDC(WGS-AAA)/prozyme	0.10±0.01	0.30±0.1	(2.8±0.1)x 10^2	0.18±0.04	1.0±0.5	(1.7±0.8)x 10^2
AdoMetDC(L8A)/prozyme	0.12±0.003	0.45±0.03	(2.5±0.2)x 10^2	>0.03	>2	*16.6±0.5
AdoMetDC(S9A)/prozyme	0.29±0.02	0.90±0.1	(3.4±0.5)x 10^2	0.23±0.01	1.4±0.1	(1.8±0.2)x 10^2
AdoMetDC(L10A)/prozyme	0.084±0.009	0.22±0.08	(3.8±0.1)x 10^2	>0.10	>2	*50±9
WT AdoMetDC/Δprozyme	0.15±0.01	0.20±0.04	(7.7±0.2)x 10^2	0.23±0.04	0.60±0.20	(4±1)x 10^2
Δ16 AdoMetDC/Δprozyme	>0.004	>2	*2.2±0.1	>0.006	>2	*3.1±0.3

Note: (*) Denotes kinetic experiments in which substrate saturation was not observed. k_{cat}/K_m($M^{-1}s^{-1}$) values were determined through linear regression (slope) of the velocity versus substrate plots and the highest substrate concentration tested was used to determine a lower estimate of K_m and k_{cat}.

CHAPTER 4

CHARACTERIZATION OF THE *LEISHMANIA MAJOR* ADOMETDC/PROZYME COMPLEX AND CROSS-SPECIES ANALYSES

Introduction

Trypanosomatids are a group of single-cell flagellate protozoa, known to cause many detrimental diseases in humans and other animals, as well as plants. Members of this group are exclusively parasitic, and most commonly found in insects. They belong to the Kinetoplastea class and have several unique features that make them peculiar organisms [117]. For example, they contain a kinetoplast, which is an arrangement of circular DNA inside a large mitochondrion, and carry out a complex form of mitochondrial RNA editing. Additional important characteristics include polycistronic transcription of all protein-encoding genes, *trans*-splicing of all mRNA transcripts, the glycolytic pathway within glycosomes, *Trypanosoma brucei* variable surface glycoproteins and *Trypanosoma cruzi* ability to escape from the phagocytic vacuoles [117].

The most important human pathologies associated with the trypanosomatid species are African trypanosomiasis, also known as sleeping sickness and caused by *Trypanosoma brucei*; south American trypanosomiasis, also known as Chagas disease and caused by *Trypanosoma cruzi*; and leishmaniasis, which comprises a set of diseases caused by various species of *Leishmania* [118]. Altogether, it is estimated that about 37 million people are infected with these parasites [117]. Unfortunately, current therapies are limited, not very effective and poorly tolerated by the patients. Thus, the development of safer drugs is urgent.

Leishmaniasis, in particular, is one of the major insect-borne diseases in developing countries and affects about 350 million people [117, 119]. A human that gets infected with pathogenic *Leishmania* could acquire a spectrum of diseases, normally divided into cutaneous (CL), diffuse cutaneous (DCL), mucocutaneous (MCL) and visceral leishmaniasis (VL), which is the most severe form and can be lethal if untreated. The parasites are transmitted to the human

host through the bite of a sand fly. During a blood meal they are injected as a metacyclic promastigote stage, phagocytized by macrophages and differentiated into the intracellular amastigote form. Subsequently, parasites proliferate in the infected cells and affect different tissues, depending on the *Leishmania* specie involved. The outcome of the infection is also determined by host genetic factors and the immune response [120].

The sub-specie *Leishmania major* causes the most common form of the disease, cutaneous leishmaniasis (CL), which is considered non-life threatening and usually cures spontaneously without any treatments. However, there have been reports of severe cases caused by *L. major* in Afghanistan. Current therapies include 200 mg of oral fluconazole, which is normally used for treating fungal infections, given daily for six-weeks [121]. Some clinical trials were performed in Iran, and showed that 400 mg of fluconazole were significantly more effective than 200 mg for curing cutaneous leishmaniasis [122]. However, it is not known if patients with CL caused by other *Leishmania* species can also be responsive to fluconazole.

The polyamine biosynthetic pathway has been a crucial tool for the development of anti-proliferative and anti-trypanosomal therapies. Inhibition of the biosynthetic enzymes has proven to be a successful approach and the best example is the clinical use of α-Difluoromethylornithine (DFMO), a suicide inhibitor of ornithine decarboxylase (ODC), for the treatment of African trypanosomiasis. DFMO has proven efficacy against other genera of protozoan parasites including *Plasmodium* species [123, 124], *Giardia* [125], and *Leishmania* as well [126, 127]. Importantly, from the trypanosomatids group, *T.cruzi* is the only parasite that does not encode an ODC gene, and therefore DFMO is not effective for treating Chagas disease [58]. The polyamine biosynthetic pathway of *Leishmania*, similar to *T. brucei* is composed of three main enzymes: ODC, ADOMETDC, and spermidine synthase (SPDSYN). Their genome do not encode a

spermine synthase gene, thus they lack spermine, which is a major polyamine in the mammalian host [126]. Genetic depletion of *ODC*, *ADOMETDC*, or *SPDSYN* in *L. donovani* promastigotes demonstrated the importance of these enzymes for parasite viability and proliferation [38-40].

During polyamine biosynthesis, AdoMetDC is in charge of catalyzing the decarboxylation of S-adenosylmethionine (AdoMet) and producing the amino propyl group that will be used for the formation of spermidine from putrescine. AdoMetDC belongs to the specific group of enzymes that utilize a covalently-bound pyruvate group as a cofactor during the decarboxylation event. This pyruvate is generated by an auto processing reaction, which also leads to cleavage of the peptide bond into the α and β chains. The human AdoMetDC enzyme is a homodimer (α2β2), the activity from which is allosterically stimulated by putrescine. Our lab recently demonstrated that the trypanosomatid AdoMetDC is allosterically activated by heterodimer formation with a catalytically dead homolog, designated prozyme, which is present only in these species [57]. Prozyme is neither processed to generate the pyruvute cofactor, nor does it display any activity on its own. However upon binding, prozyme stimulates AdoMetDC activity by $>10^3$-fold. Putrescine does not seem to have a strong effect on the activity of the *T. brucei* heterodimer, as opposed to the human homodimeric enzyme. Importantly, prozyme protein expression levels are regulated in *T. brucei*, providing a mechanism to control pathway flux that is unique to these parasites [33].

The genomes of the trypanosomatids (*T.brucei, T.cruzi* and *Leishmania*) all contain the sequence for both a functional AdoMetDC and a catalytically dead prozyme. However, only the *T. brucei* and *T. cruzi* heterodimers have been characterized. Willert et al. demonstrated that the *T. cruzi* prozyme also stimulates the activity the respective AdoMetDC, although in contrast to the *T. brucei* enzyme, the activity of the *T. cruzi* heterodimer is putrescine-dependent [58]. In

this chapter, we evaluate the ability of *L. major* AdoMetDC and prozyme to form a fully active complex, and compare it to the *T.brucei* and *T.cruzi* heterodimers. Results demonstrate that, although a heterodimeric complex could not be obtained by our standard purification methods, *L. major* prozyme is able to stimulate, by 170-fold, the activity of the respective AdoMetDC when both subunits are mixed together. Previous studies also demonstrated that prozyme and AdoMetDC from *T. brucei* and *T. cruzi* are able to form functional cross-species heterodimers, indicating that the dimer interface and mechanism of activation are conserved between the species [58]. Thus, the catalytic activity of mixed-complexes from *T. brucei*, *T. cruzi* and *L. major* species was also evaluated, and resulted in fully active enzymes further stimulated by putrescine.

Experimental Procedures

AdoMetDC and Prozyme Constructs

L.major AdoMetDC and prozyme, genes were amplified by PCR from genomic DNA, using specific primers (**Table 4.1**), and each ligated into the pET15b (Novagen, San Diego, CA) expression vector to generate N-terminal His_6-tag fusions. For purposes of co-purification, a pT7-Flag1-prozyme expression construct was provided by Oleg Volkov. Cross-species analyses were performed using the *T. cruzi* pODC29-AdoMetDC and pET15b-prozyme [58]; and T. *brucei* pET15b-AdoMetDC and pET15b-prozyme [57] plasmids, all provided by Erin Willert and which contain N-terminal His_6-tag fusions. All constructs were properly sequenced before proceeding to do kinetic analyses.

Protein Expression and Purification

E.coli BL21/DE3 cells were transformed with the construct of interest and grown at 37°C until OD_{600} reached between 0.6 - 0.8. Protein expression was induced by the addition of 0.2mM IPTG and cells were grown overnight at 20°C. Cells were harvested by centrifugation and resuspended in lysis buffer (50mM Hepes, 100mM NaCl, 10mM Imidazole, 5mM β-mercaptoethanol). Protease inhibitors were added directly to the cell lysate (Cocktail 1 (1:1000)- 1mg/mL Leupeptin, 2mg/mL Antipain and 10mg/mL Benzamidine; Cocktail 2 (1:1000)- 1mg/mL Pepstain, 1mg/mL Chymostatin; and 0.2M Phenylmethyl-sylfonyl fluoride (PMSF) in a 1:500 ratio) (Sigma, St.Louis, MO). Bacterial cells were lysed using an EmulsiFlex-C5 homogenizer, followed by centrifugation (Beckman Ti-45 rotor) at 15,000rpm for 30min. The soluble fraction was subjected to Ni^{2+} -agarose (Qiagen, Valencia, CA) column chromatography (Buffer A: 50mM Hepes pH 8, 100mM NaCl, 1mM β-mercaptoethanol, 10mM Imidazole; Buffer B: 50mM Hepes pH 8, 100mM NaCl, 1mM β-mercaptoethanol, 800mM Imidazole), as previously described [57, 66]. We attempted to obtain the *Leishmania major* heterodimeric complex by mixing the separate lysates and co-purifying the His_6- tagged AdoMetDC with the Flag-tagged prozyme. The protein containing fractions were pooled together, concentrated and diluted back in buffer A, to remove excess imidazole. Subsequently, anion-exchange column chromatography was performed for further cleaning, as previously described [57, 66]. Extinction coefficients (AdoMetDC: 61.3 $mM^{-1}cm^{-1}$, prozyme: 26.9 $mM^{-1}cm^{-1}$, determined by ExPASy Prot Param) from each enzyme were used to obtain protein concentration after measuring absorbance at 280nm. These calculations were performed by using the Beer's law equation ($A=\varepsilon lc$, where A is absorbance, ε is extinction coefficient, l is the path lengh and c is concentration).

Western Blot

To start the analysis 50ng of each recombinant protein were loaded per lane, separated by 12% SDS/PAGE, and subsequently transferred to a PVDF membrane (Hybond-P; Amersham). Membranes were blocked with 5% non-fat dry milk in Tris-buffered saline (TBS: 20 mM Tris-HCl, 137 mM NaCl, pH 7.6), overnight at 4ºC with gentle agitation. Then, blots were incubated with mouse monoclonal antibodies to His_6 and Flag tags at 1:1,000 for 1 hour at room temperature with gentle agitation. After three washes with TBS-T (0.1% Tween-20 added), blots were incubated with Horseradish peroxidase-linked donkey anti-mouse at 1:10,000 for 1 hour at room temperature. Blots were washed again with TBS-T and the antigen was visualized by using the ECL Western Blotting Analysis system (Amersham).

Steady-state Kinetic Analysis

The enzymatic activity of *L. major* AdoMetDC was assessed using a $^{14}CO_2$-based method. A constant amount of AdoMetDC (1 µM for homodimer; and 0.1/1 µM AdoMetDC/prozyme for the mixed complex) was titrated into reactions containing 25µM $^{14}CO_2$-AdoMet (American Radiolabeled Chemicals), a range of unlabeled AdoMet concentrations (25-1475 µM, Affymetrix), 100mM Hepes pH 8, 50mM NaCl, 1mM DTT and 5mM putrescine (analyses were also performed in the absence of putrescine). Test tubes were capped and placed in a water bath at 37ºC. The CO_2 liberated from the substrate would get trapped on a filter paper soaked in 80 µL of saturated $Ba(OH)_2$. After 5 minutes, reactions were quenched using 6M HCl.

The filter paper was then transferred to a scintillation vial containing 5mL of CytoScint. Samples were placed on the scintillation counter, and the counts per minute (cpm) obtained were converted into velocity (s^{-1}) values using the specific activity of the substrate. Data was fitted to the Michaelis-Menten equation to determine the steady-state kinectic parameters (k_{cat}, K_m) using Prism (GraphPad, San Diego, CA). Cross-species analyses were performed similarly. In that particular case, AdoMetDC and prozyme from different trypanosome species were added to the reaction in a 1:10 ratio of AdoMetDC to prozyme.

Results

L. major Prozyme is Able to Activate AdoMetDC from the Same Trypanosomatid Specie, Although Complex Formation Could not be Assessed through our Standard Purification Methods

From the trypanosomatids group, only the *T. brucei* and *T. cruzi* heterodimers have been characterized. Thus, in order to determine if the *L. major* AdoMetDC activity is also stimulated by the respective prozyme, enzymes were first expressed and purified from *E. coli*. *L. major* AdoMetDC undergoes a self-processing reaction to generate the active enzyme consisting of two chains, α (~34kDa) and β (~10 kDa), while prozyme runs as a single polypeptide chain with similar molecular weight as the AdoMetDC α-subunit (33kDa) (**Fig 4.1A**). To assess complex formation, His_6-tagged AdoMetDC and Flag-tagged prozyme protein lysates were mixed together and then co-purified by Ni^{2+}-agarose and anion exchange column chromatography. As fractions were collected after each purification step and analyzed through SDS-PAGE, only a

single band was observed, running close to 34kDa. However, since *L.major* α-AdoMetDC and prozyme have such similar molecular weights, we thought we might not be able to distinguish them easily on the coomassie stained gel. Thus, western blots analyses were performed using anti-His_6 (AdoMetDC) and anti-Flag (prozyme) to corroborate the presence of the homolog (**Fig 4.1B**). Results demonstrate that in the heterodimeric sample no prozyme was detected. There are two potential reasons for this issue, either the *L.major* prozyme does not bind to AdoMetDC, and therefore is not necessary for enzyme activation, or our purification approach is somehow not suitable for obtaining the heterodimeric complex.

Steady-state kinetic analyses were then performed in both *L. major* homodimeric and heterodimeric enzymes, to evaluate the ability of prozyme to stimulate AdoMetDC activity. In this particular case, the "heterodimeric" sample was obtained by mixing individually purified AdoMetDC and prozyme in the test tube. There was a requirement for excess prozyme to be used, since it has a tendency to aggregate [57]. Results indicated, as previously observed for other species homodimers [49, 57, 58], that the catalytic efficiency (k_{cat}/K_m) of *L.major* AdoMetDC was stimulated 8-fold by putresine (**Fig 4.2 and Table 4.2**). However, if it is true that this enzyme does not need prozyme to be catalytically efficient, we would expect higher rate numbers (k_{cat} = 0.0203 s^{-1}). If we compare it to the human AdoMetDC (k_{cat} = 2.6 s^{-1} and k_{cat}/K_m= 44,000 $M^{-1}s^{-1}$, in the presence of 5 mM putrescine [49]), which is fully active as a homodimer, the efficiency of the trypanosomatid enzyme is more than 300 times lesser. Interestingly, when prozyme is mixed with AdoMetDC, the homolog is able to further activate the enzyme, increasing its catalytic efficiency by 170-fold, when compared to the homodimer in the absence of putrescine, and by 40-fold in the presence of 5mM putrescine. In general, prozyme seems to have a strong effect on enzymatic rate (k_{cat}), while putrescine influences K_m (**Table 4.2**).

Normally this polyamine is associated with a decrease in K_m, as it is observed for the *L.major* homodimer. However, in the mixed complex the K_m seems to be higher when putrescine is present, although the rate increases by 10-fold.

These results demonstrate that *Leishmania* species also require prozyme to activate AdoMetDC. Thus, the fact that we could not co-purify a stable heterodimeric complex implies that the purification approach needs to be modified.

L. major AdoMetDC and Prozyme can Form Functional Swapped Complexes with other Species

AdometDC stimulation by a catalytically dead homolog, which is only present in the trypanosomatids, could represent a common mechanism for enzyme activation in these species. In fact, previous studies demonstrated that cross-species heterodimers of *T. cruzi and T. brucei* AdoMetDC and prozyme are functional, and that putrescine is required for full activation of these mixed species complexes [58]. Thus, in order to determine if swapped complexes of *L.major* AdoMetDC and prozyme with the other trypanosomatid species could also be efficient, we performed some steady-state kinetic analyses. All enzymes were purified individually and mixed in the reaction, with the same requirement for prozyme to be present in excess (1:10, AdoMetDC: prozyme). Results demonstrated that *L.major* AdoMetDC can be activated by *T. cruzi* and *T. brucei* prozymes, resulting in a 160 and 320-fold increase in catalytic efficiency, respectively (**Fig 4.3**). Putrescine further stimulates catalysis of these swapped complexes by having an effect on both k_{cat} and K_m (**Table 4.3**). *L. major* prozyme is also able to stimulate activity of *T. cruzi* AdoMetDC, although it strongly depends on the presence of putrescine.

Interestingly, not a significant increase in activity, even with putrescine, was observed when *T. brucei* AdoMetDC was mixed with *L. major* prozyme.

Discussion

Diseases caused by the trypanosomatid species threaten the life of many people each year. The polyamine biosynthetic pathway in these parasites has been a crucial tool for the development of drugs, particularly through the inhibition of key enzymes involved in the process. The recent discovery that *T. brucei* AdoMetDC activity is stimulated by $>10^3$-fold upon heterodimer formation with an inactive homolog, which is present only in the trypanosomatids, represents an alternative for further exploitation of this enzyme as a drug target. Importantly, this strong activation is also observed in *T. cruzi*, implying that it could be a common mechanism for AdoMetDC regulation in these species. The studies described herein demonstrate that the *L.major* prozyme is also able to stimulate the catalytic activity of the respective AdoMetDC, as assessed by mixing individually purified enzymes and evaluating kinetic parameters. Similar to the *T. cruzi* heterodimer [58], stimulation the *L.major* complex is more pronounced in the presence of putrescine. In addition, we showed that particular swapped complexes containing AdoMetDC and prozyme from different species (*T. brucei*, *T. cruzi* and *L.major*) are functional and, in some cases, need putrescine for better activation. Thus, prozyme requirement for AdoMetDC regulation is in fact characteristic of all trypanosomatids, and can be utilized as a means for selectively interfering with parasite survival in the human host.

Unfortunately, a stable heterodimeric complex could not be obtained by our standard purification approach. Previous studies demonstrated that the *T. brucei* and *T. cruzi* heterodimers form with very high affinity (<0.5μM), and were easily obtained following a similar protocol. There is a possibility that the *L.major* prozyme binds less tightly to AdoMetDC, and purification conditions used at some point could have been too stringent, affecting either essential interactions at the dimer interface or proper folding. Careful optimization must be performed in order to overcome this problem. However, this situation is not representative of the ability of prozyme to activate AdoMetDC in *Leishmania* species, as demonstrated by the kinetic data obtained after mixing the subunits.

Even though no crystal structure is currently available for any of the trypanosomatid heterodimeric enzymes, our observations and the fact that some swapped-species complexes are functional lead us to assume that the amino acid residues essential for the activation mechanism are conserved in all three parasites. In fact, the structural basis for the activation of AdoMetDC by prozyme was assessed in Chapter 3, particularly in *T. brucei* parasites. We demonstrated that the *T. brucei* AdoMetDC N-terminus is necessary for proper activation by prozyme and might be involved in any associated conformational changes. Specifically, residues L8 and L10 strongly influenced catalysis, but did not seem to play a role in dimerization, suggesting that they might be acting through an allosteric regulatory mechanism. Sequence alignment of the trypanosomatid AdoMetDCs shows that they all contain this N-terminal extension and the essential leucine residues are fully conserved among them. Additional analyses in *T. cruzi* and *L.major* AdoMetDCs would be necessary to determine if truncation of the N-terminus and/or mutation of these key amino acids also results in the inability of prozyme to stimulate catalysis, providing further proof of a general mechanism to regulate enzyme activity in these parasites.

Putrescine is known to stimulate the activity of the human and all trypanosomatid AdoMetDC homodimers. Interestingly, while this polyamine has no effect on the *T. brucei* heterodimer, it stimulates the activity of the *T. cruzi* and *L. major* complexes. These differences are difficult to explain since the putrescine-binding site is not very well established in the trypanosomatid AdoMetDCs. Based on the amino acids known to be essential for binding of this polyamine to the human enzyme (D174, E178, E256 and K80), Clyne et al. identified the corresponding residues in *T. cruzi* and performed a detailed mutational analysis to determine if the putrescine-binding site was fully conserved between the two species [113]. Results demonstrated that it is not, since only D174 seems to play an important role in putrescine binding to *T. cruzi* AdoMetDC and stimulating its activity, while the remaining key residues had no effect. Interestingly, D174 is also conserved in *T. brucei* and *L. major* AdoMetDCs and must have a similar function. It should be noted that this analysis is based in the homodimeric enzymes. Upon binding of prozyme, differences are observed between the trypanosomatids regarding putrescine stimulation, even though D174 is conserved between them. The explanation to this observation could be more physiological, based on the different environments in which these parasites grow and replicate in the human host [58]. *T. brucei* is an extracellular pathogen that lives in the bloodstream, where polyamine levels are low, and thus they might have been adapted to this deficit. In the contrary, *T. cruzi* and *L. major* parasites replicate intracellularly, usually a good source of polyamines, and the fact that putrescine regulates AdoMetDC/prozyme activity in these species might be due to their localization. The observation that *L.major* prozyme can activate *T. cruzi* AdometDC, but not *T. brucei* AdoMetDC, could also be explained by these environmental differences.

Our findings support, together with previous data [57, 58], that trypanosomatid species share a common mechanism to regulate AdoMetDC, which is mediated by the catalytically dead homolog, prozyme. There is an urgent need for more detailed structural information, to further understand this unique activation, and exploit it as a huge alternative for the development of more selective inhibitors. These compounds could potentially become drugs that can target not one, but several life-threatening diseases caused by each of the parasite species that belong to the trypanosomatid group.

Table 4.1. Primer sequences and restriction sites

Construct (Optimized Gene)	Restriction Site	Primer Sequence
pET15b-AdoMetDC	BamH1(F), NdeI(R)	Forward (5’ to 3’): GCAAAACATATGAACGTCTGCTCGAACACC Reverse (5’to 3’): CGTTTTGGATCCCTAGTCGGGCCCACTTTTGGC
pET15b-prozyme	BamH1(F), NdeI(R)	Forward (5’ to 3’): GCAAAACATATGTCGCTGTGGGGAGGGTTTTCG Reverse (5’to 3’): CGTTTTGGATCCTCAATCTGCGCTGCGGGC

Figure 4.1. Evaluation of *Leishmania major* AdoMetDC, prozyme and AdoMetDC/prozyme protein purifications

(A) SDS-PAGE analysis. α-AdoMetDC corresponds to the ~34kDa band, and His_6-tagged β-AdoMetDC to the ~10kDa band observed in lane 1. Recombinant His_6-tagged prozyme migrates close to 33kDa, which corresponds to the single band in lane 2. Results from co-purification (His_6-tagged AdoMetDC and Flag-tagged prozyme) are presented in lane 3; potentially indicating that prozyme is not present in the protein sample. HM= homodimer (B) Western blot analysis. 50ng of recombinant protein were loaded per lane, and different blots were probed with either anti-His_6 or anti-Flag antibodies. Lane 1 corresponds to purified recombinant *L.major* AdoMetDC, and the band observed represents the His_6-tagged β-subunit. Lane 2 corresponds to the co-purified *L. major* complex. His_6-tagged β-AdoMetDC was detected when the blot was probed with anti- His_6, but nothing was observed after it was probed with anti-Flag (lane 4), indicating the absence of prozyme in the co-purified sample. In lane three the co-purified *T. brucei* complex, containing a Flag-tagged prozyme, was loaded as a control for the Flag antibody and a nice band is observed around 37kDa.

A.

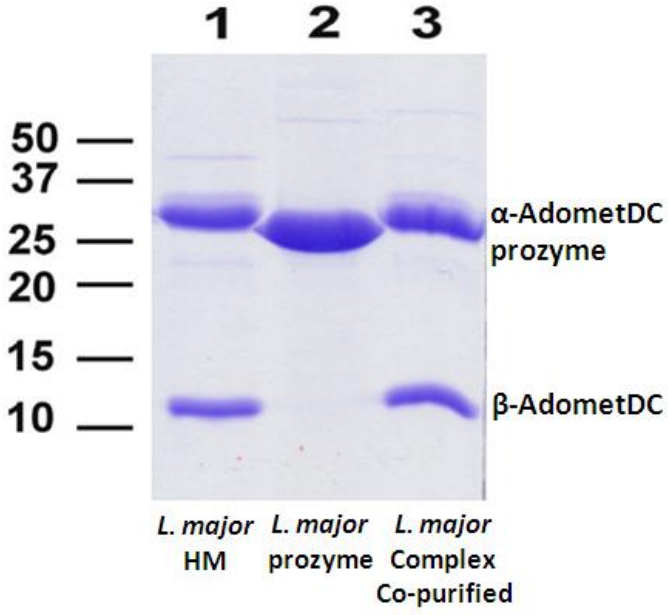
1
2
3
50
37
25
20
15
10
α-AdometDC
prozyme
β-AdometDC
L. major HM
L. major prozyme
L. major Complex Co-purified

B.

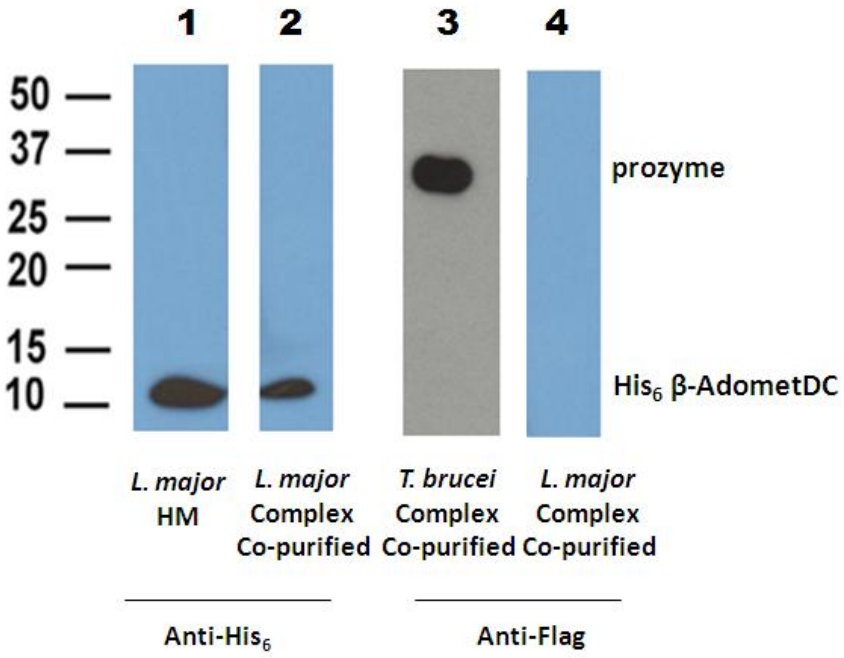
1
2
3
4
50
37
25
20
15
10
prozyme
His6 β-AdometDC
L. major HM
L. major Complex Co-purified
T. brucei Complex Co-purified
L. major Complex Co-purified
Anti-His6
Anti-Flag

Figure 4.2. Catalytic efficiency of *Leishmania major* AdoMetDC and the AdoMetDC/prozyme mixed complex

Bar graphs represent k_{cat}/K_m ($M^{-1}s^{-1}$) values for the *L.major* enzymes in the presence (purple) and absence (blue) of 5mM putrescine.

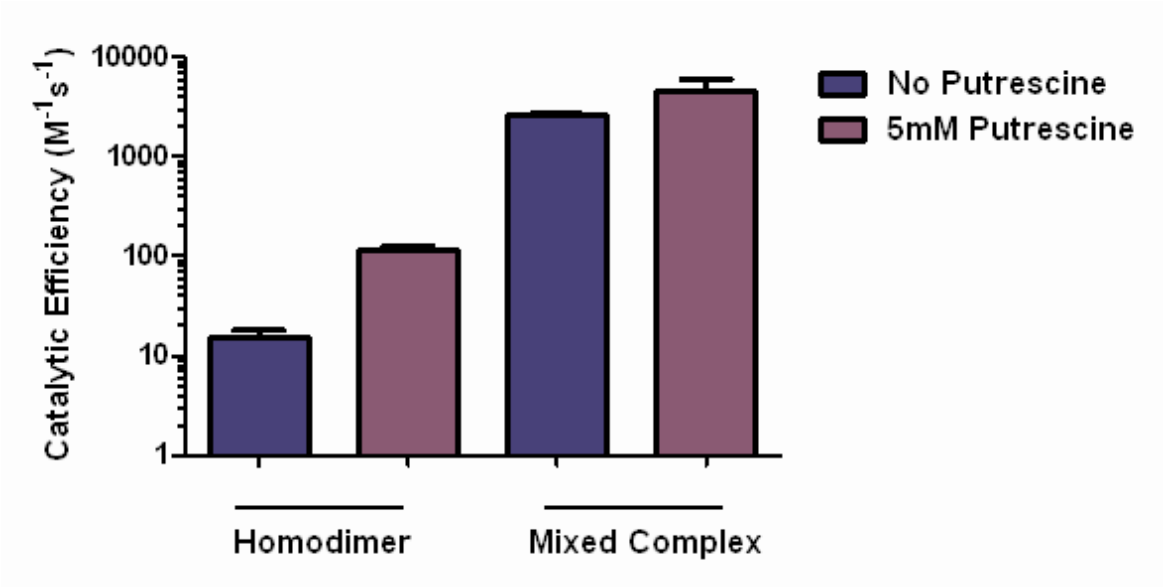
Catalytic Efficiency ($M^{-1}s^{-1}$)
10000
1000
100
10
1
No Putrescine
5mM Putrescine
Homodimer
Mixed Complex

Table 4.2. Steady-state kinetic analysis of the *Leishmania major* AdoMetDC homodimer and the AdoMetDC/prozyme mixed complex

	5mM Putrescine			No Putrescine		
Enzyme	**k_{cat} (s^{-1})**	**K_m(mM)**	**k_{cat}/K_m ($M^{-1}s^{-1}$)**	**k_{cat} (s^{-1})**	**K_m(mM)**	**k_{cat}/K_m ($M^{-1}s^{-1}$)**
L. major AdoMetDC	0.0203±0.0005	0.18±0.02	113±13	0.018±0.002	1.2±0.2	15±3
L. major AdoMetDC/prozyme (mixed)	1.0±0.1	0.22±0.07	(5±1)x 10^3	0.131±0.006	0.05±0.01	(2.6±0.1)x 10^3

Figure 4.3. Catalytic efficiency of several AdoMetDC and prozyme swapped-species complexes

Bar graphs represent k_{cat}/K_m ($M^{-1}s^{-1}$) values for each mixture in the presence (purple) and absence (blue) of 5mM putrescine. *Denotes data taken from [58] for comparison purposes. *Tb= T.brucei, Tc=T.cruzi, Lm=L.major,* A=AdoMetDC and p=prozyme.

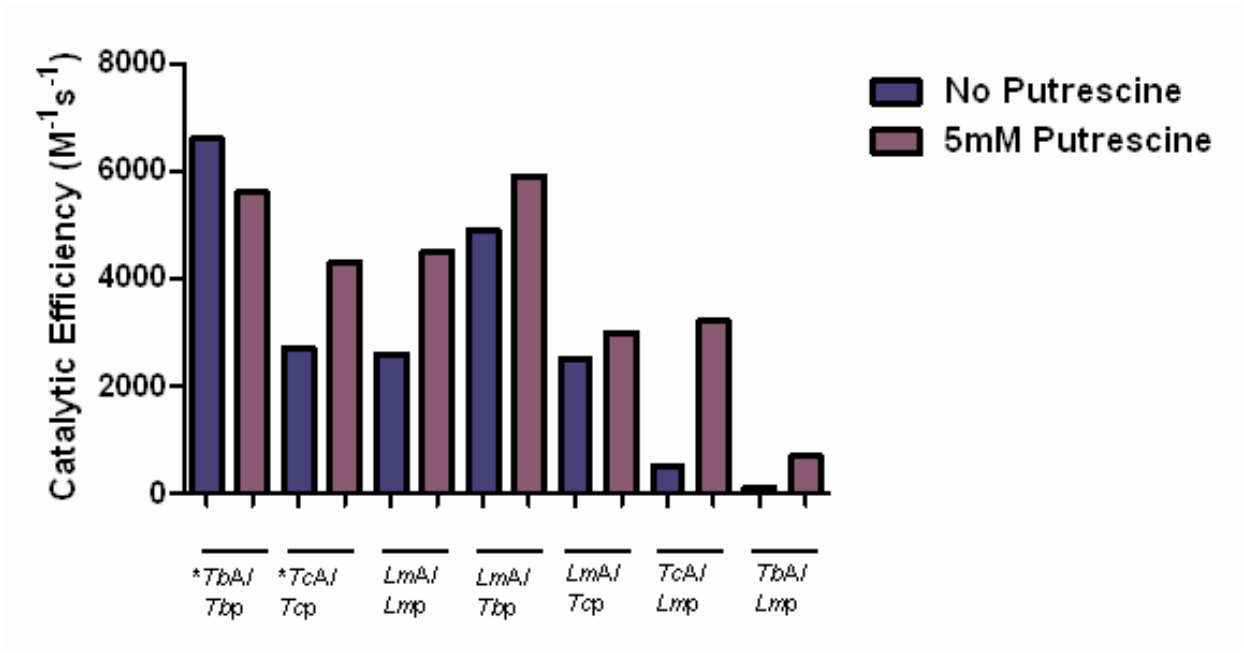
Catalytic Efficiency ($M^{-1}s^{-1}$)
8000
6000
4000
2000
0
No Putrescine
5mM Putrescine
*TbA/ Tbp
*TcA/ Tcp
LmA/ Lmp
LmA/ Tbp
LmA/ Tcp
TcA/ Lmp
TbA/ Lmp

Table 4.3. Steady-state kinetic analysis of several AdoMetDC and prozyme swapped-species complexes

	5mM Putrescine			No Putrescine		
Enzyme	**k_{cat} (s^{-1})**	**K_m(mM)**	**k_{cat}/K_m($M^{-1}s^{-1}$)**	**k_{cat} (s^{-1})**	**K_m(mM)**	**k_{cat}/K_m($M^{-1}s^{-1}$)**
**T. brucei* AdoMetDC/prozyme	1.30±0.09	0.23±0.05	(6±1)x 10^3	0.86±0.04	0.13±0.02	(7±1)x 10^3
**T. cruzi* AdoMetDC/prozyme	0.69±0.05	0.16±0.03	(4.3±0.9)x 10^3	0.53±0.04	0.20±0.04	(2.7±0.5)x 10^3
L. major AdoMetDC/prozyme	1.0±0.1	0.22±0.07	(5±1)x 10^3	0.131±0.006	0.05±0.01	(2.6±0.1)x 10^3
Lm AdoMetDC/*Tb* prozyme	1.6±0.2	0.27±0.01	(5.9±0.8)x 10^3	1.02±0.05	0.21±0.03	(4.9±0.7)x 10^3
Lm AdoMetDC/*Tc* prozyme	0.84±0.05	0.28±0.05	(3.0±0.6)x 10^3	1.25±0.07	0.50±0.07	(2.5±0.4)x 10^3
Tc AdoMetDC/*Lm* prozyme	0.59±0.04	0.18±0.04	(3.2±0.7)x 10^3	0.11±0.01	0.21±0.07	(0.5±0.1)x 10^2
Tb AdoMetDC/*Lm* prozyme	0.75±0.04	1.1±0.01	(7.0±0.3)x 10^2	0.05±0.01	0.4±0.2	(1.1±0.1)x 10^2

*Denotes data taken from [58] for comparison purposes. *Tb= T.brucei*, *Tc=T.cruzi* and *Lm=L.major*.

CHAPTER 5

CONCLUSIONS AND FUTURE PERSPECTIVES

Polyamine biosynthesis in *Trypanosoma brucei* parasites is a well-known target for the development of new anti-trypanosomal agents, since these organic compounds are known to regulate important cellular processes [13, 14, 20, 21]. AdoMetDC, a crucial enzyme involved in the biosynthetic pathway, is constantly under study and fundamental knowledge about its regulation in these species has been recently obtained. The enzyme is activated by heterodimer formation with a catalytically dead homolog, designated prozyme, which is not present outside of the trypanosomatid lineage [57]. This finding has potential implications for novel enzyme inhibition approaches. However, detailed information on structure and mechanisms of activation were still scarce. Thus, by employing several biochemical techniques, we were able to (i) determine the best conditions for obtaining high levels of soluble and fully active recombinant protein, (ii) identify specific amino acid residues in AdoMetDC that are essential for activation by prozyme, (iii) establish a possible mechanism of activation, and (iv) characterize the activity of the *Leishmania major* AdoMetDC/prozyme complex in an attempt to demonstrate that this type of activation is common to all trypanosomatid species.

Careful optimization of *T. brucei* AdoMetDC expression in *E. coli* revealed that fusion to a SUMO protein dramatically increases the production of active material. About 30 mgs of protein are now recovered from 6L of culture, after the first affinity purification step. This system proved to be effective not only for enhancing solubility and improving expression levels, but also for generating a native protein, after SUMO cleavage with a specific protease (ULP1) [79-81]. The main goal of biotechnological industries is the development of drugs for treatment of numerous human disorders. Frequently, proteins become the targets for these therapeutic drugs. Thus, producing high amounts of material for structural and functional analysis is a current major task for researchers. Of course, this has never been an easy job, since proteins have

very diverse physical-chemical properties, and one single protocol cannot be used for expression and purification of all of them. In the case of AdoMetDC, we strongly believe that inhibitors against this enzyme, as demonstrated in animal models [50, 51], could potentially become more effective therapies for the treatment of human African trypanosomiasis (HAT). The driving force behind this optimization process was to obtain enough material in order to perform a full-scale high-throughput screen (HTS) of a ~200,000 compound library to identify potential candidates that could block the enzyme. The high levels of active AdoMetDC that are been produced now will definitely allow for proper cherry picking of the hits and any further analytical validation. Our results illustrate one of the many ways in which technologies are evolving to improve recombinant protein expression in order to fulfill the research, development and commercial needs.

The structural basis for the activation of AdoMetDC by prozyme was elucidated through detailed mutational and kinetic analyses. Results demonstrated that the N-terminus of *T. brucei* AdoMetDC is necessary for this activation. The catalytic efficency (k_{cat}/K_m) of a mutant enzyme lacking the first 16 amino acid residues (Δ16 AdoMetDC), could not be stimulated by heterodimer formation with prozyme, as opposed to wild-type AdoMetDC. Catalysis rate (k_{cat}) of the mutant complex was about 18-fold slower. After specific point mutations were performed in the region, we discovered that residues L8 and L10 seem to be playing the most important role during the decarboxylation process, although putrescine rescues the detrimental effect in activity observed whenever each of these two amino acids are substituted for alanine. Interestingly, this polyamine had no significant effect neither when both leucines were simultaneously mutated to alanine, nor after the whole region was truncated. It is difficult to provide certain explanations for these observations since the putrescine-binding site has not been well established in the

trypanosomatid enzymes. Several studies have been performed on *T. cruzi* AdoMetDC, based on the human enzyme, and although D174 appears to be a common residue required for binding of putrescine, there is little similarity in the activation of the parasite and mammalian enzymes [113]. The crystal structure of human AdoMetDC bound to putrescine shows that the carbon chain of this diamine stacks against F285 and F111, and is involved in essential hydrophobic interactions to these aromatic residues [47]. From these two, only F285 is fully conserved in all trypanosomatid enzymes. No global conformational changes are observed upon binding of putrescine, just local repositioning of specific residues. However, this might be different for the parasite enzymes, which require heterodimerization with the respective prozyme for full activation. Conformational changes occurring upon binding of prozyme might account for the differences in putrescine activation observed in these species, since residues could now be placed in strategic regions that abolish the need of putrescine for further activation. Unfortunately, no structure information is available for any of the trypanosomatid enzymes, thus this hypothesis is hard to test. Our mutagenesis results on the *T. brucei* AdoMetDC/prozyme complex imply that L8 and L10, in addition to M11 and M13, could be involved in essential hydrophobic interactions during the decarboxylation process. Putrescine compensates for the absence of these side chains, when the residues are mutated to alanine, implying that the aliphatic portion of the diamine molecule could replace the hydrophobic interactions these might have been involved in. The lack of putrescine effect when the whole N-terminus is truncated could also be a consequence of key conformational changes occurring.

Possible mechanisms by which the N-terminus of AdoMetDC is involved in activation by prozyme were investigated by analytical ultracentrifugation (AUC) in the sedimentation velocity (SV) mode. Results demonstrated that although the AdoMetDC L8A/S9A/L10A mutant

heterodimer has lost catalytic activity, the affinity of both subunits is as strong as the wild-type complex, suggesting that these residues might be influencing activation through an allosteric mechanism rather than promoting dimer formation. Removal of the whole N-terminus weakens the dimer interface, as it would be expected from the lack of several residues. However, a fairly tight complex is still obtained, further supporting an allosteric effect. Based on some homology models with human AdoMetDC, which shares about 58% sequence identity with *T. brucei* AdoMetDC, it was predicted that the N-terminal region of the trypanosomatid enzyme is exposed to water in the homodimeric form. Thus, binding of prozyme could re-arrange the structure in such a way that the N-terminal region moves closer to the active site residues, or any other important residues, allowing key interactions to take place that will result in enhanced catalysis.

Studies in blood-form *T. brucei* parasites showed that depletion of either AdoMetDC or prozyme resulted in decreased spermidine and trypanothione levels, eventually leading to parasite death [33]. These observations strongly demonstrate that prozyme activation of AdoMetDC is essential, and that the heterodimer is the functional enzyme *in vivo*. Our findings lead to question if the requirement of the AdoMetDC N-terminus for activation by prozyme would be equally important in the parasites for proper growth and survival. Induction of AdoMetDC RNAi, by the addition of tetracycline to the cells, leads to growth arrest within 4 days, followed by death on day 11 [33]. Thus, the rationale is that while transfection of the WT AdoMetDC gene into this RNAi cell line should rescue the detrimental phenotype observed, transfection of Δ16 AdoMetDC might not. Although the mutant enzyme can bind to prozyme, catalysis is not stimulated and thus not enough decarboxylated AdoMet will be produced for the synthesis of spermidine, resulting on impaired cell viability. Some important details have to be

taken into consideration if these experiments were to be performed. Primarily, scrambled sequences must be obtained for the AdoMetDC and Δ16 AdoMetDC genes that will be transfected, so that RNAi induction does not target them as well. Also, selectable makers should be different for the expression and RNAi vectors. Results obtained from these experiments would further confirm the essentiality of this N-terminal region for enzyme activation, its effect on polyamine and thiol pools in the trypanosomes, and the huge role it could have for the development of new parasite-specific treatments.

The impact of identifying the AdoMetDC N-terminus as a requirement for activation by prozyme relies on the valuable information it provides for the design of new inhibitors. Structural information on the human enzyme reveals multiple areas that would allow abolishing AdoMetDC activity. These included the active site, proenzyme, and the putrescine binding site. MDL73811 is an enzyme-activated irreversible inhibitor of *T. brucei* AdoMetDC [86]. This compound is an analog of the substrate, AdoMet, and inactivates the enzyme by transamination of the pyruvate prosthetic group in the active site. Since the AdoMetDC/prozyme complex represents the active enzyme in trypanosomes, blocking heterodimer formation could be a potential approach. This will also provide huge selectivity, since mammals do not have prozyme. Importantly, small molecules could be designed to target the N-terminal region of AdoMetDC and abolish interaction with key residues during catalysis. Allosteric activation suggests a conformational change that allows seeking for compounds that lock the protein in the inactive conformation, examples from which are currently available and support the feasibility of the mechanism [114-116].

The ability of the *L. major* prozyme to activate the respective AdoMetDC was investigated through steady-state kinetic analysis. Results demonstrated that when both subunits

are mixed together, prozyme is able to increase catalytic efficiency by 170-fold when compared to the homodimer. Interestingly, complexes containing AdoMetDC and prozyme from different trypanosomatid (*T. brucei*, *T. cruzi* and *L. major*) species displayed considerable activity, which was notoriously stimulated by putrescine. These observations reinforce the idea of prozyme activation as a common regulatory mechanism in the parasites. Future experiments could be focused on elucidating the role of the AdoMetDC N-terminus in the *T. cruzi* and *L. major* heterodimers activity. The region is fully conserved in all three species, and thus we would expect it to be equally essential for activation by prozyme.

In conclusion, data presented in this thesis work sheds light on the structural requirements for increased AdoMetDC activity, through complex formation with catalytically dead homolog, in the trypanosomatid species. Crystal structures of the parasites heterodimeric enzymes are urgently needed, since they will provide further information about specific interactions, conformational changes, putrescine binding and species-specific activation, among others. This knowledge will be vital for the rational design of more fully complimentary and potent AdoMetDC inhibitors, which could eventually be used as anti-trypanosomal agents.

References

1. Malvy, D. and F. Chappuis, *Sleeping sickness.* Clin Microbiol Infect, 2011. 17(7): p. 986-95.
2. Barrett, M.P., et al., *Human African trypanosomiasis: pharmacological re-engagement with a neglected disease.* Br J Pharmacol, 2007. 152(8): p. 1155-71.
3. Brun, R., et al., *Human African trypanosomiasis.* Lancet, 2010. 375(9709): p. 148-59.
4. Simarro, P.P., et al., *The human African trypanosomiasis control and surveillance programme of the World Health Organization 2000-2009: the way forward.* PLoS Negl Trop Dis, 2011. 5(2): p. e1007.
5. WHO, *http://www.who.int/mediacentre/factsheets/fs259/en/index.html.* African Trypanosomiasis Fact Sheet.
6. Pays, E., et al., *The trypanolytic factor of human serum.* Nat Rev Microbiol, 2006. 4(6): p. 477-86.
7. Kirchhoff, L.V., *Epidemiology of American trypanosomiasis (Chagas disease).* Adv Parasitol, 2011. 75: p. 1-18.
8. Rassi, A., Jr., A. Rassi, and J.A. Marin-Neto, *Chagas disease.* Lancet, 2010. 375(9723): p. 1388-402.
9. Pays, E., L. Vanhamme, and D. Perez-Morga, *Antigenic variation in Trypanosoma brucei: facts, challenges and mysteries.* Curr Opin Microbiol, 2004. 7(4): p. 369-74.
10. Taylor, J.E. and G. Rudenko, *Switching trypanosome coats: what's in the wardrobe?* Trends Genet, 2006. 22(11): p. 614-20.
11. Barrett, M.P., et al., *Drug resistance in human African trypanosomiasis.* Future Microbiol, 2011. 6(9): p. 1037-47.
12. Priotto, G., et al., *Nifurtimox-eflornithine combination therapy for second-stage African Trypanosoma brucei gambiense trypanosomiasis: a multicentre, randomised, phase III, non-inferiority trial.* Lancet, 2009. 374(9683): p. 56-64.
13. Tabor, C.W. and H. Tabor, *Polyamines.* Annu Rev Biochem, 1984. 53: p. 749-90.
14. Casero, R.A., Jr. and L.J. Marton, *Targeting polyamine metabolism and function in cancer and other hyperproliferative diseases.* Nat Rev Drug Discov, 2007. 6(5): p. 373-90.
15. Gerner, E.W. and F.L. Meyskens, Jr., *Polyamines and cancer: old molecules, new understanding.* Nat Rev Cancer, 2004. 4(10): p. 781-92.
16. Childs, A.C., D.J. Mehta, and E.W. Gerner, *Polyamine-dependent gene expression.* Cell Mol Life Sci, 2003. 60(7): p. 1394-406.
17. Park, M.H., *The post-translational synthesis of a polyamine-derived amino acid, hypusine, in the eukaryotic translation initiation factor 5A (eIF5A).* J Biochem, 2006. 139(2): p. 161-9.
18. Wolff, E.C., et al., *Posttranslational synthesis of hypusine: evolutionary progression and specificity of the hypusine modification.* Amino Acids, 2007. 33(2): p. 341-50.
19. Williams, K., *Modulation and block of ion channels: a new biology of polyamines.* Cell Signal, 1997. 9(1): p. 1-13.
20. Bacchi, C.J., et al., *Polyamine metabolism: a potential therapeutic target in trypanosomes.* Science, 1980. 210(4467): p. 332-4.
21. Birkholtz, L.M., et al., *Polyamine homoeostasis as a drug target in pathogenic protozoa: peculiarities and possibilities.* Biochem J, 2011. 438(2): p. 229-44.
22. Boncher, T., et al., *Polyamine-based analogues as biochemical probes and potential therapeutics.* Biochem Soc Trans, 2007. 35(Pt 2): p. 356-63.

23. Shantz, L.M. and V.A. Levin, *Regulation of ornithine decarboxylase during oncogenic transformation: mechanisms and therapeutic potential.* Amino Acids, 2007. 33(2): p. 213-23.
24. Fairlamb, A. and S. Le Quesne, *Polyamine metabolism in Trypanosomes*, in *Trypanosomiasis and Leishmaniasis*, G. Hide, et al., Editors. 1997, CAB International: Wallingford, Oxon, UK. p. 149-161.
25. Fairlamb, A.H., et al., *Trypanothione: a novel bis(glutathionyl)spermidine cofactor for glutathione reductase in trypanosomatids.* Science, 1985. 227(4693): p. 1485-7.
26. El-Sayed, N.M., et al., *Comparative genomics of trypanosomatid parasitic protozoa.* Science, 2005. 309(5733): p. 404-9.
27. Oza, S., et al., *A single enzyme catalyses formation of trypanothione from glutathione and spermidine in Trypanosoma cruzi.* J. Biol. Chem., 2002. 277: p. 35853-35861.
28. Oza, S.L., et al., *Properties of trypanothione synthetase from Trypanosoma brucei.* Mol Biochem Parasitol, 2003. 131(1): p. 25-33.
29. Heby, O., S.C. Roberts, and B. Ullman, *Polyamine biosynthetic enzymes as drug targets in parasitic protozoa.* Biochem Soc Trans, 2003. 31(2): p. 415-9.
30. Heby, O., L. Persson, and M. Rentala, *Targeting the polyamine biosynthetic enzymes: a promising approach to therapy of African sleeping sickness, Chagas' disease, and leishmaniasis.* Amino Acids, 2007. 33(2): p. 359-66.
31. Li, F., et al., *Trypanosoma brucei brucei: characterization of an ODC null bloodstream form mutant and the action of alpha-difluoromethylornithine.* Exp Parasitol, 1998. 88(3): p. 255-7.
32. Li, F., et al., *Procyclic Trypanosoma brucei cell lines deficient in ornithine decarboxylase activity.* Mol Biochem Parasitol, 1996. 78(1-2): p. 227-36.
33. Willert, E.K. and M.A. Phillips, *Regulated expression of an essential allosteric activator of polyamine biosynthesis in African trypanosomes.* PLoS Pathog, 2008. 4(10): p. e1000183.
34. Taylor, M.C., et al., *Validation of spermidine synthase as a drug target in African trypanosomes.* Biochem J, 2008. 409(2): p. 563-9.
35. Huynh, T.T., et al., *Gene knockdown of gamma-glutamylcysteine synthetase by RNAi in the parasitic protozoa Trypanosoma brucei demonstrates that it is an essential enzyme.* J Biol Chem, 2003. 278(41): p. 39794-800.
36. Krieger, S., et al., *Trypanosomes lacking trypanothione reductase are avirulent and show increased sensitivity to oxidative stress.* Mol Microbiol, 2000. 35(3): p. 542-52.
37. Ariyanayagam, M.R., et al., *Phenotypic analysis of trypanothione synthetase knockdown in the African trypanosome.* Biochem J, 2005. 391(Pt 2): p. 425-32.
38. Roberts, S.C., et al., *Genetic analysis of spermidine synthase from Leishmania donovani.* Mol Biochem Parasitol, 2001. 115(2): p. 217-26.
39. Jiang, Y., et al., *Ornithine decarboxylase gene deletion mutants of Leishmania donovani.* J Biol Chem, 1999. 274(6): p. 3781-8.
40. Roberts, S.C., et al., *S-adenosylmethionine decarboxylase from Leishmania donovani. Molecular, genetic, and biochemical characterization of null mutants and overproducers.* J Biol Chem, 2002. 277(8): p. 5902-9.
41. Roberts, S.C., et al., *Arginase plays a pivotal role in polyamine precursor metabolism in Leishmania. Characterization of gene deletion mutants.* J Biol Chem, 2004. 279(22): p. 23668-78.
42. Tolbert, W.D., et al., *Mechanism of human S-adenosylmethionine decarboxylase proenzyme processing as revealed by the structure of the S68A mutant.* Biochemistry, 2003. 42(8): p. 2386-95.

43. Ekstrom, J.L., et al., *Structure of a human S-adenosylmethionine decarboxylase self-processing ester intermediate and mechanism of putrescine stimulation of processing as revealed by the H243A mutant.* Biochemistry, 2001. 40(32): p. 9495-504.
44. Ekstrom, J.L., et al., *The crystal structure of human S-adenosylmethionine decarboxylase at 2.25 A resolution reveals a novel fold.* Structure, 1999. 7(5): p. 583-95.
45. Pegg, A.E., et al., *S-adenosylmethionine decarboxylase: structure, function and regulation by polyamines.* Biochem Soc Trans, 1998. 26(4): p. 580-6.
46. Bale, S. and S.E. Ealick, *Structural biology of S-adenosylmethionine decarboxylase.* Amino Acids, 2010. 38(2): p. 451-60.
47. Bale, S., et al., *Structural basis for putrescine activation of human S-adenosylmethionine decarboxylase.* Biochemistry, 2008. 47(50): p. 13404-17.
48. Bennett, E.M., et al., *Monomeric S-adenosylmethionine decarboxylase from plants provides an alternative to putrescine stimulation.* Biochemistry, 2002. 41(49): p. 14509-17.
49. Beswick, T.C., E.K. Willert, and M.A. Phillips, *Mechanisms of allosteric regulation of Trypanosoma cruzi S-adenosylmethionine decarboxylase.* Biochemistry, 2006. 45(25): p. 7797-807.
50. Bacchi, C.J., et al., *Cure of murine Trypanosoma brucei rhodesiense infections with an S-adenosylmethionine decarboxylase inhibitor.* Antimicrob Agents Chemother, 1992. 36(12): p. 2736-40.
51. Bitonti, A.J., et al., *Cure of Trypanosoma brucei brucei and Trypanosoma brucei rhodesiense infections in mice with an irreversible inhibitor of S-adenosylmethionine decarboxylase.* Antimicrob Agents Chemother, 1990. 34(8): p. 1485-90.
52. Bacchi, C.J., et al., *In vivo trypanocidal activities of new S-adenosylmethionine decarboxylase inhibitors.* Antimicrob Agents Chemother, 1996. 40(6): p. 1448-53.
53. Bacchi, C., *Resistance to clinical drugs in african trypanosomes.* Parasitology Today, 1993. 9: p. 190-193.
54. Goldberg, B., et al., *Effects of carboxylmethylation and polyamine synthesis inhibitors on methylation of Trypanosoma brucei cellular proteins and lipids.* J. Euk. Mikcrobiol., 1997. 44: p. 352-358.
55. Goldberg, B., et al., *Kinetics of S-adenosylmethionine cellular transport and protein methylation in Trypanosoma brucei brucei and Trypanosoma brucei rhodesiense.* Arch Biochem Biophys, 1999. 364(1): p. 13-8.
56. Goldberg, B., et al., *A unique transporter of S-adenosylmethionine in African trypanosomes.* FASEB J, 1997. 11(4): p. 256-60.
57. Willert, E.K., R. Fitzpatrick, and M.A. Phillips, *Allosteric regulation of an essential trypanosome polyamine biosynthetic enzyme by a catalytically dead homolog.* Proc Natl Acad Sci U S A, 2007. 104(20): p. 8275-80.
58. Willert, E.K. and M.A. Phillips, *Cross-species activation of trypanosome S-adenosylmethionine decarboxylase by the regulatory subunit prozyme.* Mol Biochem Parasitol, 2009. 168(1): p. 1-6.
59. Baneyx, F., *Recombinant protein expression in Escherichia coli.* Curr Opin Biotechnol, 1999. 10(5): p. 411-21.
60. Malys, N., et al., *Protein production in Saccharomyces cerevisiae for systems biology studies.* Methods Enzymol, 2011. 500: p. 197-212.
61. Kost, T.A., J.P. Condreay, and D.L. Jarvis, *Baculovirus as versatile vectors for protein expression in insect and mammalian cells.* Nat Biotechnol, 2005. 23(5): p. 567-75.
62. Rosser, M.P., et al., *Transient transfection of CHO-K1-S using serum-free medium in suspension: a rapid mammalian protein expression system.* Protein Expr Purif, 2005. 40(2): p. 237-43.

63. Lee, P.S. and K.H. Lee, *Escherichia coli--a model system that benefits from and contributes to the evolution of proteomics.* Biotechnol Bioeng, 2003. 84(7): p. 801-14.
64. Stanley, B.A., L.M. Shantz, and A.E. Pegg, *Expression of mammalian S-adenosylmethionine decarboxylase in Escherichia coli. Determination of sites for putrescine activation of activity and processing.* J Biol Chem, 1994. 269(11): p. 7901-7.
65. Persson, K., I. Holm, and O. Heby, *Cloning and sequencing of an intronless mouse S-adenosylmethionine decarboxylase gene coding for a functional enzyme strongly expressed in the liver.* J Biol Chem, 1995. 270(10): p. 5642-8.
66. Osterman, A., et al., *Formation of functional cross-species heterodimers of ornithine decarboxylase.* Biochemistry, 1994. 33(46): p. 13662-7.
67. Bradford, M.M., *A rapid and sensitive method for the quantitation of microgram quantities of protein utilizing the principle of protein-dye binding.* Anal Biochem, 1976. 72: p. 248-54.
68. Chou, C.P., *Engineering cell physiology to enhance recombinant protein production in Escherichia coli.* Appl Microbiol Biotechnol, 2007. 76(3): p. 521-32.
69. Francis, D.M. and R. Page, *Strategies to optimize protein expression in E. coli.* Curr Protoc Protein Sci, 2010. Chapter 5: p. Unit 5 24 1-29.
70. Ferrer, M., et al., *Expression of a temperature-sensitive esterase in a novel chaperone-based Escherichia coli strain.* Appl Environ Microbiol, 2004. 70(8): p. 4499-504.
71. Svensson, F. and L. Persson, *Regulation of ornithine decarboxylase and S-adenosylmethionine decarboxylase in a polyamine auxotrophic cell line.* Mol Cell Biochem, 1996. 162(2): p. 113-9.
72. Murray, E.E., J. Lotzer, and M. Eberle, *Codon usage in plant genes.* Nucleic Acids Res, 1989. 17(2): p. 477-98.
73. Plotkin, J.B., H. Robins, and A.J. Levine, *Tissue-specific codon usage and the expression of human genes.* Proc Natl Acad Sci U S A, 2004. 101(34): p. 12588-91.
74. Gutierrez, G., L. Marquez, and A. Marin, *Preference for guanosine at first codon position in highly expressed Escherichia coli genes. A relationship with translational efficiency.* Nucleic Acids Res, 1996. 24(13): p. 2525-7.
75. Hatfield, G.W. and D.A. Roth, *Optimizing scaleup yield for protein production: Computationally Optimized DNA Assembly (CODA) and Translation Engineering.* Biotechnol Annu Rev, 2007. 13: p. 27-42.
76. Young, C.L., Z.T. Britton, and A.S. Robinson, *Recombinant protein expression and purification: a comprehensive review of affinity tags and microbial applications.* Biotechnol J, 2012. 7(5): p. 620-34.
77. Kapust, R.B., et al., *The P1' specificity of tobacco etch virus protease.* Biochem Biophys Res Commun, 2002. 294(5): p. 949-55.
78. Zuo, X., et al., *Enhanced expression and purification of membrane proteins by SUMO fusion in Escherichia coli.* J Struct Funct Genomics, 2005. 6(2-3): p. 103-11.
79. Butt, T.R., et al., *SUMO fusion technology for difficult-to-express proteins.* Protein Expr Purif, 2005. 43(1): p. 1-9.
80. Marblestone, J.G., et al., *Comparison of SUMO fusion technology with traditional gene fusion systems: enhanced expression and solubility with SUMO.* Protein Sci, 2006. 15(1): p. 182-9.
81. Peroutka Iii, R.J., et al., *SUMO fusion technology for enhanced protein expression and purification in prokaryotes and eukaryotes.* Methods Mol Biol, 2011. 705: p. 15-30.
82. Pegg, A.E., *Mammalian polyamine metabolism and function.* IUBMB Life, 2009. 61(9): p. 880-94.
83. Willert, E. and M.A. Phillips, *Regulation and function of polyamines in African trypanosomes.* Trends Parasitol, 2012. 28(2): p. 66-72.

84. Marton, L.J. and A.E. Pegg, *Polyamines as targets for therapeutic intervention.* Annu Rev Pharmacol Toxicol, 1995. 35: p. 55-91.
85. Spinks, D., et al., *Design, synthesis and biological evaluation of Trypanosoma brucei trypanothione synthetase inhibitors.* ChemMedChem, 2012. 7(1): p. 95-106.
86. Barker, R.H., Jr., et al., *Novel S-adenosylmethionine decarboxylase inhibitors for the treatment of human African trypanosomiasis.* Antimicrob Agents Chemother, 2009. 53(5): p. 2052-8.
87. Hanfrey, C., et al., *A dual upstream open reading frame-based autoregulatory circuit controlling polyamine-responsive translation.* J Biol Chem, 2005. 280(47): p. 39229-37.
88. Pegg, A.E., *Regulation of ornithine decarboxylase.* J Biol Chem, 2006. 281(21): p. 14529-32.
89. Pegg, A.a.P., H., *S-Adenosylmethionine decarboxylase (rat liver). .* In: Tabor H, Tabor CW, editors. Methods in enzymology, Academic Press, 1983. 94th ed. : p. pp. 234–239.
90. Schuck, P., *Size-distribution analysis of macromolecules by sedimentation velocity ultracentrifugation and lamm equation modeling.* Biophys J, 2000. 78(3): p. 1606-19.
91. Schuck, P., et al., *Size-distribution analysis of proteins by analytical ultracentrifugation: strategies and application to model systems.* Biophys J, 2002. 82(2): p. 1096-111.
92. Brautigam, C.A., *Using Lamm-Equation modeling of sedimentation velocity data to determine the kinetic and thermodynamic properties of macromolecular interactions.* Methods, 2011. 54(1): p. 4-15.
93. Dam, J., et al., *Sedimentation velocity analysis of heterogeneous protein-protein interactions: Lamm equation modeling and sedimentation coefficient distributions c(s).* Biophys J, 2005. 89(1): p. 619-34.
94. Bevington, P.R., and Robinson, D. K. , *Data reduction and error analysis for the physical sciences.* 1992. 2nd ed.(WCB/McGraw-Hill, Boston, MA).
95. Johnson, M.L., *Why, when, and how biochemists should use least squares.* Anal Biochem, 1992. 206(2): p. 215-25.
96. Laue, T.M., et al., *Computer-aided interpretation of analytical sedimentation data for proteins*, in *Analytical Ultracentrifugation in Biochemistry and Polymer Science*, S.E. Harding, A.J. Rowe, and J.C. Horton, Editors. 1992, The Royal Society of Chemistry: Cambridge, UK. p. 90-125.
97. DeLano, W.L., *The PyMOL Molecular Graphics System, DeLano Scientific LLC, San Carlos, CA.* 2002.
98. Gilbert, G.A. and R.C.L. Jenkins, *Boundary problems in the sedimentation and electrophoresis of complex systems in rapid reversible equilibrium.* Nature, 1956. 177: p. 853-854.
99. Brown, P.H., A. Balbo, and P. Schuck, *Characterizing protein-protein interactions by sedimentation velocity analytical ultracentrifugation*, in *Current Protocols in Immunology*. 2008, John Wiley & Sons. p. 18.15.1-18.15.39.
100. Yamashina, I., *The action of enterokinase on trypsinogen.* Biochim Biophys Acta, 1956. 20(2): p. 433-4.
101. Chen, J.M., et al., *Evolution of trypsinogen activation peptides.* Mol Biol Evol, 2003. 20(11): p. 1767-77.
102. Jeno, P., J.R. Green, and M.J. Lentze, *Specificity studies on enteropeptidase substrates related to the N-terminus of trypsinogen.* Biochem J, 1987. 241(3): p. 721-7.
103. Davie, E.W. and H. Neurath, *Identification of a peptide released during autocatalytic activation of trypsinogen.* J Biol Chem, 1955. 212(2): p. 515-29.
104. Deshmukh, A.S., et al., *The role of N-terminus of Plasmodium falciparum ORC1 in telomeric localization and var gene silencing.* Nucleic Acids Res, 2012.
105. Shi, H., et al., *RNA interference in Trypanosoma brucei: role of the n-terminal RGG domain and the polyribosome association of argonaute.* J Biol Chem, 2009. 284(52): p. 36511-20.

106. Zhang, X., et al., *Role of the helical structure of the N-terminal region of Plasmodium falciparum merozoite surface protein 2 in fibril formation and membrane interaction.* Biochemistry, 2012. 51(7): p. 1380-7.
107. Jain, R., et al., *N- and C-terminal domains of the calcium binding protein EhCaBP1 of the parasite Entamoeba histolytica display distinct functions.* PLoS ONE, 2009. 4(4): p. e5269.
108. Moyersoen, J., et al., *Characterization of Trypanosoma brucei PEX14 and its role in the import of glycosomal matrix proteins.* Eur J Biochem, 2003. 270(9): p. 2059-67.
109. Luginbuehl, E., et al., *The N terminus of phosphodiesterase TbrPDEB1 of Trypanosoma brucei contains the signal for integration into the flagellar skeleton.* Eukaryot Cell, 2010. 9(10): p. 1466-75.
110. Schimanski, B., et al., *The second largest subunit of Trypanosoma brucei's multifunctional RNA polymerase I has a unique N-terminal extension domain.* Mol Biochem Parasitol, 2003. 126(2): p. 193-200.
111. Daniels, J.P., K. Gull, and B. Wickstead, *The trypanosomatid-specific N terminus of RPA2 is required for RNA polymerase I assembly, localization, and function.* Eukaryot Cell, 2012. 11(5): p. 662-72.
112. Li, X., et al., *The N terminus of antizyme promotes degradation of heterologous proteins.* J Biol Chem, 1996. 271(8): p. 4441-6.
113. Clyne, T., L.N. Kinch, and M.A. Phillips, *Putrescine activation of Trypanosoma cruzi S-adenosylmethionine decarboxylase.* Biochemistry, 2002. 41(44): p. 13207-16.
114. Cherry, M. and D.H. Williams, *Recent kinase and kinase inhibitor X-ray structures: mechanisms of inhibition and selectivity insights.* Curr Med Chem, 2004. 11(6): p. 663-73.
115. Nagar, B., et al., *Crystal structures of the kinase domain of c-Abl in complex with the small molecule inhibitors PD173955 and imatinib (STI-571).* Cancer Res, 2002. 62(15): p. 4236-43.
116. Regan, J., et al., *Pyrazole urea-based inhibitors of p38 MAP kinase: from lead compound to clinical candidate.* J Med Chem, 2002. 45(14): p. 2994-3008.
117. Lopes, A.H., Souto-Padrón, T., Dias, F.A., Gomes, M.T., Rodrigues, G.C., and L.T. Zimmermann, Alves e Silva, T.L. and Vermelho, A.B., *Trypanosomatids: Odd Organisms, Devastating Diseases.* The Open Parasitology Journal, 2010. 4: p. 30-59.
118. Wikipedia, *http://en.wikipedia.org/wiki/Trypanosomatid*. Trypanosomatid.
119. WHO, *http://www.who.int/vaccine_research/diseases/soa_parasitic/en/index3.html*. Leishmaniasis.
120. Ivens, A.C., et al., *The genome of the kinetoplastid parasite, Leishmania major.* Science, 2005. 309(5733): p. 436-42.
121. Alrajhi, A.A., et al., *Fluconazole for the treatment of cutaneous leishmaniasis caused by Leishmania major.* N Engl J Med, 2002. 346(12): p. 891-5.
122. Emad, M., et al., *Superior efficacy of oral fluconazole 400 mg daily versus oral fluconazole 200 mg daily in the treatment of cutaneous leishmania major infection: a randomized clinical trial.* J Am Acad Dermatol, 2011. 64(3): p. 606-8.
123. Bitonti, A.J., et al., *Bis(benzyl)polyamine analogs inhibit the growth of chloroquine-resistant human malaria parasites (Plasmodium falciparum) in vitro and in combination with alpha-difluoromethylornithine cure murine malaria.* Proc Natl Acad Sci U S A, 1989. 86(2): p. 651-5.
124. Assaraf, Y.G., et al., *Cytostatic effect of DL-alpha-difluoromethylornithine against Plasmodium falciparum and its reversal by diamines and spermidine.* Parasitol Res, 1987. 73(4): p. 313-8.
125. Gillin, F.D., D.S. Reiner, and P.P. McCann, *Inhibition of growth of Giardia lamblia by difluoromethylornithine, a specific inhibitor of polyamine biosynthesis.* J Protozool, 1984. 31(1): p. 161-3.

126. **Roberts, S.C., et al., *Leishmania donovani polyamine biosynthetic enzyme overproducers as tools to investigate the mode of action of cytotoxic polyamine analogs.* Antimicrob Agents Chemother, 2007. 51(2): p. 438-45.**

127. **Mukhopadhyay, R. and R. Madhubala, *Effect of a bis(benzyl)polyamine analogue, and DL-alpha-difluoromethylornithine on parasite suppression and cellular polyamine levels in golden hamster during Leishmania donovani infection.* Pharmacol Res, 1993. 28(4): p. 359-65.**